CHEMICAL ALTERATION AND EROSION OF POLYMERIC MATERIALS INDUCED BY EXPOSURE TO SIMULATED LOW EARTH ORBIT CONDITIONS

By

MICHAEL L. EVERETT

A DISSERTATION PRESENTED TO THE GRADUATE SCHOOL
OF THE UNIVERSITY OF FLORIDA IN PARTIAL FULFILLMENT
OF THE REQUIREMENTS FOR THE DEGREE OF
DOCTOR OF PHILOSOPHY

UNIVERSITY OF FLORIDA

2006

I dedicate this dissertation to my parents.

ACKNOWLEDGMENTS

I would like to thank Gar B. Hoflund, Jason F. Weaver, and Helena Hagelin-Weaver for their guidance, their help, and their support throughout my time at the University of Florida. They have taught me a great deal and I am honored to have worked with them. I would also like to thank Seung-Hoon Oh and Bryan Fitzsimmons for their assistance and friendship. I would finally like to thank my parents, my sister, my entire family and all my friends for their support throughout the years.

TABLE OF CONTENTS

page

LIST OF TABLES

Table page

LIST OF FIGURES

Abstract of Dissertation Presented to the Graduate School
of the University of Florida in Partial Fulfillment of the
Requirements for the Degree of Doctor of Philosophy

CHEMICAL ALTERATION AND EROSION OF POLYMERIC MATERIALS INDUCED BY EXPOSURE TO SIMULATED LOW EARTH ORBIT CONDITIONS

By

Michael L. Everett

December 2006

Chair: Gar B. Hoflund
Major Department: Chemical Engineering

In this study the chemical alteration and erosion of poly (tetrafluoroethylene) (PTFE Teflon) by electrons and inert gas ions as well as poly (vinyl fluoride) (Tedlar) and poly (ethylene tetrafluoroethylene) (Tefzel) by hyperthermal atomic oxygen (AO) and vacuum ultraviolet radiation (VUV) (115-400 nm) have been examined using X-ray photoelectron spectroscopy (XPS).

For each polymer sample and each treatment, XPS spectra were taken following various exposure times until no further chemical changes were evident via XPS with increased exposure time. The following steady state values were obtained for each sample and treatment in the study. For PTFE Teflon following the electron exposure, the F/C atom ratio reduced from 1.99 to 1.55 after 25 h and no O was adsorbed to the surface indicating that no reactive sites were formed during the erosion process. After the He^+ exposures the F/C atom ratio decreased from 2.07 to 1.12. A small amount of O was chemisorbed, indicating that only a small amount of reactive sites were formed. The high-resolution XPS C 1s data indicate that new chemical states of carbon formed as the F was removed.

For Tedlar, the F/C atom ratio was reduced from 0.45 to 0.018 after just 2 h exposure to the AO flux, forming a graphitic or amorphous carbon-like layer on the surface. After VUV

exposure the F/C atom ratio decreased from 0.34 to 0.04 after 24 h of exposure time. For both Tedlar studies exposure to O_2 or air nearly doubled the oxygen content at the surface, indicating a large amount of reactive sites formed at the surface during AO and VUV exposures.

For Tefzel, after 24 h of AO exposure the F/C atom ratio decreased from 0.74 to 0.02. After 200 h of VUV radiation the F/C atom ratio decreased from 0.70 to 0.03. Like Tedlar, the near-surface region became a graphitic or amorphous carbon-like layer. Exposure of the AO-damaged surface to O_2 or air nearly doubled the oxygen content in the near-surface region due to dissociative oxygen adsorption at reactive sites formed at the surface during AO exposure. C-H bonds are important sites for attack during erosion by hyperthermal AO for both Tefzel and Tedlar.

CHAPTER 1
INTRODUCTION

Overview

A novel electron stimulated desorption (ESD) hyperthermal atomic oxygen (AO) source, an ultraviolet (UV) radiation lamp and an ion sputtering gun were used to induce chemical changes to the surface of a PTFE Teflon® film, a Tedlar® film and a Tefzel® film. The changes were studied by X-ray photoelectron spectroscopy (XPS). The goal of this study is to examine and attempt to understand the chemical alterations of these polymer surfaces when impacted by hyperthermal (~5 eV) AO, UV radiation, electron irradiation and He^+ ion exposure the way it may occur in low earth orbit (LEO). The average energy and energy spread of the AO from this source are similar to AO in LEO. Also, the UV lamp used covers the range of UV radiation that occurs in LEO, vacuum ultraviolet (VUV) (115-200 nm). There are two types of bonds in PTFE Teflon: C-C bonds and C-F bonds with bond strengths of approximately 83 and 116 kcal/mole, respectively. Tefzel and Tedlar also contain these bonds as well as C-H bonds with bond strengths of 99 kcal/mole. The UV radiation used in this study is energetic enough to break these bonds. PTFE Teflon was exposed to AO and VUV in a separate study, and the results are compared with those from the electron and ion exposures in this study. Tedlar and Tefzel were exposed to AO and VUV only.

Literature Review

Polymers are attractive and desirable materials for use in space applications because they are lightweight and typically much easier to process using techniques such as extrusion, casting and injection molding at relatively low temperatures compared to metals and ceramics. They also tend to be more flexible and offer a wide variety of choices from optically transparent to opaque, rubbery to stiff and conducting to insulating. PTFE Teflon is one material that is widely

used as a thermal blanket for spacecraft flying in LEO [1]. Thermal control is provided by lining the PTFE Teflon with aluminum or silver. The PTFE Teflon has a high thermal emittance, and this system reflects a large fraction of the incident solar energy.

However, over the last two decades, it has been well established that polymers undergo severe degradation resulting in reduced spacecraft lifetimes. These materials degrade because spacecraft surfaces are exposed to high fluxes of AO, bombardment by low- and high-energy charged particles, thermal cycling and the full spectrum of solar radiation. Atomic oxygen is the main constituent of the atmosphere in LEO. It is formed by dissociation of molecular oxygen by ultraviolet radiation from the sun, resulting in an AO concentration of approximately 10^8 atoms/cm^3. The reverse reaction in which an oxygen molecule forms from AO does not have a high reaction rate because it requires a teratomic collision. The third atom is required to dissipate the energy released by formation of O_2. The actual flux of ~10^{14} atoms/cm^2-s impinging on a spacecraft is high due to orbiting speeds of approximately 8 km/s. At these relative speeds thermal AO collides with a kinetic energy of ~4.5 eV. These highly energetic collisions not only result in surface chemical reactions but also can lead to a pure physical sputtering of the surface atoms in the absence of any chemical changes. Many studies have been conducted in an effort to determine the mechanism of this degradation primarily caused by surface reactions with AO [2-9]. However, these studies have all been carried out after exposing these highly reactive surfaces to air prior to analysis, thus introducing artifacts that do not represent the true space environment. Recent studies have shown that exposure to air chemically alters the reactive surfaces formed during AO exposure [10-13]. It is, therefore, essential that analysis of polymers exposed to AO be carried out in-situ to avoid artifacts induced by air exposure.

Several studies have been conducted on the deterioration of fluorinated polymers retrieved from spacecraft subjected to the LEO environment. The outer layer of Teflon-fluorinated ethylene propylene® (FEP) multi-layer insulation on the Hubble space telescope (HST) was significantly cracked at the time of the second HST servicing mission, 6.8 years after it was launched into LEO [14, 15]. Comparatively minor embrittlement and cracking were also observed in the FEP materials retrieved from solar-facing surfaces on the HST at the time of the first servicing mission (3.6 years of exposure). Furthermore, an increased deterioration of fluorinated polymers may result from the synergistic effect of VUV radiation and charged particles such as electrons and ions in the presence of AO [16]. This point remains to be demonstrated.

Intuitively, low-energy AO would not be expected to break these bonds, and this has been found experimentally [4]. Gindulyte, Massa, Banks and Miller [17] have carried out a quantum mechanical study on the erosion of PTFE Teflon by AO. They conclude that AO in LEO possesses enough translational energy to erode PTFE Teflon by breaking C-C bonds. They did not consider breakage of C-F bonds based on electronegativity arguments.

O-Atom Source Characteristics

A photograph and schematic diagram illustrating the operational principles of the ESD AO source are shown in Figures 1-1a and 1-1b, respectively. Ultrahigh-purity molecular oxygen dissociatively adsorbs on the high-pressure (2 Torr) side of a thin metallic Ag-alloy membrane maintained at elevated temperature (~400°C) and permeates through the membrane to the UHV side. There the chemisorbed atoms are struck by a directed flux of primary electrons, which results in ESD of the O atoms forming a continuous flux. The primary electrons are produced by thermionic emission from a coiled hot filament supported around the perimeter of the membrane.

An electron reflector (lens assembly) surrounds the filament. It produces a potential field, which creates a uniform flux of electrons over the membrane surface. These primary electrons have a kinetic energy of 1000 eV and provide two functions: ESD of the O atoms and heating of the membrane surface. Another lens is placed between the reflector and the sample for removal of all charged particles including secondary electrons and O^+ and O^- ions produced during the ESD process.

Several processes have to function in series at sufficiently high rates for this system to work, including dissociative chemisorption of the molecular gas on the metal surface, permeation of atomic oxygen through the membrane and formation of the neutral flux by ESD. Since these processes occur in series, the slowest one determines the magnitude of the AO flux. The sticking coefficient of O_2 on polycrystalline Ag (step 1) is fairly small (< 0.001) so it is necessary to use a high pressure on the upstream side of the membrane. However, the permeation rate through the membrane is proportional to the reciprocal of the membrane thickness. This means that it is desirable to have a high pressure and a thin membrane, but this can lead to membrane failure. The ESD rate can be increased by increasing the primary electron current to the membrane, but this increases the temperature of the membrane and can result in evaporation of Ag, which is unacceptable.

The AO produced by this source has been shown to be hyperthermal (energies greater than 0.01 to 0.02 eV), but the neutral energy distribution has not been measured. Corallo et al. [18] have measured the energy distribution of O ions emitted by ESD from a Ag(110) surface and found that this distribution has a maximum of ~5 eV and a full-width at half maximum of 3.6 eV. This ion energy distribution sets an upper bound for the neutral energy distribution because ESD neutrals are generally believed to be less energetic than ESD ions based on models of the ESD

process. This point has been discussed often in the ESD literature but not actually demonstrated. Since neutral ESD species are difficult to detect, very few ESD studies of neutral species have appeared in the literature. The neutral atom flux has been detected by using a quadrupole mass spectrometer [19, 20] in the appearance potential (AP) mode to allow the atoms to be distinguished from residual gases and background gas products formed by collisions of the neutrals with the walls of the UHV system. In this experiment the ion acceleration potential was set at 0.0 V. Calibration studies have demonstrated that the ions entering the quadrupole section must have a minimum kinetic energy of 2.0 eV to reach the detector so the ESD neutrals detected have a minimum energy of 2.0 eV. Therefore, the hyperthermal AO produced by this ESD source have energies greater than 2 eV but possibly less than the ion energy distribution. Furthermore, these mass spectrometric experiments have shown that the AO-to-O^+ ratio is about 10^8 and that the O^+-to-O^- ratio is about 100.

Several approaches have been used to measure the magnitude of the hyperthermal AO flux and reasonable agreement was obtained between the various methods. The flux from the ESD AO source is approximately $2x10^{15}$ atoms/cm^2-s. One of the most reliable methods for flux determination is the measurement of a ZrO_2 film growth rate [21]. A Zr flux was generated by e-beam evaporation and the flux was calibrated using a quartz-crystal monitor. Based on the facts that stoichiometric ZrO_2 was produced and that no O_2 is present in the AO flux, the AO flux was calculated. By doubling the Zr flux, stoichiometric ZrO was grown [22]. The AO flux has also been determined by measuring the chemisorption rate of AO on polycrystalline Au using ion scattering spectroscopy [23]. The flux determined using this method is in excellent agreement with that determined using the oxide growth rate method.

Ultraviolet Source Characteristics

The UV source used in this study was a Hamamatsu water-cooled deuterium lamp (model L1835). It had an MgF_2 window allowing UV light with wavelengths ranging from 115 to 400 nm to pass through to the sample in a 2.5 mm diameter aperture. The aperture was approximately 15 cm from the sample and the lamp operated at a power of 150 W. Based on the power level and the ASTM solar spectral irradiance tables [24], the irradiance level is most likely more than twenty times that found in LEO. Typically the output from windowed VUV sources like the one used in this study degrades rapidly due to accumulation of contamination on the window. This was not a problem in this study because the VUV source is housed in the same chamber as the AO source [25], which keeps this chamber very clean. The AO source was not operated when this sample was in the chamber.

X-ray Photoelectron Spectroscopy

X-ray photoelectron spectroscopy (XPS), also known as electron spectroscopy for chemical analysis (ESCA), is a photoemission technique used to determine the composition and chemical state distribution of solid surfaces. It is performed by irradiating the surface with X-rays under vacuum and measuring the kinetic energy distribution of the emitted electrons. An electrostatic charged particle energy analyzer is used to obtain the spectral peaks generated from the kinetic energies of the emitted electrons. The corresponding binding energies specific to each individual element are then calculated from the following equation:

$$E_b = h\nu - E_k + \Delta\phi$$

where E_b is the binding energy (BE) in the solid, E_k is the kinetic energy of the emitted electron and $\Delta\phi$ is the work function difference between the sample and the detector material assuming there is no electrical charging at the sample surface [26].

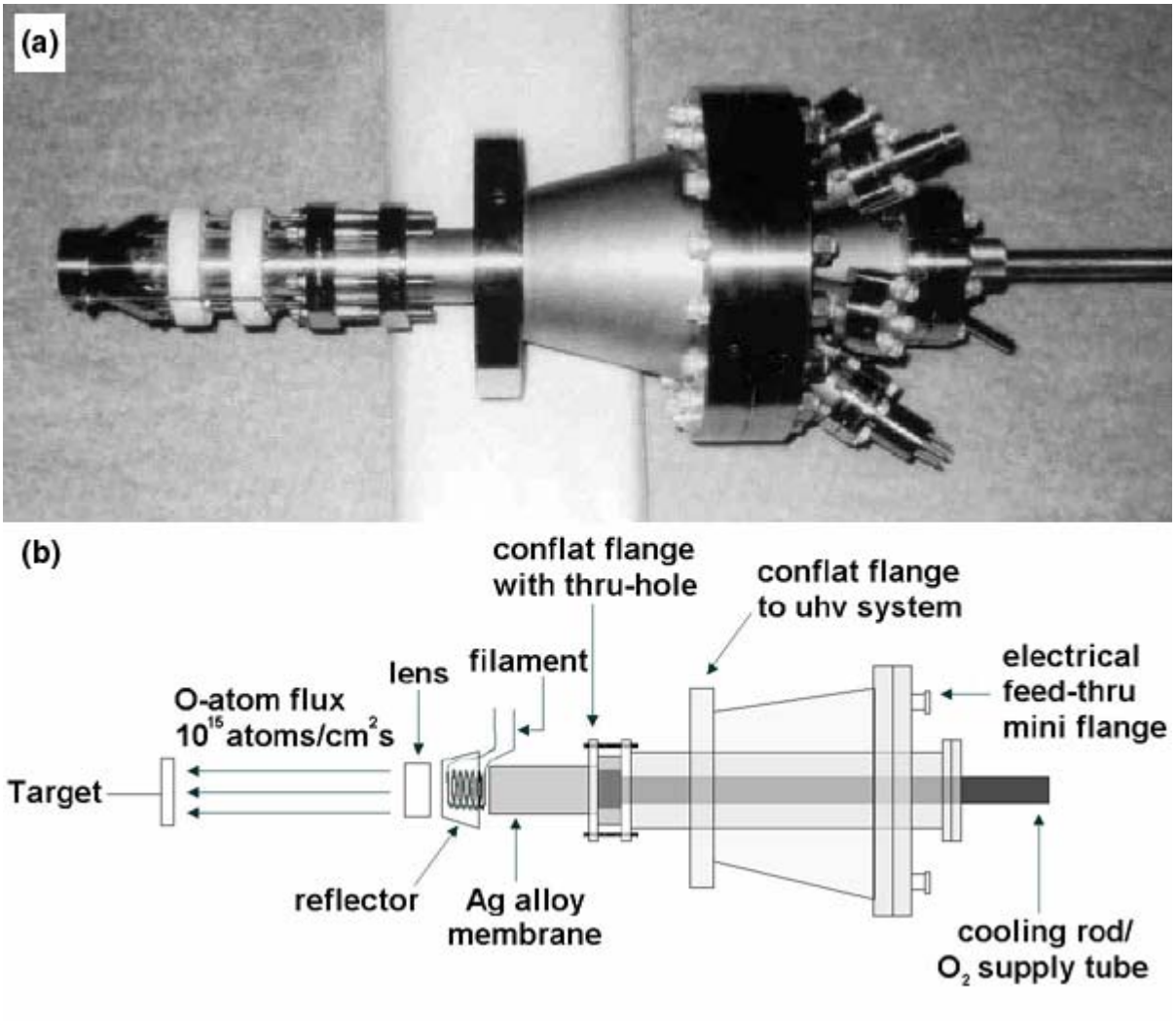

Figure 1-1. Atomic oxygen source (a) Photograph of ESD AO source. (b) Schematic illustrating operational principles of ESD AO source.

CHAPTER 2
CHEMICAL ALTERATION OF POLY (TETRAFLUOROETHYLENE) PTFE TEFLON INDUCED BY EXPOSURE TO ELECTRONS AND INERT-GAS IONS

In addition to other factors such as atomic oxygen and vacuum ultraviolet radiation, charged particles such as electrons and ions are two other factors in LEO that can affect the surface chemistry of a polymer [16]. In this study XPS was used to characterize the surface of a PTFE Teflon film before and after exposures of varying lengths to 1 keV electrons and 1 keV He^+ ions, as well as O_2 and air. The goal of the study was to determine how these treatments affect the PTFE Teflon surface so that a better understanding of its space survivability can be obtained.

Experimental

Electron Source Characteristics

The ~1.0 keV electrons were generated in this study by operating the AO source mentioned in Chapter 1 without oxygen present in the source and setting the electrostatic lens voltage to 0.0 V. Primary electrons (1 keV) from the filament struck a Ag membrane generating 1-keV electrons and a low, broad background of secondary electrons [27]. The electron flux used was approximately 5 μamp/mm^2.

Ion Source Characteristics

The ion source used in this study was a PHI Model 04-161 Sputter Ion Gun with a PHI Model 20-045 Sputter Ion Gun Control. The ion source was operated at a primary beam energy of 1.0 keV with an emission current of 4 mA. The source was operated within an ultra-high vacuum chamber backfilled to a pressure of $1x10^{-5}$ Torr He. The sample was exposed at an

incident angle of ~60º and a distance of 8 cm from the source. The flux was ~$5x10^{13}$ ions/cm^2s with the instrument settings used.

Surface Characterization

An as-received E.I. du Pont Nemours & Co., Inc. PTFE Teflon film was wiped with ethanol and inserted into an ultra-high vacuum (UHV) chamber (base pressure <$1.0x10^{-10}$ Torr). XPS measurements were performed using a double-pass cylindrical mirror analyzer (DPCMA) (PHI Model 25-270AR). XPS survey spectra were taken in the retarding mode with a pass energy of 50 eV, and high-resolution XPS spectra were taken with a pass energy of 25 eV using Mg $K\alpha$ X-rays (PHI Model 04-151 X-ray source). Data collection was accomplished using a computer interfaced, digital pulse counting circuit [28] followed by smoothing with digital-filtering techniques [29]. The sample was tilted 30 degrees off the axis of the DPCMA, and the DPCMA accepted electrons emitted into a cone 42.6 ± 6 degrees off the DPCMA axis.

XPS spectra were first obtained from the as-entered, solvent-cleaned sample. The sample was then transferred *in-vacuo* into an adjoining UHV chamber that houses the electron source via a magnetically coupled rotary/linear manipulator. There the surface was exposed to a flux of electrons or ions and re-examined after various exposure times. The sample was not exposed to air after the exposures and before collecting XPS data. However, after the exposures the surface was exposed *in-vacuo* to O_2 in another adjoining vacuum chamber to determine how this would affect the electron- or ion-exposed surface. The sample was maintained at room temperature during the exposures with a temperature increase to about 50°C due to exposure to the X-ray source during XPS data collection. The substrate temperature was determined using a chromel-alumel thermocouple.

Results and Discussion

Electron Exposures

The XPS survey spectrum obtained from the as-received PTFE Teflon surface prior to electron exposure is shown in Figure 2-1a. This spectrum is identical to that given for PTFE in the polymer XPS handbook by Beamson and Briggs [30] with the characteristic C 1s, F 1s, F 2s and F (KLL) peaks. There is no O 1s peak, which would appear near a binding energy (BE) of 530 eV. There are two states of carbon present indicated by a large peak due to PTFE Teflon at a BE of 292.5 eV and a small peak due to adventitious carbon at 284.6 eV. These C 1s features are more apparent in the high resolution XPS spectrum shown in Figure 2-2Aa. The corresponding F 1s spectrum shown in Figure 2-2Ba exhibits a single broad peak centered at 689.7 eV, which is characteristic of Teflon [30]. Estimates of the near-surface compositions have been made from the peak areas in the high-resolution spectra using published atomic sensitivity factors [31] with the assumption of a homogeneous surface region. XPS probes the near-surface region of the sample and yields a weighted average composition with the atomic layers near the surface being weighted more heavily since the photoemitted electrons from these layers have a lower probability of scattering inelastically. The sampling depth is ~4-6 nm, and ~10% of the signal originates from the outermost atomic layer [32]. This near-surface region is nonhomogeneous because the electrons and ions react most strongly with the outermost few atomic layers. Therefore, the region that reacts to the greatest extent with the electrons and ions also makes the largest contribution to the XPS signal. This fact implies that XPS is an excellent technique for studying erosion of spacecraft materials. Even though the distribution functions involving the depth of chemical reactions in the near-surface region and the XPS determination of the weighted average composition of the near-surface region are complex, the compositional values provide a trend which is indicative of the chemical alterations occurring during electron or

ion exposure. The compositions determined using the homogeneous assumption are shown in Table 2-1 before and after various exposures to electrons and research-grade O_2. The F/C atom ratio obtained from the as-entered sample is 1.99, which is very close to the stoichiometric value of 2.0.

After 2 h of exposure to the electron flux, distinct changes in the C 1s features are apparent in Figure 2-1b. Based on the high resolution C 1s feature shown in Figure 2-2Ab, the feature due to adventitious carbon has been completely removed. The overall height of the high-BE peak due to PTFE Teflon is decreased and a broad structure is apparent on the low-BE side. Although distinct peaks cannot be discerned, at least two peaks are present. A shoulder is also present at 294.8 eV. No detectable changes are observed in the F 1s, F 2s or F (KLL) peaks in Figure 2-1b, nor are any observed in the high resolution F 1s spectrum (Figure 2-2Bb). The C concentration is increased from 33.5 to 41.5 at% and the F concentration dropped from 66.5 to 58.5 at% resulting in a decrease in the F/C atom ratio to 1.41.

The surface was then exposed to the electron flux for another 23 h for a total of 25 h. The data in Table 2-1 indicate that the F content is slightly increased while the C content is slightly decreased resulting in an increase in the F/C atom ratio from 1.41 to 1.55. This increase is consistent with the changes in the C 1s shown in Figure 2-2Ac. The peak at 292.5 eV due to carbon in PTFE Teflon is increased in size relative to the shoulder. The features on the shoulder at 290.0 and 288.0 eV are more pronounced and there may be another small contribution just above 288.0 eV. Furthermore, the shoulder at 294.8 eV was eliminated by this exposure. No changes are apparent in the F 1s peak (Figure 2-2Bc).

Assigning these peaks to specific species is quite difficult for several reasons. Defining localized species, which yield features at specific BEs, may not be possible. For example,

$F - \overset{|}{\underset{|}{C}} - F$ species are present in PTFE and FEP Teflon and Tefzel but the C 1s BEs are 292.48 and 290.9 eV respectively. Also, $H - \overset{|}{\underset{|}{C}} - H$ species are present in Tefzel and Tedlar with BEs of 286.44 and 285.74 eV respectively. XPS BEs result from the chemical environment around the given element. This fact implies that the chemical environment is larger than the species defined in PTFE Teflon, Tefzel and Tedlar. Since there are distinct peaks in these spectra, there are distinct chemical environments, but defining the nature of these chemical environments is difficult. Since the electron-exposed PTFE Teflon surface is a damaged surface in that the composition is changed to a great extent, the structure is most likely altered in the following manner. The two states with BEs of 290.0 and 288.5 eV may be carbons that have lost one and two fluorines respectively. The presence of regions of lower concentrations of F implies that electron density on the C atoms is not decreased to such a large extent by withdrawal toward the F resulting in increased C 1s BEs.

The surface was then exposed to 120 Torr O_2 for 20 min. Negligible changes are observed in the XPS survey spectrum (not shown). The C concentration increases to 39.5 at%, the F concentration decreases to 60.5 at% and the F/C atom ratio drops to 1.53; all of which are similar to those after the 25-h e^- exposure. No oxygen is adsorbed onto the surface. The surface was then exposed to 760 Torr O_2 for another 90 minutes. Negligible changes to the XPS survey spectra (not shown) are observed with the exception of the appearance of a very small peak at 530 eV, which is due to a small amount of oxygen adsorbed at the surface. The area under the O 1s feature is not large enough to quantify but is indicative of an O concentration less than 1 at% in the near-surface region.

The high-resolution XPS spectra obtained after the two O_2 exposures exhibit subtle changes in the C 1s features (Figure 2-2Ad and 2-2Ae) while no changes to the F 1s spectra (Figure 2-2Bd and 2-2Be) are apparent. After the 20-min O_2 exposure, the high-BE C 1s peak (Figure 2-2Ad) broadens further on the low-BE side. The shoulder at 290.0 eV has a more definitive peak shape. The low-BE feature at 288.0 eV becomes more narrow and prominent, whereas the portion at 288.5 eV is decreased. After the additional 90-min O_2 exposure the spectrum resembles that prior to any O_2 exposure. The peak at 288.5 eV becomes larger than the shoulder at 288.0 eV, and the peak at 290.0 eV becomes less prominent.

The surface was again exposed to the electron flux for 23 additional h (48 h total). The XPS survey spectrum (not shown) indicates no changes to the F 1s, F 2s or F (KLL) peaks and that the small feature due to O is completely removed. The low-BE C 1s feature appears as a more defined peak, similar to that obtained after the 25-h electron exposure. The C composition of the surface increases to 40.3 at%, the F 1s concentration decreases to 59.7 at% and the F/C atom ratio decreases to 1.48. As before, there is no noticeable change in the high-resolution F 1s spectrum shown in Figure 2-2Bf. Several changes to the C 1s spectrum are observed in Figure 2-2Af. The features at 290.0 and 288.0 eV begin to reemerge as peaks with the continued electron exposure. The high BE peak at 292.5 eV becomes broader with a shoulder now appearing on its high-BE side at 294.8 eV. This shoulder having a higher BE than carbon in the PTFE Teflon environment indicates that electron-deficient species are formed under electron bombardment. This may occur by emission of F^- species leaving carbon species which have lost an electron pair. The nuclei of these species then attract the C 1s electrons more strongly resulting in a larger C 1s BE. This feature is also apparent after the 2-h electron exposure (Figure 2-2Ab).

He^+ Exposures

The XPS survey spectrum obtained from the as-received PTFE Teflon surface prior to ion exposure is identical to that shown in Figure 2-1a and does not change after a 1-h exposure to 0.5 keV He^+ (not shown). As found above, two states of carbon are present due to PTFE Teflon at a BE of 292.5 eV and a small peak due to adventitious carbon at 284.6 eV (Figure 2-3Aa). The F/C atom ratio is 2.07 (Table 2-2), which is close to the expected value of 2.00. Comparison of the as-received survey spectrum and the He^+-exposed survey spectrum (not shown), as well as the high resolution C 1s and F 1s spectra (Figures 2-3Aa, 2-3Ab, 2-3Ca, 2-3Cb), indicate that there are no detectable changes to the surface induced by exposure to 0.5 keV He^+. The F/C atom ratio increases slightly to 2.18.

Changes in the C 1s peak are observed in Figure 2-3Ac after a 2-h exposure to 1-keV He^+. The adventitious carbon peak is reduced in size and at least one new state of carbon is apparent as a shoulder at 287.5 eV on the low-BE side of the C 1s peak. The F/C atom ratio is decreased to 1.79; a loss of nearly 18% of the F in the near-surface region. Negligible changes in the fluorine peaks are observed in Figure 2-3Cc. After an additional 2 h of He^+ exposure there is an increase in the size of the shoulder on the C 1s peak (Figure 2-3Ad). The C 1s feature is broader, the height of the shoulder is increased and multiple carbon states are apparent. The low-BE feature from the previous exposure now appears to be a peak centered at 288.0 eV while another peak forms at 290.0 eV. The F/C atom ratio drops to 1.51, another 15% decrease in F concentration in the near-surface region. No changes are apparent in the F 1s, F 2s and F (KLL) peaks.

Another 4 h of He^+ exposure (8 h total) yields further change in the C 1s features as do 2 more subsequent hours. The high-resolution C 1s spectrum in Figure 2-3Ae indicates the presence of five distinct carbon features. The peaks at 288.0 and 290.0 eV each become more

defined and make larger contributions to the carbon content at the surface. The F/C atom ratio is further reduced to 1.37; a loss of approximately 9% of the remaining near-surface F or 33% of the original F concentration. Also, a shoulder forms on the high-BE side of the PTFE Teflon C 1s peak at 292.5 eV.

These changes are enhanced further by another 2-h He^+ exposure. The high resolution F 1s spectrum (Figure 2-3Cf) indicates that the F 1s peak shape remains constant. The F/C atom ratio after this treatment only decreases nominally to 1.35. Assigning peaks to specific species is again difficult for the reasons stated above. Since the He^+-exposed surface is a damaged surface in that the composition is altered to a great extent, the structure is most likely altered in the following manner. The two states with BEs of 290.0 and 288.5 eV may be carbons that have lost one and two fluorines respectively. The presence of lower concentrations of F implies that electron density on the C atoms is not decreased to such a large extent by withdrawal toward the F resulting in decreased C 1s BEs. The shoulder at 294.8 eV, having a higher BE than carbon in the PTFE Teflon environment, indicates that electron-deficient species are formed under He^+ bombardment most likely by emission of F^- species leaving carbon species which have lost an electron pair. The nuclei of these species then attract the C 1s electrons more strongly resulting in a larger C 1s BE.

The sample was then exposed to research-grade O_2 at 150 Torr for 20 min and the XPS spectrum (not shown) indicates that only a very small amount (<1 at%) of O_2 chemisorbs on the surface. This suggests that most of the broken bonds formed by the He^+ exposure cross-link on the PTFE Teflon surface. The F/C atom ratio did however increase to 1.45. This may be due to removal of reactive C species by reaction with O_2 to form CO and CO_2. The C 1s and F 1s high resolution spectra are shown in Figures 2-3Ag and 2-3Cg respectively. As before the F 1s

feature apparently is not altered by the O_2 exposure, but the C 1s shoulders are significantly altered in that they are decreased in intensity. This is consistent with loss of these species by reaction with O_2.

Five more h of He^+ exposure (15 h total) following the O_2 treatment results in complete removal of the O 1s feature in the survey spectrum (not shown). The C 1s feature shown in Figure 2-3Ah indicates that the shoulders become significantly larger and more well-defined. The peaks at 288.0 and 290.0 eV become larger with respect to the PTFE Teflon peak at 292.5 eV. Also, the PTFE Teflon peak has become narrower and the shoulder on its high-BE side has become larger and more prominent. The F/C atom ratio decreases further to 1.27. After another 4 h of He^+ exposure (19 h total), it decreases further to 1.12. Approximately 46% of the fluorine originally present in the near-surface region is removed by this He^+ exposure. In the XPS spectrum in Figure 2-4a, changes to the C 1s feature are evident in that the two separate peaks merge into one large, broad feature. Furthermore, the 288.0-eV feature is broadened toward the low-BE side and is now considerably larger than the 290.0-eV feature.

After 19 h of He^+ exposure, the sample was removed from the UHV system, exposed to air at room temperature for 90 min and returned to the UHV system for analysis. The XPS spectrum obtained after this exposure is shown in Figure 2-4b. Two noticeable changes from Figure 2-4a are the presence of an O 1s feature near 535 eV and further changes to the C 1s feature which now has two peaks of nearly equal heights. The F 1s, F 2s and F (KLL) features remain unchanged and no features due to N are evident. The C 1s features in Figure 2-3Aj are less defined after the air exposure and the feature as a whole is broader. The low-BE features are increased in height relative to the PTFE Teflon feature at 292.5 eV. The F 1s peak in Figure 2-

3Cj remains unchanged. The O 1s spectrum in Figure 2-3Bj appears as a broad feature with two peaks at 534.6 eV and 535.8 eV. The F/C atom ratio is decreased to 0.99.

Ar^+ Exposures

A fresh PTFE Teflon sample was then sputtered with 1-keV Ar^+ for various times, and the resulting data are compared with those obtained after 1-keV He^+ exposures. Both 1-keV He^+ and 1-keV Ar^+ have the same kinetic energy, but the velocity of the 1-keV He^+ is 3.16 times that of the 1-keV Ar^+ due to the mass difference while the ratio of the Ar^+ momentum to the He^+ momentum is 3.16. The F/C atom ratio decreases with Ar^+ exposure similarly to the He^+ exposure but about twice as fast. In 8 h a steady-state F/C atom ratio of 1.13 is attained using 1-keV Ar^+ while 19 h is required to attain a steady-state F/C atom ratio of 1.12 with 1-keV He^+. This increased damage rate with Ar^+ is most likely due to the fact that Ar^+ has a larger cross section than He^+ [32].

The C 1s XPS spectra obtained after various Ar^+ exposures are shown in Figure 2-5. After a 1-h, 1-keV Ar^+ exposure, the spectrum shown in Figure 2-5b was obtained. Compared with the spectrum from the as-entered PTFE Teflon, the adventitious carbon is removed and carbon states with BEs of 287.5 and 290.0 eV are apparent. These changes are similar to those observed after a 2-h, 1-keV He^+ exposure (Figure 2-3c). The spectrum shown in Figure 2-5c was obtained after an 8-h exposure to 1-keV Ar^+. The C 1s feature at 286.9 eV is quite prominent while other features are not except for the peak at 292.5 eV due to PTFE Teflon. The C 1s spectrum shown in Figure 2-5d was obtained after a 20-min exposure to 150 Torr O_2. The shoulders at ~295 and 290.5 eV are more prominent, and the low-BE energy feature is shifted to a higher BE by about 0.5 eV and broadened. The near-surface region O concentration is approximately 1.4 at% after this treatment.

A comparison of the C 1s spectra obtained after exposure for 8 h to 1-keV He^+ and exposure for 8 h to 1-keV Ar^+ is shown in Figure 2-6. The spectra are quite different with regard to the carbon chemical states formed. Exposures to He^+ produces the two prominent damage states with BEs of 290.0 and 288.0 eV as discussed above. These two states may contribute to the C 1s spectrum obtained after Ar^+ exposure, but they are not apparent. Instead, a large, broad peak is present at a BE of 286.9 eV which extends down to a BE of about 284 eV. The low-BE portion of the feature is due to a graphitic form of carbon which has a BE of about 285 eV. The presence of F may result in an increased BE for this graphitic species due to withdrawal of electrons by the F. The He^+ exposure also produces a higher-BE species at about 295 eV due to emission of F^- leaving electron-deficient C species. This state is not present after exposure to Ar^+.

Comparison of He^+, e^-, AO and VUV Data

In two previous studies the chemical alteration of PTFE Teflon by hyperthermal AO [33] and VUV radiation [34] have been studied. A comparison of C 1s features obtained from PTFE Teflon after exposure to He^+, e^-, VUV and hyperthermal (~5 eV) AO are shown in Figure 2-7. These are all steady-state exposures in that longer exposures do not result in different spectra. These four spectra are all quite different, but they all contain the same four features at 288.0, 290.0, 292.5 and 294.5 eV. None of these spectra exhibit a feature due to graphitic carbon as found in the case of Ar^+ exposure. The greatest alteration occurs for the hyperthermal-AO exposure. The feature due to PTFE Teflon is quite small as is the high-BE feature at 294.5 eV. The predominant peak at 288.0 eV is due to C atoms that have lost two F atoms, and the next largest feature at 290.0 eV is due to C atoms that have lost one F atom.

Exposure to He^+ results in less alteration than AO exposure. In this case the peak due to PTFE Teflon is the predominant peak. The lower-BE peaks are large and again have a similar

structure to those obtained after AO exposure and VUV exposure. The high-BE shoulder at 294.5 eV is present on the PTFE Teflon peak which remains well defined.

Less alteration occurs with the 1-keV e^- exposure than the He^+ exposure. The lower-BE C 1s states are present but they are not well defined. The peak due to PTFE Teflon is predominant, but it has a large shoulder at about 291.5 eV. The nature of the chemical species responsible for this shoulder is not understood. The high-BE feature at 294.5 eV is present as a shoulder on the PTFE Teflon peak, but it is fairly small indicating that electron stimulated desorption (ESD) of F^- occurs less frequently than ESD of F neutrals.

The least amount of alteration occurs with VUV radiation of PTFE Teflon. The lower-BE features at 288.0 and 290.0 eV have a similar structure to those in the C 1s spectrum obtained after AO exposure, but they are smaller than the peak due to PTFE Teflon which is the predominant peak. Unlike the other spectra, the high-BE peak at 294.5 eV is quite large and almost as large as the PTFE Teflon peak.

Summary

In this study the chemical alterations at a PTFE Teflon surface caused by exposure to primary electrons, 1.0 keV He^+ and 1.0 keV Ar^+ have been studied using XPS. A 2-h exposure to electrons results in a decrease in the F/C atom ratio from 1.99 to 1.41 and the formation of three new carbon chemical states assigned as C bonded to only one F, C bonded to other C and C which have lost a pair of electrons by emission of F^-. Adventitious C is not present in significant quantities on any of the surfaces examined in this study and what little is there initially is removed by a 2-h exposure to both electrons and He^+. Another 23 h of electron exposure results in a further decrease of the F/C atom ratio to 1.55 and an increase in the concentration of the three new carbon states, although the PTFE Teflon state still predominates. Exposure of this electron-exposed surface to O_2 results in chemisorption of a very small amount

of O due to bonding at reactive sites. The fact that so little O_2 chemisorbs indicates that the surface carbon may bond to other carbon, which is consistent with the formation of the new C chemical states. Further exposure of this surface to electrons for another 23 h results in removal of the chemisorbed oxygen and a further reduction in the F/C atom ratio to 1.48.

A 2-h exposure of a fresh PTFE Teflon surface to 1.0 keV He^+ ions reduces the initial F/C atom ratio from 2.07 to 1.79. Another 8 h of He^+ exposure further reduces the F/C atom ratio to 1.35 and the formation of three new carbon chemical states also assigned as C bonded to only one F, C bonded to other C and C which have lost a pair of electrons by emission of F^-. Exposure of this He^+-altered surface to O_2 results in chemisorption of a very small amount of O at reactive sites. The fact that so little O_2 chemisorbs indicates that the surface carbon, which have lost F atoms, bond to other carbon, which is consistent with the formation of the new C chemical states. Nine more hours of He^+ exposure results in further reduction of the F/C atom ratio to 1.12 with the lower-BE carbon states beginning to predominate. Finally this surface was exposed to air at room temperature and some O was chemisorbed resulting in a near-surface concentration of 1.9 at%. A fresh PTFE Teflon surface was also exposed to 1-keV Ar^+ for various periods. Chemical alterations of PTFE Teflon occur about twice as fast with 1-keV Ar^+ versus 1-keV He^+. This is believed to be due to the fact that Ar^+ has a larger interaction (sputtering) cross section than He^+. Comparison of the C 1s spectra obtained after exposure to 1-keV Ar^+ and 1-keV He^+ for 8 h indicates that different carbon chemical states are formed by Ar^+. Specifically a significant amount of carbonaceous or graphitic carbon is formed by Ar^+ exposure. This species is not formed by any of the other exposures.

The C 1s spectra obtained in this study using electrons and 1-keV He^+ have been compared with C 1s spectra obtained using VUV and hyperthermal AO. The spectra compared are steady-

state in that extended exposures do not produce different spectra. Similar carbon species are present after all of the exposures, but the relative amounts vary greatly. The largest alteration is due to hyperthermal AO followed by He^{+}, e^{-} and VUV. None of these treatments result in the formation of a graphitic species.

Table 2-1. Near-surface compositions (at%) of PTFE Teflon after Various Electron Treatments

	F	C	F/C
as entered	66.5	33.5	1.99
e^- 2 h	58.5	41.5	1.41
e^- 25 h	60.8	39.2	1.55
O_2 20 min	60.5	39.5	1.53
O_2 90 min	60.6	39.4	1.54
e^- 48 h	59.7	40.3	1.48

Table 2-2. Near-surface compositions (at%) of PTFE Teflon after Various He^+ Treatments

	F	O	C	F/C	O/C
as entered	67.4	0.0	32.6	2.07	0.0
0.5 keV He^+ 1 h	68.5	0.0	31.5	2.18	0.0
He^+ 2 h	64.1	0.0	35.9	1.79	0.0
He^+ 4 h	60.2	0.0	39.8	1.51	0.0
He^+ 8 h	75.8	0.0	42.2	1.37	0.0
He^+ 10 h	57.4	0.0	42.6	1.35	0.0
O_2 20 min	59.2	0.0	40.8	1.45	0.0
He^+ 15 h	55.9	0.0	44.1	1.27	0.0
He^+ 19 h	52.9	0.0	47.1	1.12	0.0
Air 90 min	48.9	1.9	49.2	0.99	0.04

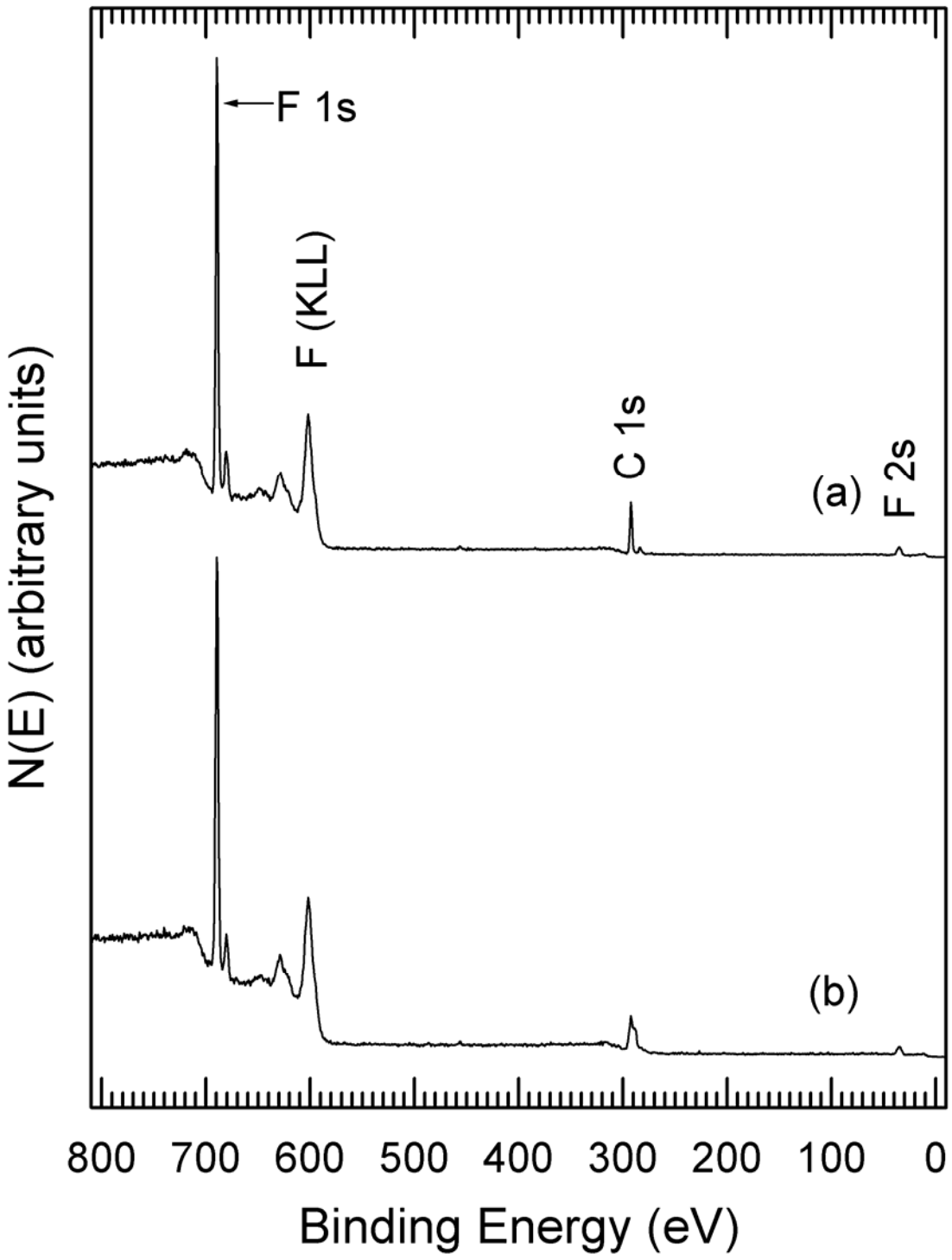

Figure 2-1. XPS survey spectra obtained from electron-exposed PTFE Teflon (a) as entered and (b) after a 2-h exposure to electrons.

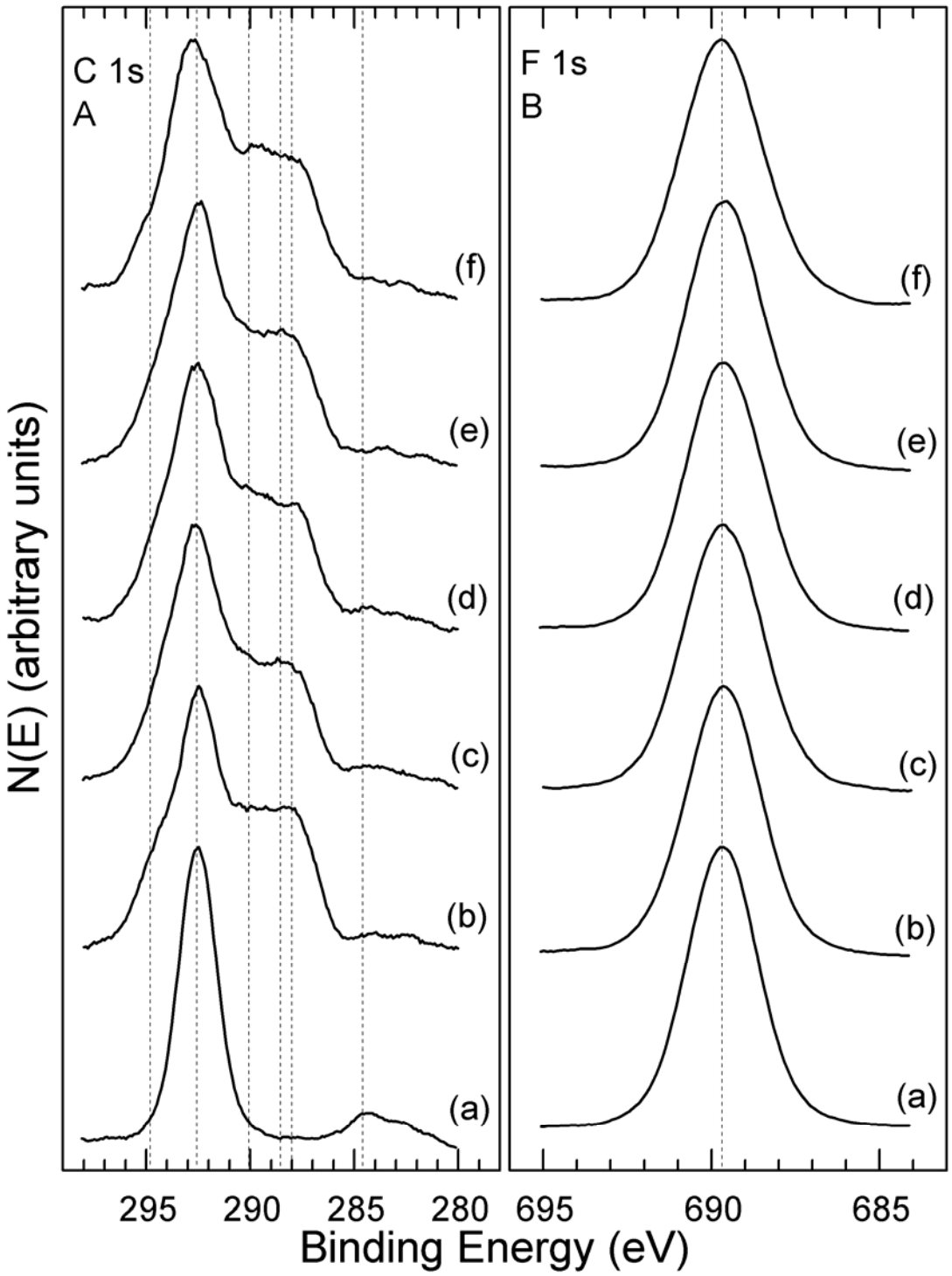

Figure 2-2. High-resolution XPS obtained from electron-exposed PTFE Teflon (A) C 1s and (B) F 1s (a) as entered, (b) after exposure to electrons for 2 h, (c) after exposure to electrons for a total of 25 h, (d) after exposure to research-grade O_2 at room temperature and 120 Torr for 20 min, (e) after exposure to research-grade O_2 at room temperature and 760 Torr for 90 min, (f) after exposure to electrons for a total of 48 h.

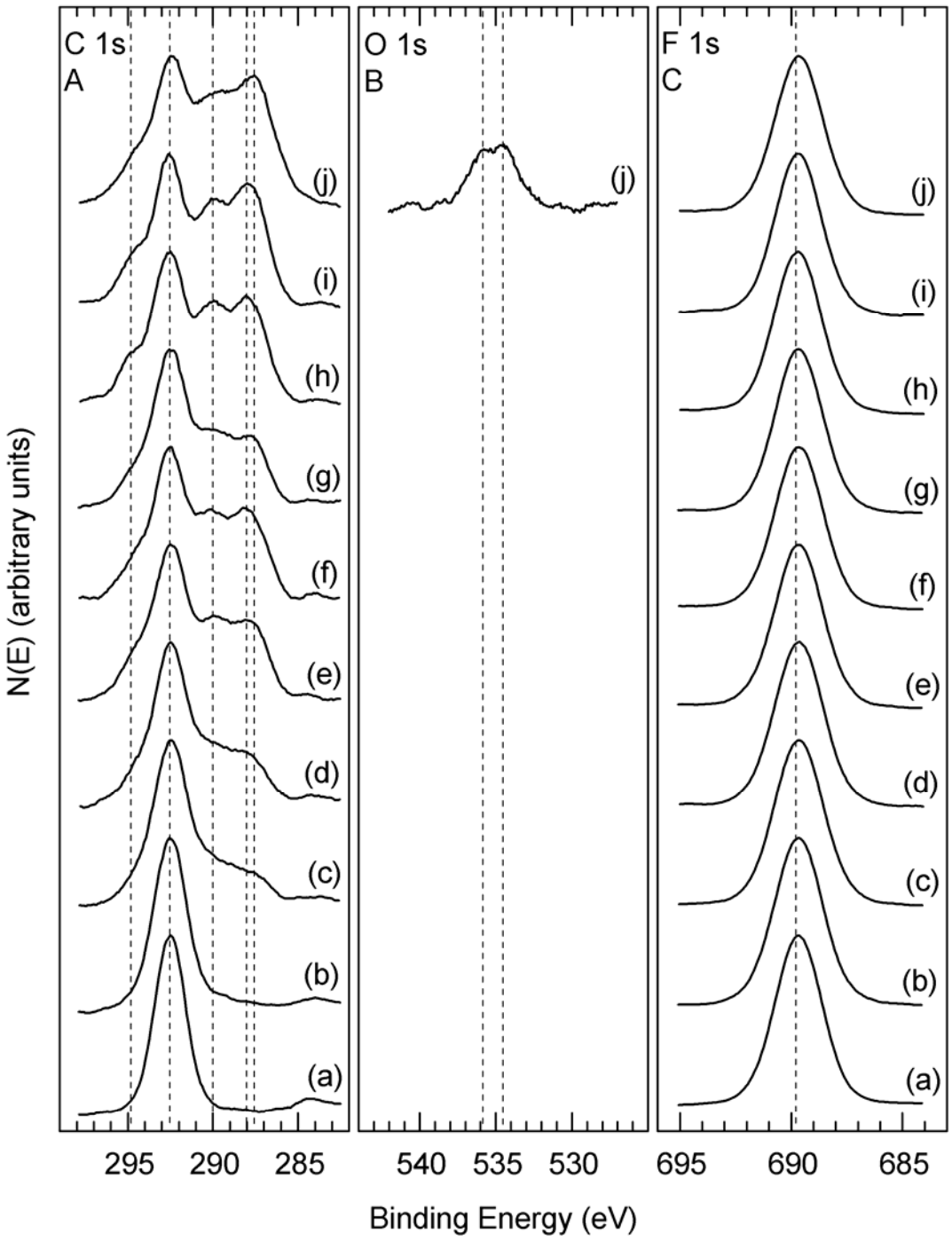

Figure 2-3. High-resolution XPS obtained from He^+-exposed PTFE Teflon (A) C 1s, (B) O 1s and (C) F 1s (a) as entered, (b) after exposure to 0.5 keV He^+ for 1 h, (c) after exposure to 1.0 keV He^+ for 2 h, (d) after exposure to He^+ for a total of 4 h, (e) after exposure to He^+ for a total of 8 h, (f) after exposure to He^+ for a total of 10 h, (g) after exposure to research-grade O_2 at room temperature and 150 Torr for 20 min, (h) after exposure to He^+ for a total of 15 h, (i) after exposure to He^+ for a total of 19 h and (j) after exposure to air for 90 min at room temperature.

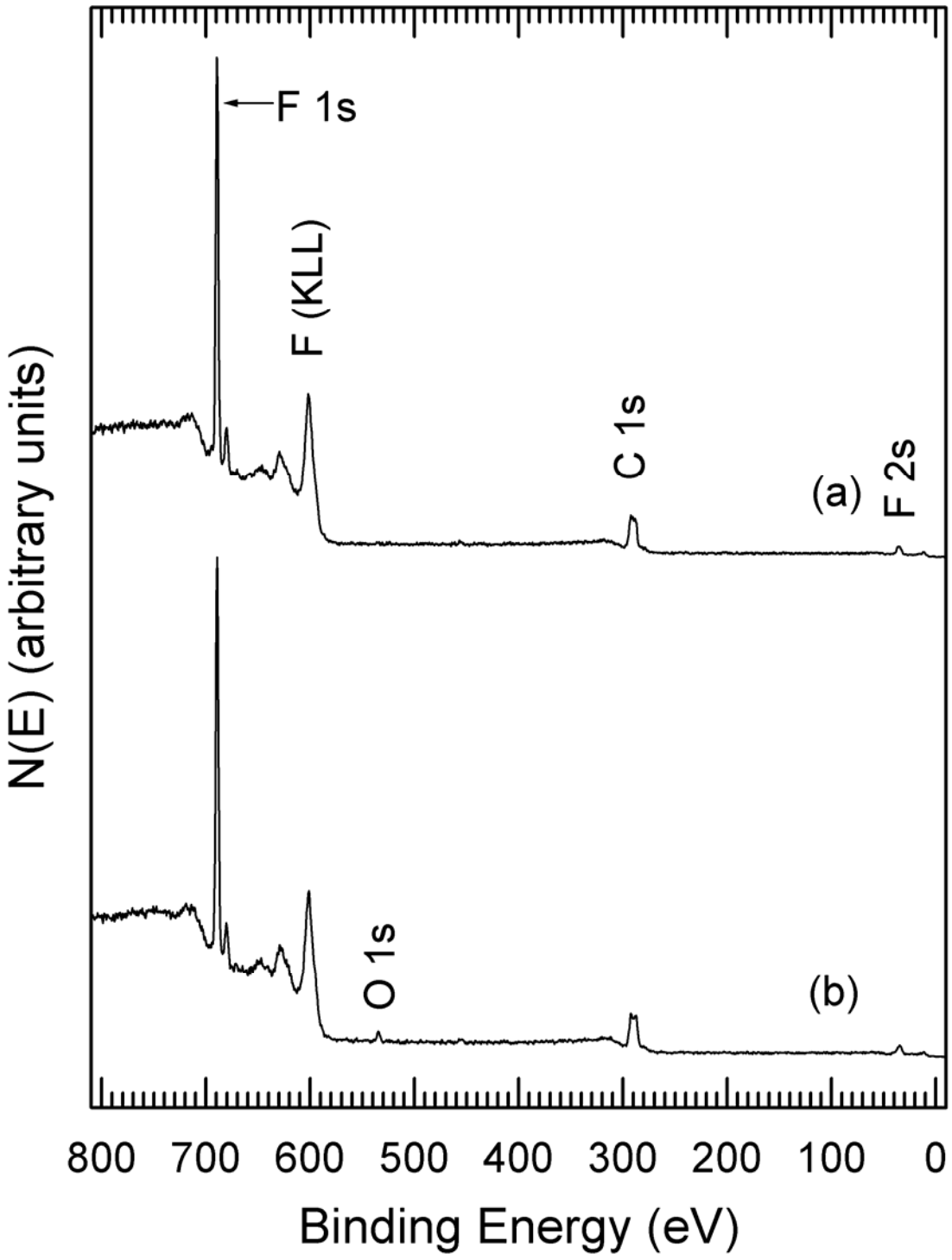

Figure 2-4. XPS survey spectra obtained from He^+-exposed PTFE Teflon (a) after a 19-h exposure to He^+ and (b) after a 90-min exposure to air at room temperature.

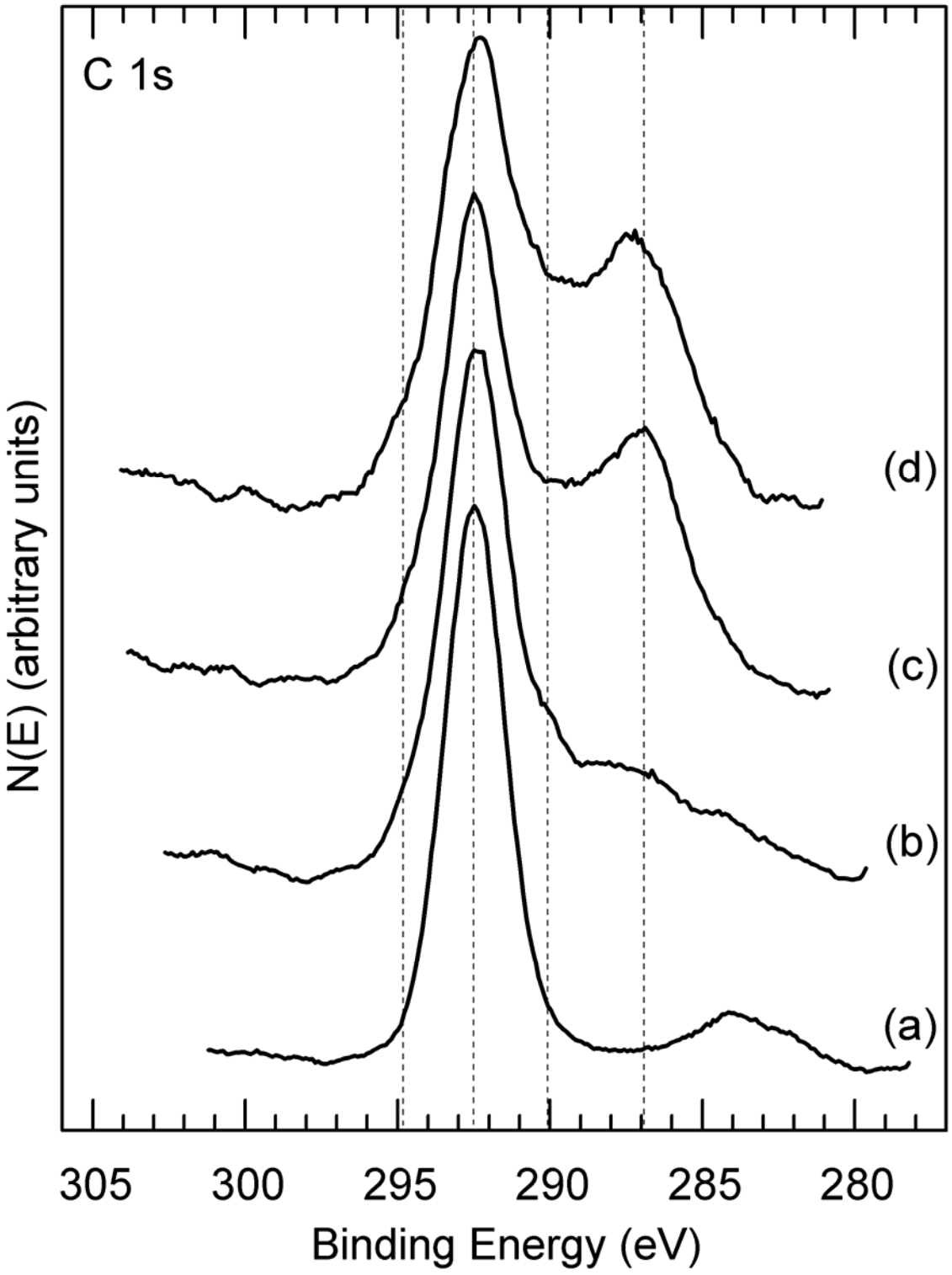

Figure 2-5. High-resolution XPS C 1s spectra obtained from Ar^+-exposed PTFE Teflon (a) as entered, (b) after exposure to 1 keV Ar^+ for 1 h, (c) after exposure to 1 keV Ar^+ for 8 h and (d) after exposure to research-grade O_2 at room temperature and 150 Torr for 20 min.

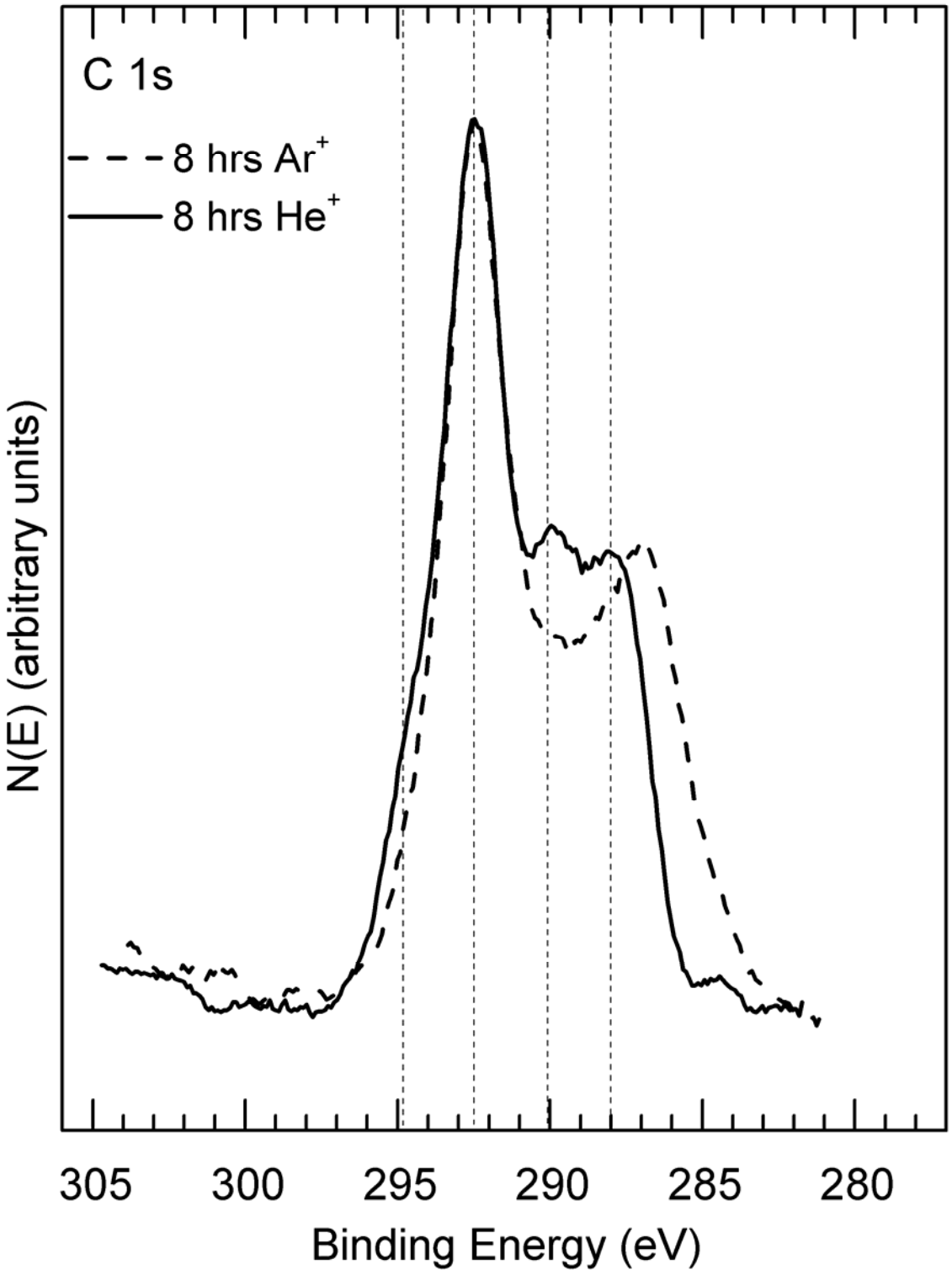

Figure 2-6. High-resolution XPS C 1s spectra obtained from PTFE Teflon after exposure to 1 keV He^+ for 8 h compared to C 1s spectra obtained after exposure to 1 keV Ar^+ for 8 h.

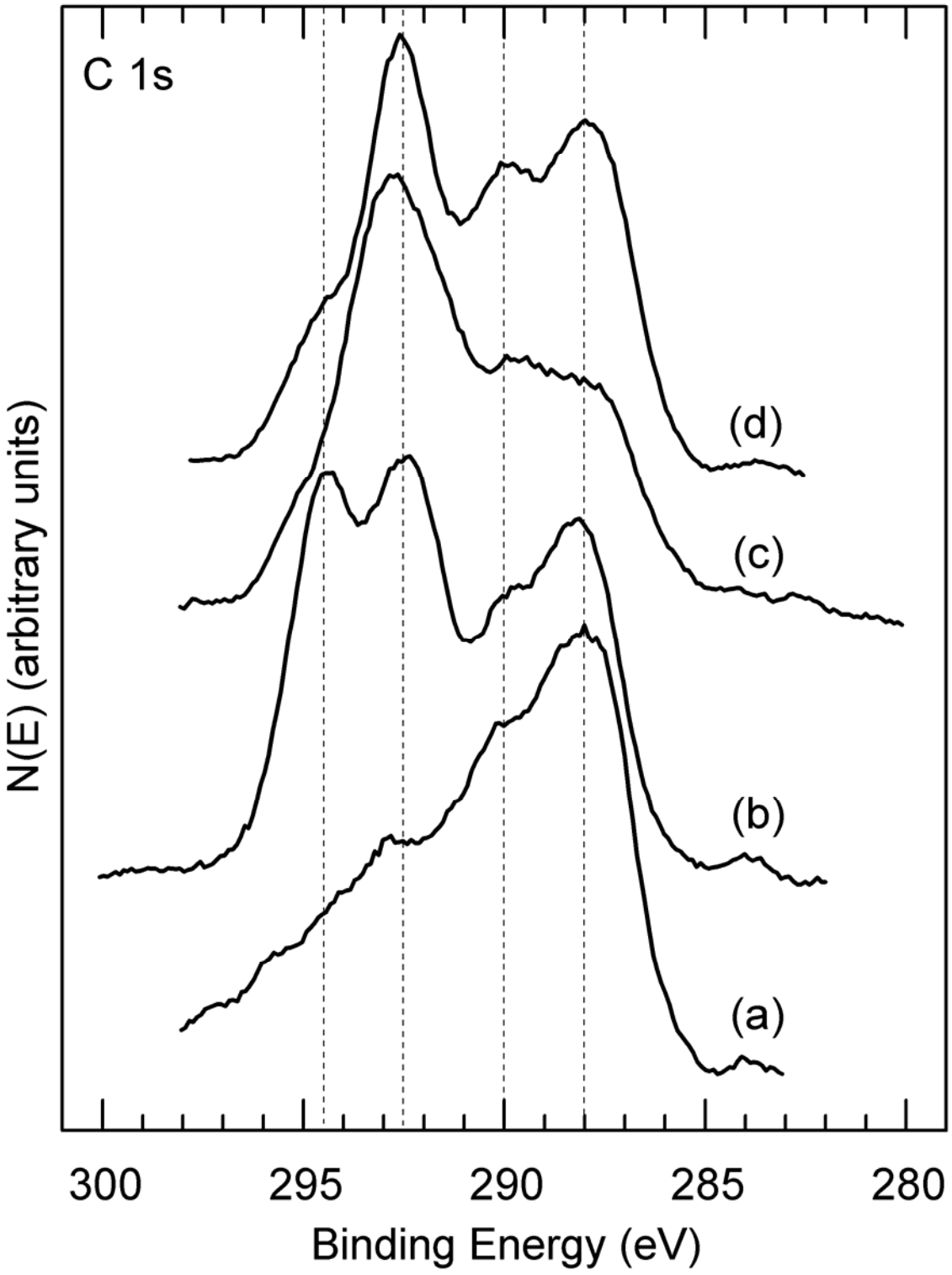

Figure 2-7. High-resolution XPS C 1s spectra obtained from PTFE Teflon after various exposures: to (a) AO for 74 h, (b) VUV for 74 h, (c) 1-keV e^- for 48 h and (d) 1-keV He^+ for 19 h. These spectra are all steady state because longer exposures do not result in different spectra.

CHAPTER 3
CHEMICAL ALTERATION OF POLY (VINYL FLORIDE) TEDLAR INDUCED BY HYPERTHERMAL ATOMIC OXYGEN

One of the main constituents in LEO is hyperthermal AO, which is known to degrade polymers. In this study XPS was used to characterize the surface of a Tedlar film before and after exposures of varying lengths to AO, as well as O_2 and air. The goal of the study was to determine how hyperthermal AO affects the Tedlar surface so that a better understanding of its space survivability can be obtained.

This chapter reprinted from Applied Surface Science, Volume 239, G.B. Hoflund and M.L. Everett, Title, pp 367-375, Copyright 2005 with permission from Elsevier.

Experimental

An as-received E.I. du Pont Nemours & Co., Inc. Tedlar film was wiped with methanol and inserted into the UHV chamber (base pressure $<1.3 \times 10^{-10}$ Torr). XPS measurements were performed using a double-pass cylindrical mirror analyzer (DPCMA) (PHI Model 25-270AR). XPS survey spectra were taken in the retarding mode with a pass energy of 50 eV, and high-resolution XPS spectra were taken with a pass energy of 25 eV using Mg $K\alpha$ X-rays (PHI Model 04-151 X-ray source). Data collection was accomplished using a computer interfaced, digital pulse-counting circuit [28] followed by smoothing with digital-filtering techniques [29]. The sample was tilted 30 degrees off the axis of the DPCMA, and the DPCMA accepted electrons emitted into a cone 42.6 ± 6 degrees off the DPCMA axis.

XPS spectra were first obtained from the as-entered, solvent-cleaned sample. The sample was then transferred via a magnetically coupled rotary/linear manipulator into an adjoining UHV chamber that houses the ESD AO source described in Chapter 1. There the surface was exposed to a hyperthermal AO flux and re-examined after various exposure times. The samples were not exposed to air after the AO exposures and before collecting XPS data. However, after the AO

exposures the surfaces were exposed to O_2 or air to determine how this would affect the AO-exposed surfaces. The approximate normal distance between the sample face and source in this study was 15 cm, at which distance the flux was about 2.0 x 10^{15} atoms/cm^2-s for the instrument settings used. The sample was maintained at room temperature during the AO exposures with a temperature increase to 50°C due to exposure to the X-ray source during XPS data collection. The substrate temperature was determined using a chromel-alumel thermocouple. Polymer structural repeat units, F-to-C ratios and reference XPS binding energies (BEs) used in this study are given in Table 3-1.

Results and Discussion

XPS survey spectra obtained from the as-entered Tedlar before and after 2 h of AO exposure are shown in Figure 3-1a and b respectively. The predominant peaks apparent in these spectra include the C 1s, O 1s, O Auger (KLL), F 1s, F Auger (KLL) and F 2s. Significant changes in relative peak heights are observed for the C and F features following the AO exposure. Estimates of the near-surface compositions have been made from the peak areas in the high-resolution spectra using published atomic sensitivity factors [31] with the assumption of a homogeneous surface region. XPS probes the near-surface region of the sample and yields a weighted average composition with the atomic layers near the surface being weighted more heavily since the photoemitted electrons from these layers have a lower probability of scattering inelastically. The sampling depth is ~4-6 nm, and ~10% of the signal originates from the outermost atomic layer [32]. This near-surface region is nonhomogeneous because the AO reacts most strongly with the outermost few atomic layers. Therefore, the region that reacts to the greatest extent with AO also makes the largest contribution to the XPS signal. This fact implies that XPS is an excellent technique for studying AO erosion of spacecraft materials. Even though the distribution functions involving the depth of chemical reactions in the near-surface

region and the XPS determination of the weighted average composition of the near-surface region are complex, the compositional values provide a trend which is indicative of the chemical alterations occurring during AO exposure.

The compositions determined using the homogeneous assumption are shown in Table 3-2 before and after various exposures to AO and O_2 or air. The F/C atom ratio obtained from the as-entered sample is 0.45 which is close to the stoichiometric value of 0.5. The near-surface region also contains about 7.2 at% of O giving an O/C atom ratio of 0.11. The source of this surface O is not known. It may have accumulated during preparation of the Tedlar, and it may be present in the bulk of the polymer.

After a 2-h AO exposure (survey spectrum shown in Figure 3-1b), the F/C atom ratio is decreased from 0.45 to 0.018: i.e., nearly all of the F is removed from the near-surface region, and the O/C atom ratio is significantly reduced from 0.11 to 0.04. Furthermore, the chemical composition of the outermost 30-50 Å consists of 94.2 at% C. The major constituent of stoichiometric Tedlar would be hydrogen at 50 at%. Unfortunately, XPS is relatively insensitive to H because it has no core level electrons. Therefore, H is not measured although it is certainly present at least initially. Both AO and H are highly reactive. AO most likely reacts with H in the near-surface region to form H_2O, which desorbs leaving the carbonaceous layer. The structure of this carbonaceous layer has not been determined and most likely is quite complex. It may be partially graphitic, and it may contain amorphous regions as well as double and triple and unsaturated bonds. It may be considered to be a charcoal-like layer produced after just 2 h of AO exposure. All further experiments are carried out on this layer and not on a Tedlar layer. The XPS spectrum obtained after a 24-h AO exposure (Figure 3-2a) is quite similar to that obtained after the 2-h AO exposure. According to the compositional data in Table 3-2, the F

content is similar, but the O content is slightly increased. This is probably due to adsorption of O at unsaturated bonds formed by further erosion of the C-rich layer.

After exposure of this surface to O_2 at 150 Torr and room temperature for 20 min, the XPS O 1s peak is clearly increased (Figure 3-2b). The compositional data in Table 3-2 indicate that the O/C at ratio is increased from 0.07 to 0.12. This increase is due to dissociative chemisorption of O_2 at reactive sites formed during the erosion process. The amount of O_2 adsorbed provides a measure of the concentration of reactive sites formed during AO exposure. A charcoal or graphite surface would not adsorb any O_2 under these exposure conditions. The O_2-exposed surface was then exposed to AO for an additional 1 h (25 h total) and another 2 h (27 h total). The resulting XPS survey spectra are shown in Figure 3-3a and b respectively. The O 1s peak is decreased in size relative to the C 1s peak. This is supported by the compositional information in Table 3-2 in which the O/C at ratio decreases from 0.12 to 0.07. Furthermore, the F/C atom ratio increases from 0.012 to 0.018. The O/C and F/C atom ratios are quite similar to those obtained after the 24-h AO exposure.

Then the surface was exposed to air at room temperature for 90 min. The XPS survey spectrum obtained after this treatment is shown in Figure 3-4a. The O 1s feature is quite large again relative to the C 1s peak. The F/C and O/C atom ratios have values of 0.012 and 0.12 respectively which are identical to those obtained after the 20-min O_2 exposure. This fact indicates that the O_2 and air exposures are equivalent in that both exposures are large enough to saturate the AO-exposed surface with O. Next the surface was exposed to AO for an additional 43 h (70 h total). The XPS survey spectrum obtained from this surface (Figure 3-4b) has an O 1s feature which is reduced to about one-half the size of that of the air-exposed surface. The compositional data indicate that the O/C atom ratio is decreased from 0.12 to 0.08. This value is

slightly higher than the value of 0.7 attained after AO exposures because the F content continues to decrease during the long AO exposure. It attains a value of 0.6 at% in the near-surface region with a F/C atom ratio of 0.006.

The high-resolution XPS C 1s, O 1s and F 1s features are shown in Figure 3-5A, B and C respectively. The C 1s feature obtained from the as-entered Tedlar (Figure 3-5Aa) consists of two peaks with maxima at 285.7 and 287.9 eV. This is consistent with reference spectra obtained from Tedlar [30]. The feature at 285.7 eV is assigned as due to C bonded as $-\overset{H}{\underset{H}{\overset{|}{\underset{|}{C}}}}-$, and the feature at 287.9 eV is assigned to C bonded as $-\overset{F}{\underset{H}{\overset{|}{\underset{|}{C}}}}-$. The peaks should be the same size since these two types of C are present in stoichiometric Tedlar in equal amounts, and this is the case in the reference spectra [30]. Stoichiometric Tedlar also contains no O. The as-entered sample in this study contained about 7 at%. This O is most likely bonded in the near-surface region as C-OH groups, which have a C 1s binding energy (BE) of about 286.5 eV [30]. The presence of these groups adds structure to the lower BE feature thereby increasing its intensity. It seems reasonable that $F-\overset{|}{\underset{|}{C}}-OH$ groups would have a higher C 1s BE than $F-\overset{|}{\underset{|}{C}}-H$ groups. Since features are not apparent at BEs above 289 eV,

$F - \overset{|}{C} - H$ species are not present. The O 1s feature obtained from the as-entered Tedlar

(Figure 3-5Ba) is consistent with the assertions above. The peak is symmetrical. This fact is consistent with the presence of only one chemical state of O. Furthermore, the BE of this peak is 532.9 eV which is the median of the narrow range (ΔE = 0.35 eV) reported by Beamson and Briggs [30]. The F 1s peak is also symmetrical with a BE of 686.9 eV. This is characteristic of

F in $- \overset{F}{\overset{|}{C}}\overset{|}{H} -$ groups [30].

The C 1s, O 1s and F 1s spectra obtained after the 2-h AO exposure are shown in Figure 3-5Ab, 3-5Bb and 3-5Cb respectively. The C 1s feature consists of a single symmetrical peak with a BE of 284.6, which is characteristic of a graphitic or an amorphous charcoal-like C film. This is reasonable since the near-surface region contains 94.2 at% C and small amounts of O and F (Table 3-2). By comparing Figures 3-5Ba and 3-5Bb, it is apparent that the chemical nature of O in the near-surface region is changed by the 2-h AO exposure. This exposure decreases the O concentration from 7.2 to 4.0 at%. The chemical state at 532.9 eV is reduced in intensity while chemical states with BEs in the range from 530.6 to 532.3 eV are formed. The chemical nature of these O species is not known, but they may be C-O-C, C-OH or C=O groups [30]. The fact that these AO-exposed surfaces are quite damaged makes species assignment very difficult. The F 1s peak is greatly decreased in size (the F/C at ratio is reduced from 0.45 to 0.018), and it is broadened toward lower BEs with a distinct shoulder at about 684.5 eV. These values are lower

than any reported F 1s values for organic materials containing F. One possibility is that the F may be interacting with O, H or C with broken bonds.

The various chemical species observed for C, O and F after the 2-h AO exposure are observed after all the various treatments but in different relative amounts. The C 1s feature does not change shape or position with any of the treatments. This is reasonable since in each case the C content is near 90 at%. The changes in the O 1s feature with the various treatments are more prominent. At least four O species are present after the 24-h AO exposure. After the 20-min O_2 exposure, the O 1s feature is symmetrical but broadened around the species with a BE of 532.3 eV. This is quite likely due to a C=O species formed by dissociative chemisorption of O_2 at reactive C sites. After another 1 h and 3 h of AO exposure the higher BE and lower BE features become more prominent until the shape of the O 1s feature (Figure 3-5Bf) is quite similar to that obtained after the 24-h AO exposure (Figure 3-5Bc). Then the sample was exposed to air for 90 min. The O 1s feature obtained after this treatment (Figure 3-5Bg) is quite similar to that obtained after the 20-min O_2 exposure (Figure 3-5Bd) except that it is more narrow indicating the predominance of the 532.3-eV chemical state. After another 47-h AO exposure, the shape of the O 1s feature (Figure 3-5Bh) becomes characteristic of an AO-exposed surface. The F 1s feature after AO exposure is difficult to interpret for two reasons. The F concentration is quite low ranging from 0.6 to 2.0 at% thereby yielding small peaks, and the peaks apparent do not correspond with previously assigned species. In a very short period (<2 h), the F/C atom ratio is decreased from 0.45 to 0.018 and then remains small throughout the rest of the study.

Summary

In this study a Tedlar film has been exposed to a flux of $2x10^{15}$ atoms/cm^2-s of 5-eV AO for various times, and the chemical alterations at the surface have been monitored using XPS. After a 2-h exposure, the F/C and O/C atom ratios decrease from 0.45 and 0.11 to 0.018 and 0.04

respectively. Nearly all of the F is removed, the O content is decreased from 7.2 to 4.0 at% and the C content is increased from 63.7 to 94.2 at%. This AO exposure transforms the near-surface region of Tedlar into a carbonaceous layer, which may be graphitic or amorphous. This is also confirmed by the high resolution C 1s spectra which show that the two C 1s features characteristic of Tedlar are converted to a single peak characteristic of amorphous or graphitic carbon. Although hydrogen cannot be detected in the XPS spectra, it most likely reacts rapidly with the AO to form water, which desorbs. Longer AO exposures do not significantly alter the chemical composition or nature of the carbonaceous film. This film is certainly attacked chemically by AO to form CO and/or CO_2 resulting in erosion, but the erosion rate has not been determined in this study. Based on the XPS data, the thickness of the carbonaceous film is at least 5 nm.

Exposure of the AO-exposed carbonaceous film to either O_2 or air increases the oxygen content of the near-surface region by about 60%. The oxygen adsorbs at reactive sites formed during AO exposure. These reactive sites most likely do not cross bond due to geometrical bond constraints. The amount of O_2 that chemisorbs provides a measure of the concentration of these reactive sites in the near-surface region. Further exposure to AO removes this chemisorbed oxygen to the level prior to the O_2 or air exposure.

Table 3-1. Polymer Name, XPS Binding Energies, F/C Ratio and Structure

Polymer	Binding Energy (eV)			
	C 1s		F 1s	F:C
	1	2		
Tedlar, Poly(vinyl fluoride) (PVF) $[-CH_2-CHF-]_n$	285.74	287.91	686.94	1:2

Table 3-2. Near-surface compositions of Tedlar after Various Treatments (at%)

	F	O	C	F/C	O/C
as entered	29.0	7.2	63.7	0.45	0.11
AO 2 h	1.7	4.0	94.2	0.018	0.04
AO 24 h	2.0	6.3	91.7	0.022	0.07
O_2 20 min	1.1	10.4	88.5	0.012	0.12
AO 25 h	1.3	7.0	91.7	0.014	0.08
AO 27 h	1.7	6.7	91.6	0.018	0.07
Air 90 min	1.1	10.5	88.4	0.012	0.12
AO 70 h	0.6	7.3	92.1	0.006	0.08

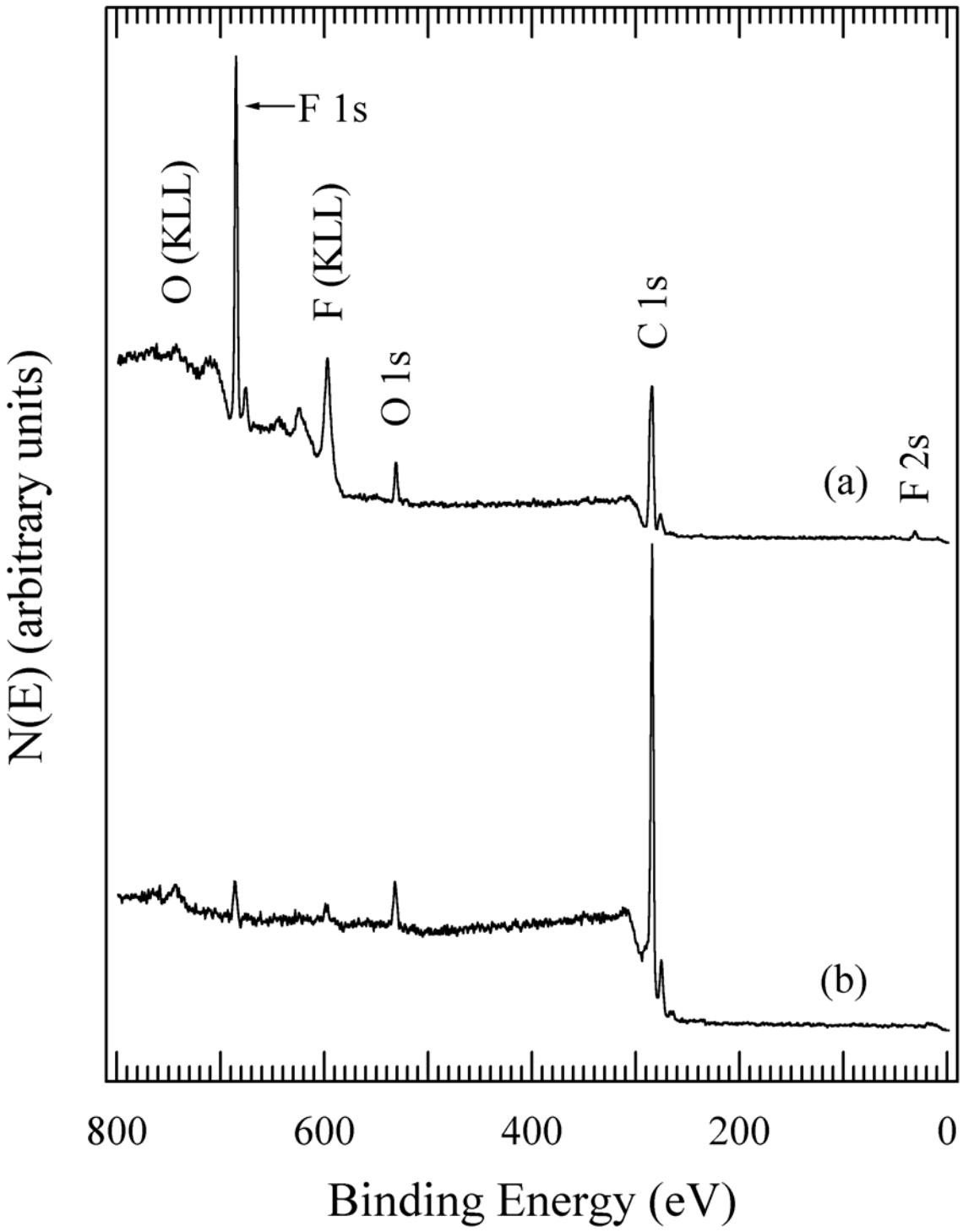

Figure 3-1. XPS survey spectra obtained from AO-exposed Tedlar (a) as entered and (b) after 2 h exposure to AO.

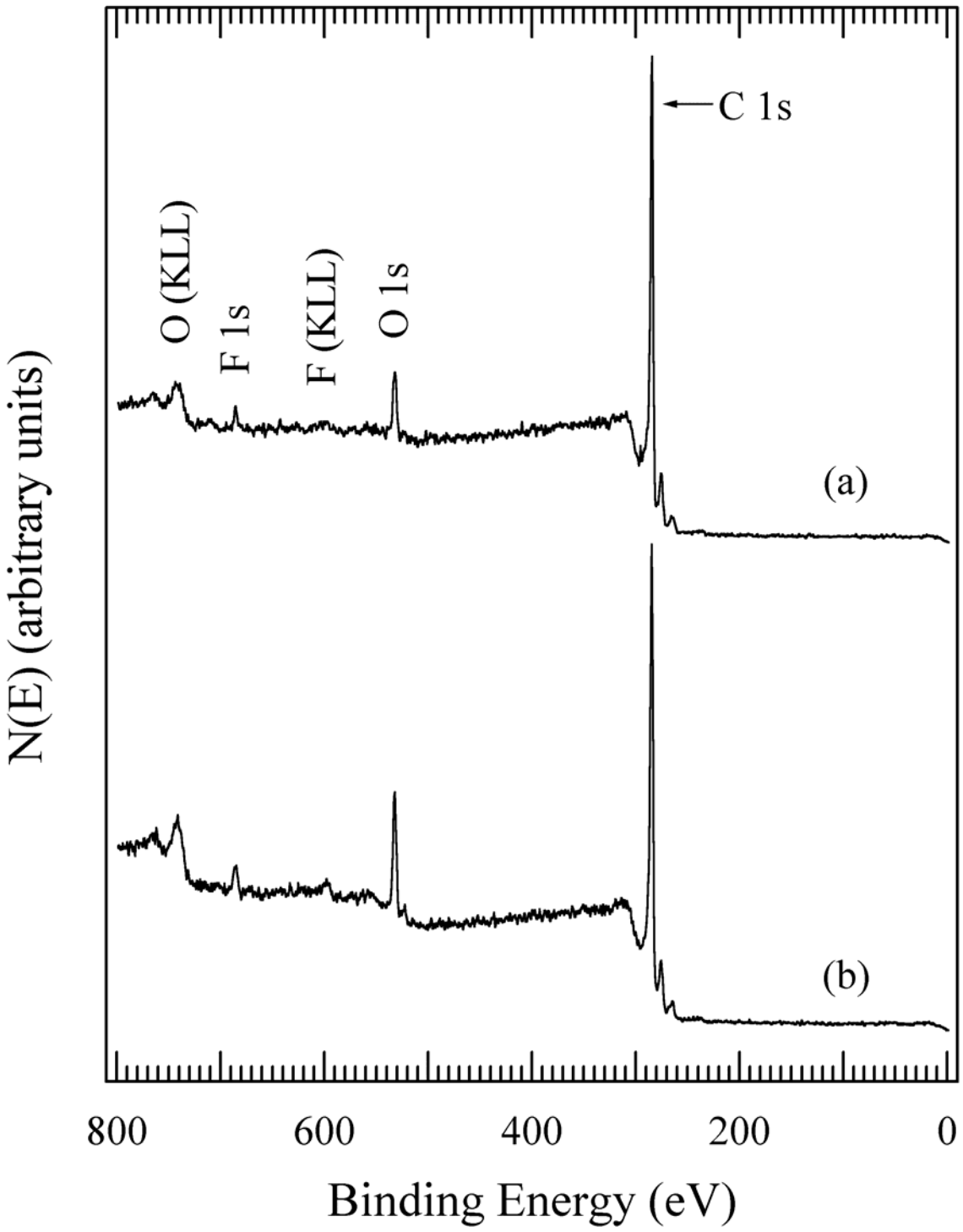

Figure 3-2. XPS survey spectra obtained from AO-exposed Tedlar (a) after 24 h exposure to AO and (b) after 20 min exposure to O_2 at 150 Torr and room temperature.

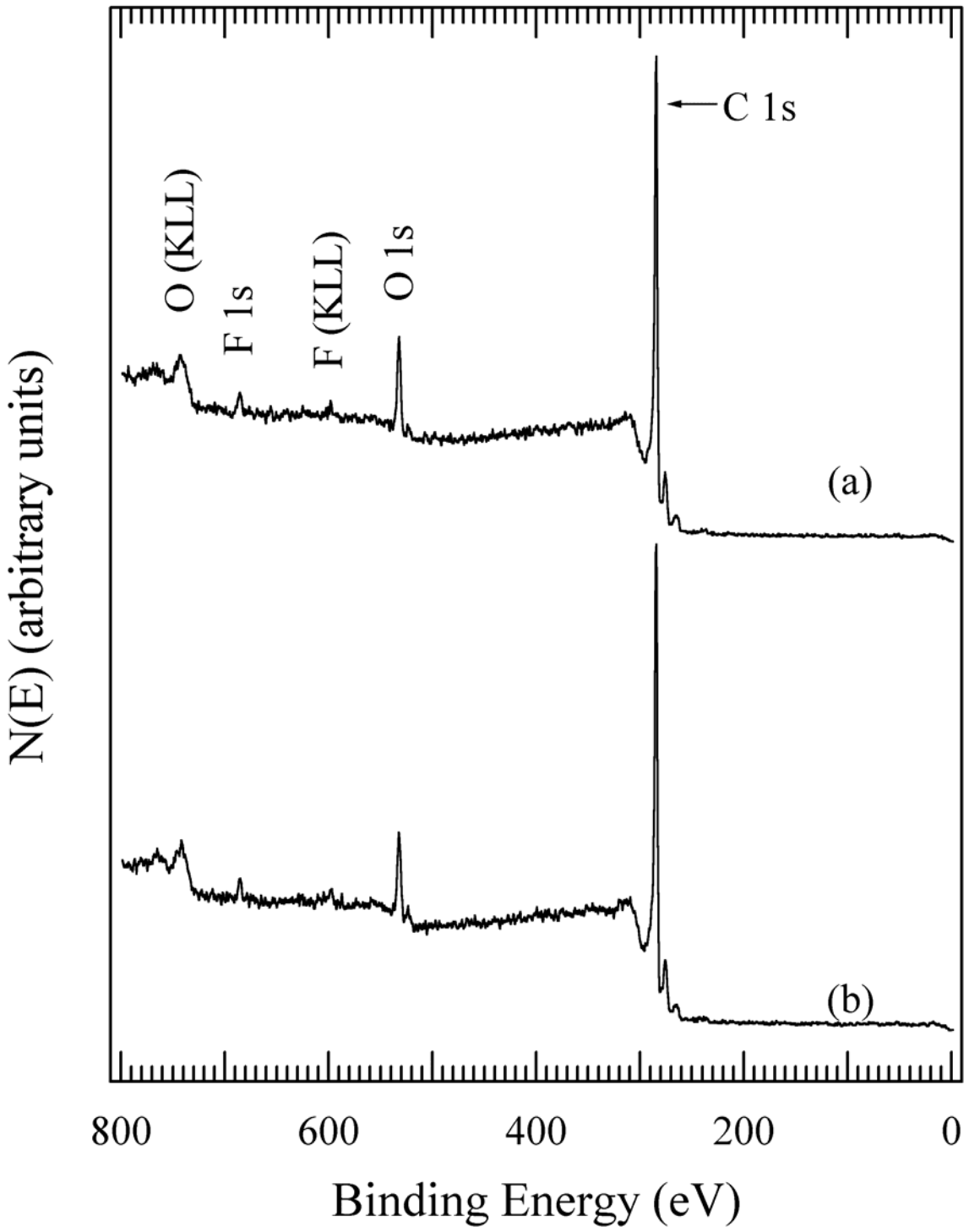

Figure 3-3. XPS survey spectra obtained from AO-exposed Tedlar (a) after 25 h exposure to AO and (b) after 27 h exposure to AO.

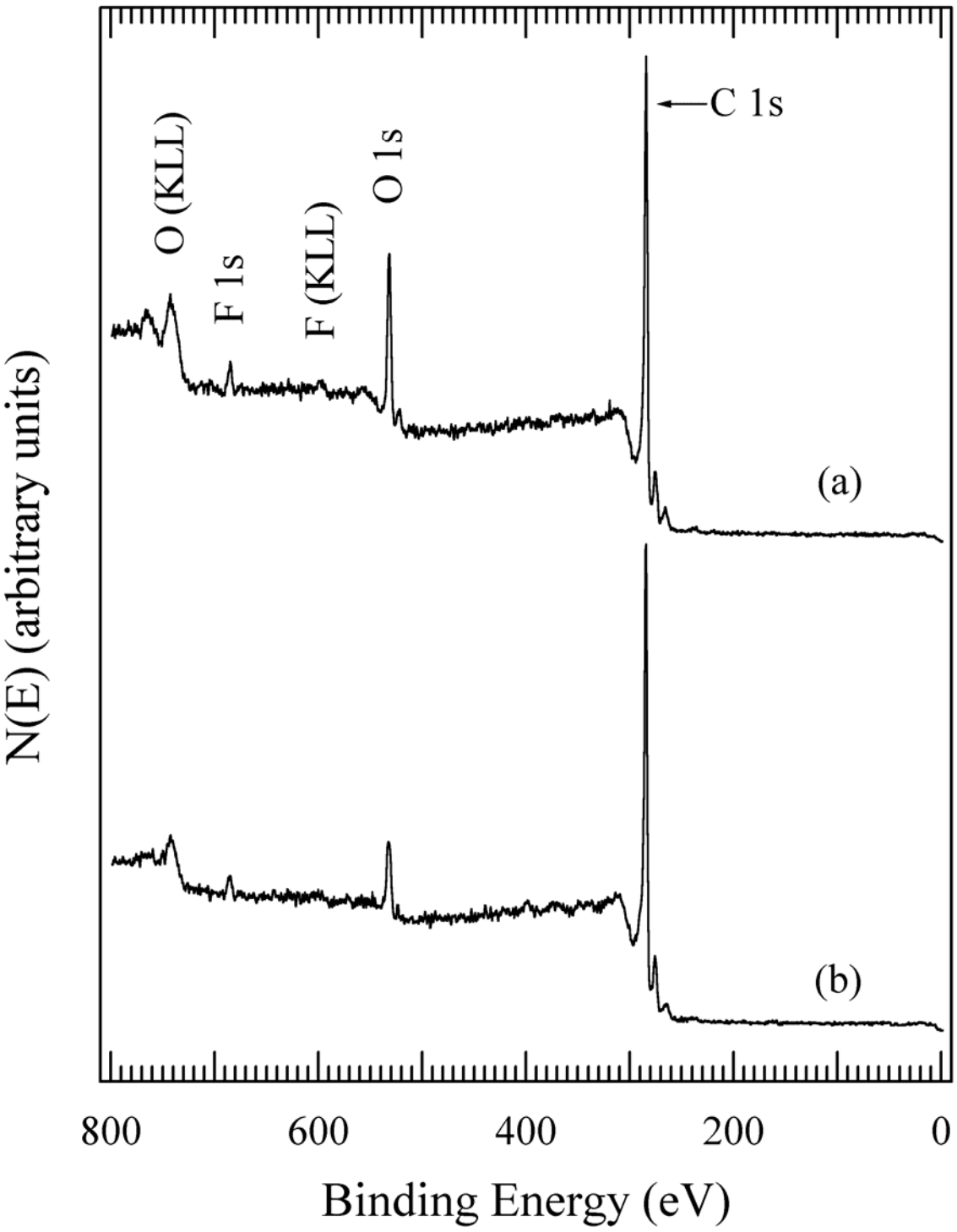

Figure 3-4. XPS survey spectra obtained from AO-exposed Tedlar (a) after air exposure for 90 min at room temperature and (b) after 70 h exposure to AO.

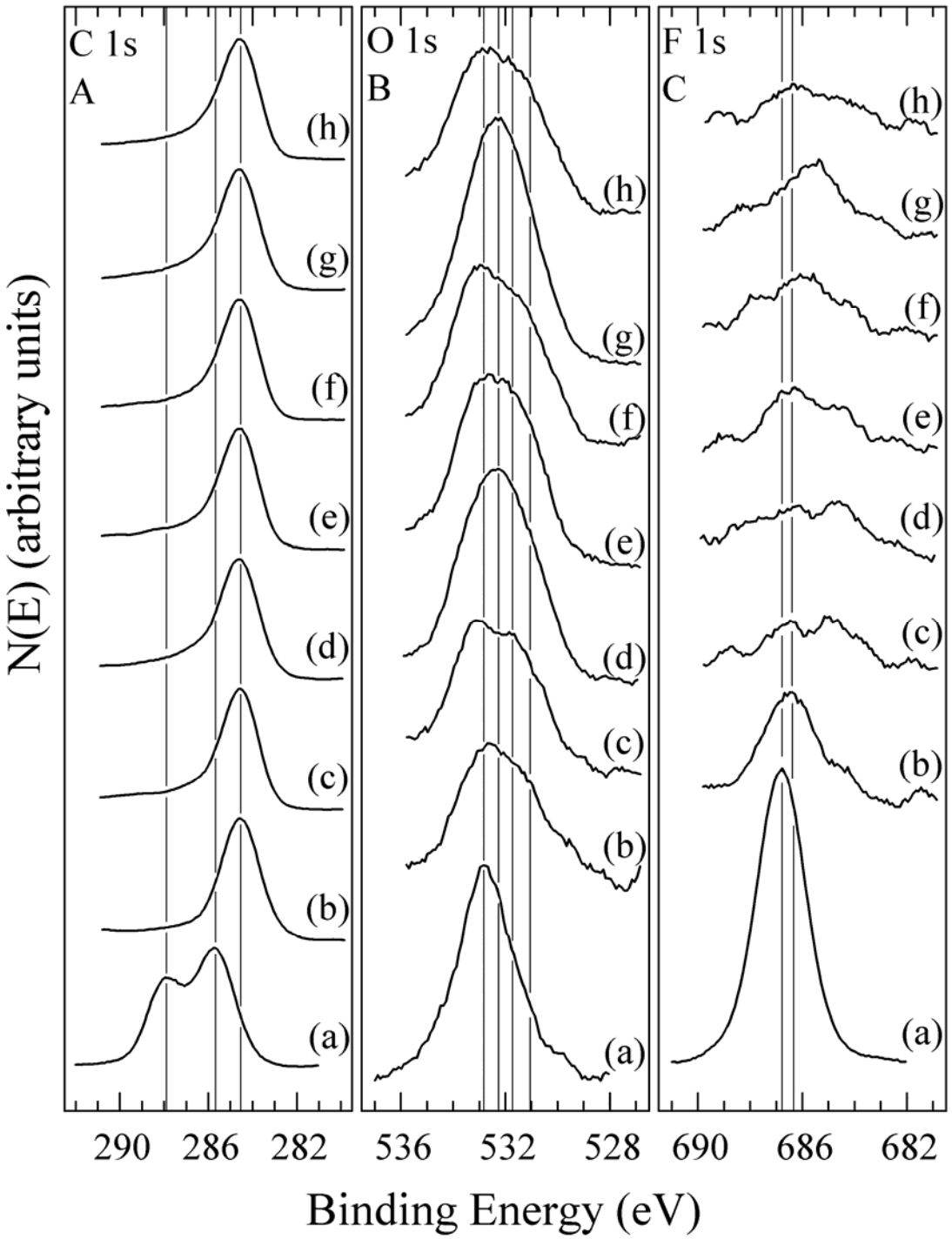

Figure 3-5. High-resolution spectra obtained from AO-exposed Tedlar (A) C 1s, (B) O 1s and (C) F 1s (a) as-entered, (b) after a 2-h AO exposure, (c) after a 24-h AO exposure, (d) after a 20-min exposure to O_2 at 150Torr and room temperature, (e) after a 25-h exposure to AO, (f) after a 27-h exposure to AO, (g) after a 90-min exposure to air at room temperature and (h) after a 70-h AO exposure.

CHAPTER 4
CHEMICAL ALTERATION OF POLY (VINYL FLUORIDE) TEDLAR INDUCED BY EXPOSURE TO VACUUM ULTRAVIOLET RADIATION

In LEO objects are subjected to the full spectrum of solar radiation. One such range of light is VUV (115-200 nm), which is known to degrade polymers. In this study XPS was used to characterize the surface of a Tedlar film before and after exposures of varying lengths to UV radiation (115-400 nm), as well as O_2 and air. The goal of the study was to determine how VUV radiation affects the Tedlar surface so that a better understanding of its space survivability can be obtained.

This chapter reprinted from Applied Surface Science, Volume 252, M.L. Everett and G.B. Hoflund, Title, pp 3789-3798, Copyright 2006 with permission from Elsevier.

Experimental

An as-received E.I. du Pont Nemours & Co., Inc. Tedlar film was wiped with ethanol and inserted into the UHV chamber (base pressure $<1.0 \times 10^{-10}$ Torr). XPS measurements were performed using a double-pass, cylindrical-mirror analyzer (DPCMA) (PHI Model 25-270AR). XPS survey spectra were taken in the retarding mode with a pass energy of 50 eV, and high-resolution XPS spectra were taken with a pass energy of 25 eV using Mg $K\alpha$ X-rays (PHI Model 04-151 X-ray source). The X-ray source was a flood source, and the DPCMA accepted photoelectrons from a spot 4 mm in diameter. The precision manipulator used allowed for analysis of the same spot after each treatment. The sample was tilted 30 degrees off the axis of the DPCMA, and the DPCMA accepted electrons emitted into a cone 42.6 ± 6 degrees off the DPCMA axis. The sample temperature was maintained at room temperature during the VUV exposures but rose to 50°C during exposure to the X-ray source according to a chromel-alumel thermocouple. The analysis chamber was pumped by a 400 l/s ion pump, a 180 l/s

turbomolecular pump and a 4000 l/s cryopump containing a Ti sublimation system. The pressure was maintained at ~$2x10^{-10}$ Torr during collection of XPS data. Under these conditions carbon contamination did not accumulate on the surfaces studied. Data collection was accomplished using a computer-interfaced, digital-pulse-counting circuit [28] followed by smoothing with digital-filtering techniques [29]. Charging did not present a diffuculty in this study. The spectrum taken from Tedlar was shifted so that the C 1s and F 1s peaks were at the same binding energies (BEs) of reference spectra [30]. All other spectra were shifted by this same value.

XPS spectra were first obtained from the as-entered, solvent-cleaned sample. The sample was then transferred into an adjoining UHV chamber that houses the VUV source via a magnetically coupled rotary/linear manipulator. This chamber contains a 120 l/s ion pump, which produces a base pressure in the low 10^{-9} Torr range during operation of the VUV source. An atomic oxygen (AO) source is also housed in this chamber. This chamber is kept very clean because AO reacts with any contamination to form products, which are pumped away. Many experiments have been performed including the oxidation of a cleaned Si(111) surface by AO which demonstrates that hydrocarbon contamination does not accumulate at surfaces in this chamber. This also keeps the VUV source window clean so periodic cleaning with diamond paste was not necessary. There the surface was exposed to a VUV radiation and re-examined after various exposure times. The samples were not exposed to air after the VUV exposures and before collecting XPS data. However, after the VUV exposures the surfaces were exposed to O_2 or air to determine how this would affect the VUV-exposed surfaces. The specific treatments used were (1) exposure to VUV for 2 h, (2) exposure to VUV for a total of 24 h, (3) exposure to research-grade O_2 at room temperature and 1 atm for 20 min, (4) exposure to VUV for a total of

27 h, (5) exposure to VUV for a total of 29 h, (6) exposure to air for 11 h at room temperature and (7) exposure to VUV for a total of 31 h. XPS spectra were collected after each treatment.

Results and Discussion

XPS survey spectra obtained from the Tedlar film before and after a 2-h VUV exposure are shown in Figure 4-1a and b respectively. Spectrum a matches that shown in the polymer XPS handbook by Beamson and Briggs [30] in that the C 1s, O 1s, F 1s, F Auger (KLL) and F 2s peaks are present. The O 1s peak, which appears near a binding energy (BE) of 530 eV, is present in a larger quantity than in the reference spectrum provided by Beamson and Briggs. Estimates of the near-surface compositions have been made from the peak areas in the high-resolution spectra using published atomic sensitivity factors [32] with the assumption of a homogeneous surface region. XPS probes the near-surface region of the sample and yields a weighted average composition with the atomic layers near the surface being weighted more heavily since the photoemitted electrons from these layers have a lower probability of scattering inelastically. The sampling depth is ~4-6 nm, and ~10% of the signal originates from the outermost atomic layer [32]. This near-surface region is nonhomogeneous because the VUV radiation reacts most strongly with the outermost few atomic layers. Therefore, the region that reacts to the greatest extent with VUV radiation also makes the largest contribution to the XPS signal. This fact implies that XPS is an excellent technique for studying erosion of spacecraft materials by VUV radiation. Even though the distribution functions involving the depth of chemical reactions in the near-surface region and the XPS determination of the weighted average composition of the near-surface region are complex, the compositional values provide a trend which is indicative of the chemical alterations occurring during VUV exposure. The compositions determined using the homogeneous assumption are shown in Table 4-1 before and after various exposures to VUV radiation, O_2 and air. The F/C atom ratio obtained from the as-

entered sample is 0.34, which is less than the stoichiometric value of 0.50. This difference could be attributed to C contamination from hydrocarbons and the presence of surface oxygen.

After a 2-h VUV exposure (survey spectrum shown in Figure 4-1b), the F/C atom ratio is decreased from 0.34 to 0.17: i.e., about 50% of the F is removed from the near-surface region by this short exposure. None of the C, O, or F features appear to change shapes or positions in the survey spectra obtained before and after the 2-h VUV exposure. These changes are more apparent in the high-resolution spectra shown in Figure 4-2. The C 1s, O 1s and F 1s features obtained from the as-entered Tedlar are shown in Figure 4-2Aa, 4-2Ba and 4-2Ca respectively and in Figure 4-2Ab, 4-2Bb and 4-2Cb for the surface exposed to VUV for 2 h. The C 1s feature obtained from the as-entered Tedlar consists of two narrow peaks with a BEs of 285.7 and 287.9 eV. It is also broadened toward the low-BE side possibly due to the presence of hydrocarbon contamination. The two peaks overlap each other more so than in the reference spectrum. The F 1s feature is a single, well-defined peak centered at 686.9 eV, which also matches the reference spectrum. The O 1s feature is a broad peak centered about 532.7 eV.

The C 1s feature obtained after the 2-h VUV exposure consists of a predominant peak centered at 285.2 eV, and the feature at 287.9 eV is reduced to a small, broad hump on the high-BE side of the larger peak. Assigning the peaks to specific species is quite difficult for several reasons. As explained in Chapter 2, defining localized species, which yield features at specific BEs, is difficult and may not be possible. Since there are distinct peaks in these spectra, there are distinct chemical environments, but defining the nature of this chemical environment may not be possible. Furthermore, the VUV-exposed surface is a damaged surface in that the composition is altered to a great extent and the structure is most likely altered in the manner

discussed below. The O 1s feature becomes a less defined peak as the chemisorbed oxygen is removed from the surface. Also the F 1s peak is reduced in size.

An XPS survey spectrum obtained from the Tedlar surface after a 24-h VUV exposure is shown in Figure 4-3a. The increased VUV exposure results in a decrease in the F/C atom ratio from 0.17 to 0.04 (Table 4-1). The F 1s peak is decreased in size almost to that of the O 1s peak, although the O surface concentration is further decreased to 1.6 at%. The C 1s spectrum shown in Figure 4-2Ac now consists of only one peak with a BE of 285.2 eV. The broad F 1s feature shown in Figure 4-2Cc indicates further loss of F, which has now been reduced by about 88%. These results demonstrate that VUV exposure destroys the Tedlar structure by removing F from the near-surface region. The C state at a BE of 285.2 eV is due to F depletion. The presence of lower concentrations of F implies that electron density on the C atoms is not decreased to such a large extent by withdrawal toward the F resulting in increased C 1s BEs.

Next the 24-h, VUV-exposed Tedlar surface was exposed to O_2 for 20 min at room temperature and 1 atm. The XPS survey spectrum obtained from this surface is shown in Figure 4-3b. There appears to be negligible differences in the C 1s features, but the sizes of the O 1s and O (KLL) features are increased. The shapes of the F, F 1s, F 2s and F (KLL) features remain unchanged but the size is slightly increased. The surface O/C ratio rose from 0.04 to 0.08 (Table 4-1) while the F/C atom ratio did not change. This increase is due to dissociative chemisorption of O_2 at reactive sites formed during the erosion process. The amount of O_2 that chemisorbs provides a measure of the concentration of reactive sites in the near-surface region. Previous studies have shown that AO-exposed Kapton [10], Tedlar [35] and Tefzel [36] chemisorb very large amounts of molecular oxygen indicating that these surfaces contain a high concentration of reactive sites. These reactive sites are probably present because cross bonding cannot occur due

to geometrical constraints. The amount of molecular oxygen chemisorbed on VUV-exposed Tedlar is similar to that of AO-exposed Tedlar, indicating that the concentration of reactive species is quite appreciable.

Differences in the high-resolution XPS spectra are more apparent than in the survey spectra. The C 1s spectrum shown in Figure 4-2Ad exhibits a broadening on the high-BE side due to the formation of oxygen-containing species. The F 1s spectrum (Figure 4-2Cd) exhibits a broader peak and a different structure than after the 24 h VUV exposure indicating that the chemical environment is altered by O chemisorption. The O 1s spectrum (Figure 4-2Bd) is broader and exhibits a more pronounced shoulder on the high-BE side confirming the chemisorption of O at the C sites, which have lost fluorine.

The XPS survey spectra obtained after another 1 and then 3 h of VUV exposure are shown in Figure 4-4a and 4-4b respectively. After the additional 1 h of VUV exposure (27 h total VUV), the O 1s and O (KLL) features are decreased in size with no apparent changes in the C and F features. The O/C atom ratio is decreased from 0.08 to 0.06 and the F/C atom ratio is increased from 0.04 to 0.06. After two more hours of VUV (29 total h), the survey spectrum exhibits a slight decrease in the size of the O features as well as a decrease in the size of the F (KLL) feature. The F/C atom ratio decreases from 0.06 to 0.03 while the O/C atom ratio remains unchanged at 0.06.

The C 1s spectra obtained after the additional 1- and 3-h VUV exposures (Figures 4-2Ae and 2Af) are similar to that obtained after the 24-h VUV exposure (Figure 4-2Ac). The O 1s spectra (Figures 4-2Be and 4-2Bf) exhibit a decrease in peak height and width after the 27-h VUV exposure but no further changes after the 29-h exposure. The F 1s spectra (Figures 4-2Ce and 4-2Cf) do not change in size and shape following the 27-h VUV exposure but decrease in

size after the 29-h VUV exposure. The mechanism of both F and O removal is photon stimulated desorption (PSD) which breaks the chemisorption bonds and creates an antibonding potential [36].

The surface was then exposed to air for 11 h at room temperature. This treatment is quite different than an exposure to research purity O_2 because air contains water, hydrocarbons, alcohols and CO_2 which can adsorb at a surface. The XPS survey spectra obtained after this treatment is shown in Figure 4-5a. A very large increase in both the O 1s and O (KLL) peaks is apparent along with a corresponding decrease in the C 1s peak and smaller decreases in the F 1s and F (KLL) peaks. No features due to N appear in the spectrum. The high-resolution C 1s, O 1s and F 1s spectra are shown in Figures 4-2Ag, 4-2Bg and 4-2Cg respectively. The O/C atom ratio increases from 0.06 to 0.18 by this treatment, and the F/C atom ratio increases from 0.03 to 0.04.

The final treatment was an exposure to the VUV radiation for another 2 h (31 h total). The survey spectrum obtained after this VUV exposure is shown in Figure 4-5b. The O 1s features decrease after the two additional hours of VUV exposure. Increases of the C 1s, F 1s and F (KLL) peaks are apparent again, just as they were after the O_2 exposure. The amount of adsorbed O at the surface is much greater after the air exposure than after the O_2 exposure indicating that the O_2 exposure was not large enough to saturate all of the available reactive sites formed during the erosion process. This implies that the sticking coefficient for chemisorption of O_2 at the reactive sites is small, most likely because the O_2 bond must be broken. After another 2 h of VUV exposure, the O/C atom ratio (Table 4-1) is decreased from a value of 0.18 to 0.14 while the F/C atom ratio remains at 0.04. This appears to be the steady-state value for the F/C atom ratio. The corresponding high-resolution C 1s, O 1s and F 1s spectra are shown in

Figures 4-2Ah, 4-2Bh and 4-2Ch respectively. The C 1s and F 1s peaks exhibit negligible change while the O 1s peak is decreased in size.

Comparison: Tedlar Erosion by VUV Versus AO

Both VUV and AO [35, Chapter 3] induce chemical alterations at a Tedlar surface, which result in erosion. A comparison of the high-resolution C 1s spectra obtained from VUV-exposed Tedlar (solid lines) and AO-exposed Tedlar (dashed lines) is shown in Figure 4-6. The spectra obtained from the two as-entered samples (Figure 4-6a) are identical as expected, and the AO- and VUV-exposed Tedlar spectra from the 24-h exposures and beyond are all quite similar in that the two peaks have been reduced to one peak at a lower BE (Figure 4-6c to h). There is one major difference between the AO- and VUV- exposed C 1s spectra. With 2 h of AO exposure (Figure 4-6b), the peak at BE 287.9 eV disappears and the peak at 285.7 eV shifts to a value of 284.6 eV, which is the C 1s BE of graphitic carbon. With 2 h of VUV exposure (Figure 4-6b), a small peak at 287.9 eV still exists, though it is nearly completely removed by the VUV. The peak at 285.7 eV shifts to lower BE as well, but only to 285.2 eV. After the 24-h exposures, the C 1s peaks change minimally in both sets of spectra but the two peaks have a difference of 0.6 eV BE. This suggests that AO and VUV lead to the formation of different carbon species at the surface.

Summary

In this study the chemical alterations at a Tedlar surface caused by exposure to VUV radiation (115-400 nm) have been studied using XPS. A 2-h exposure to VUV radiation results in a decrease in the F/C atom ratio from 0.34 to 0.17 and a significant reduction of carbon that is bonded to F. Also, surface oxygen is removed by this treatment lowering the O/C atom ratio from 0.08 to 0.05. Another 22 h of VUV exposure results in a further decrease of the F/C atom ratio to 0.04 and the O/C atom ratio to 0.04. Exposure of this VUV-exposed surface to O_2 results

in chemisorption of O due to bonding at reactive sites thereby raising the O/C atom ratio to 0.08. Further exposure of this surface to VUV radiation for 3 h results in reduction of the chemisorbed oxygen while another 2 h results in further F removal, yielding an F/C ratio of 0.03. Then this VUV-exposed surface was exposed to air for 11 h, and a large amount of O_2 is chemisorbed raising the O/C atom ratio from 0.06 to 0.18. Another 2 h of VUV exposure results in removal of some of the chemisorbed O and attainment of a steady-state F/C atom ratio of 0.04.

Similar experiments were also carried out on Tedlar using hyperthermal AO, and the resulting XPS data have been compared with the corresponding XPS data obtained using VUV radiation. The results are similar with both methods removing much of the F within 2 h and nearly all of the F within 24 h. The two different treatments do however form carbon species with different BEs indicating that different carbonaceous structures form by the two treatments.

Table 4-1. Near-surface compositions of Tedlar after various treatments (at%)

	F	C	O	F/C	O/C
as entered	23.8	70.5	5.5	0.34	0.08
UV 2 h	14.1	82.0	3.9	0.17	0.05
UV 24 h	3.4	94.9	1.6	0.04	0.04
O_2 20 min	3.4	89.6	7.0	0.04	0.08
UV 27 h	5.0	89.8	5.2	0.06	0.06
UV 29 h	2.7	91.7	5.7	0.03	0.06
Air 11 h	3.7	81.8	14.6	0.04	0.18
UV 31 h	3.8	84.8	11.4	0.04	0.14

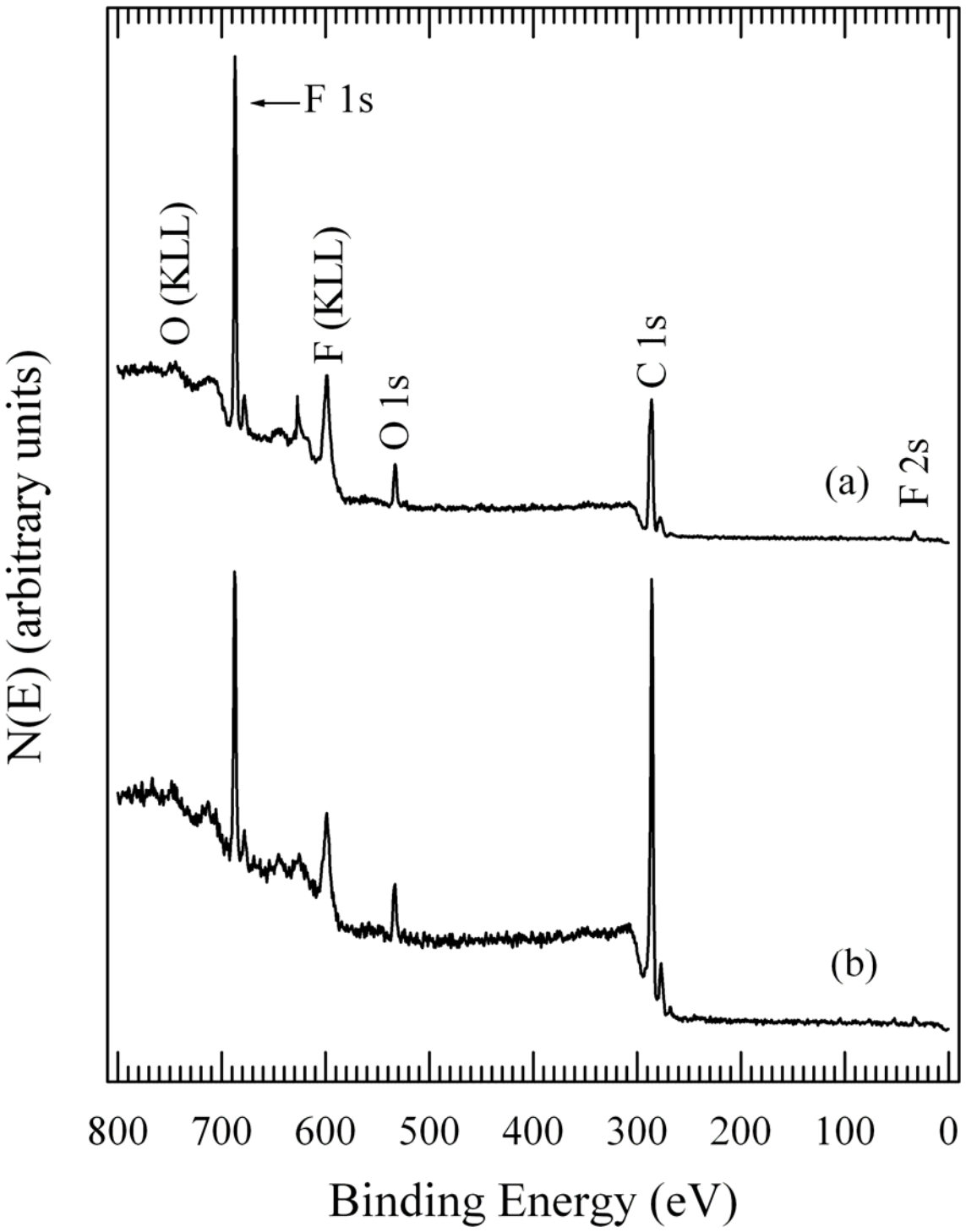

Figure 4-1. XPS survey spectra obtained from VUV-exposed Tedlar (a) as entered and (b) after a 2-h exposure to VUV radiation.

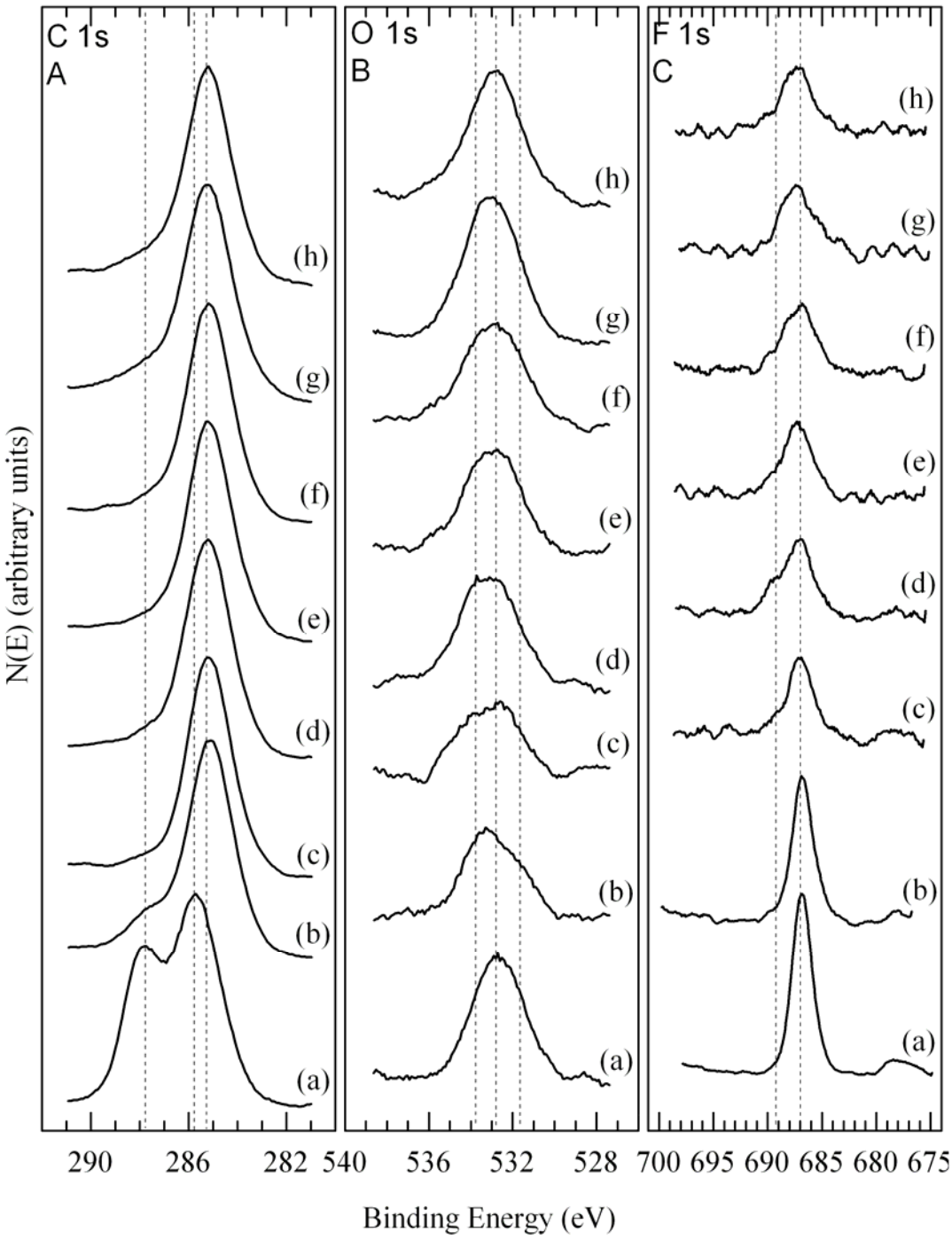

Figure 4-2. High-resolution XPS spectra obtained from VUV-exposed Tedlar (A) C 1s and (B) F 1s (a) as entered, (b) after exposure to VUV for 2 h, (c) after exposure to VUV for a total of 24 h, (d) after exposure to O_2 at room temperature and 1 atm for 20 min, (e) after exposure to VUV for a total of 27 h, (f) after exposure to VUV for a total of 29 h, (g) after exposure to air for 11 h at room temperature and (h) after exposure to VUV for a total of 31 h.

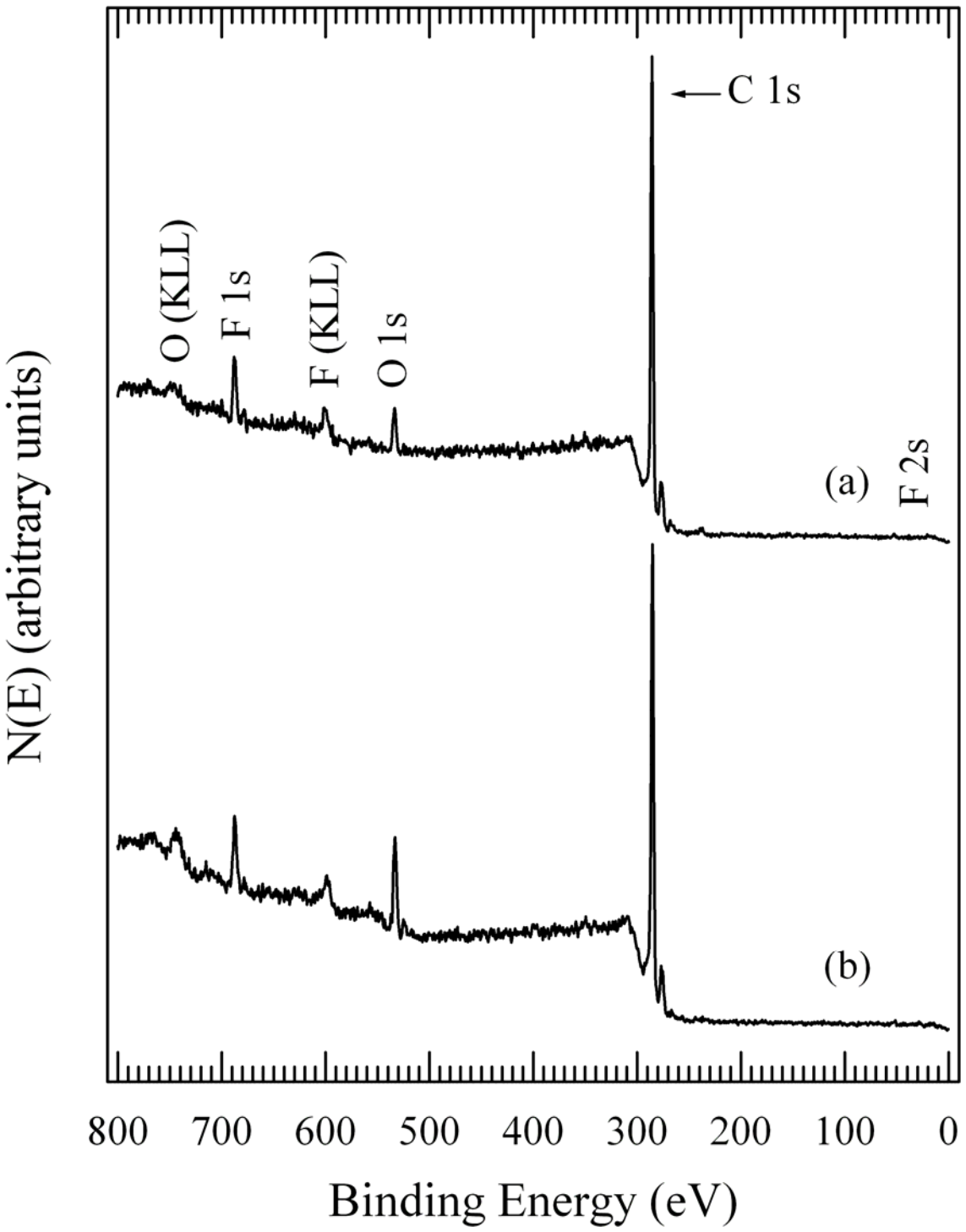

Figure 4-3. XPS survey spectra obtained from VUV-exposed Tedlar (a) after a 24-h exposure to VUV radiation and (b) after a 20-min exposure to O_2 at room temperature and 1 atm.

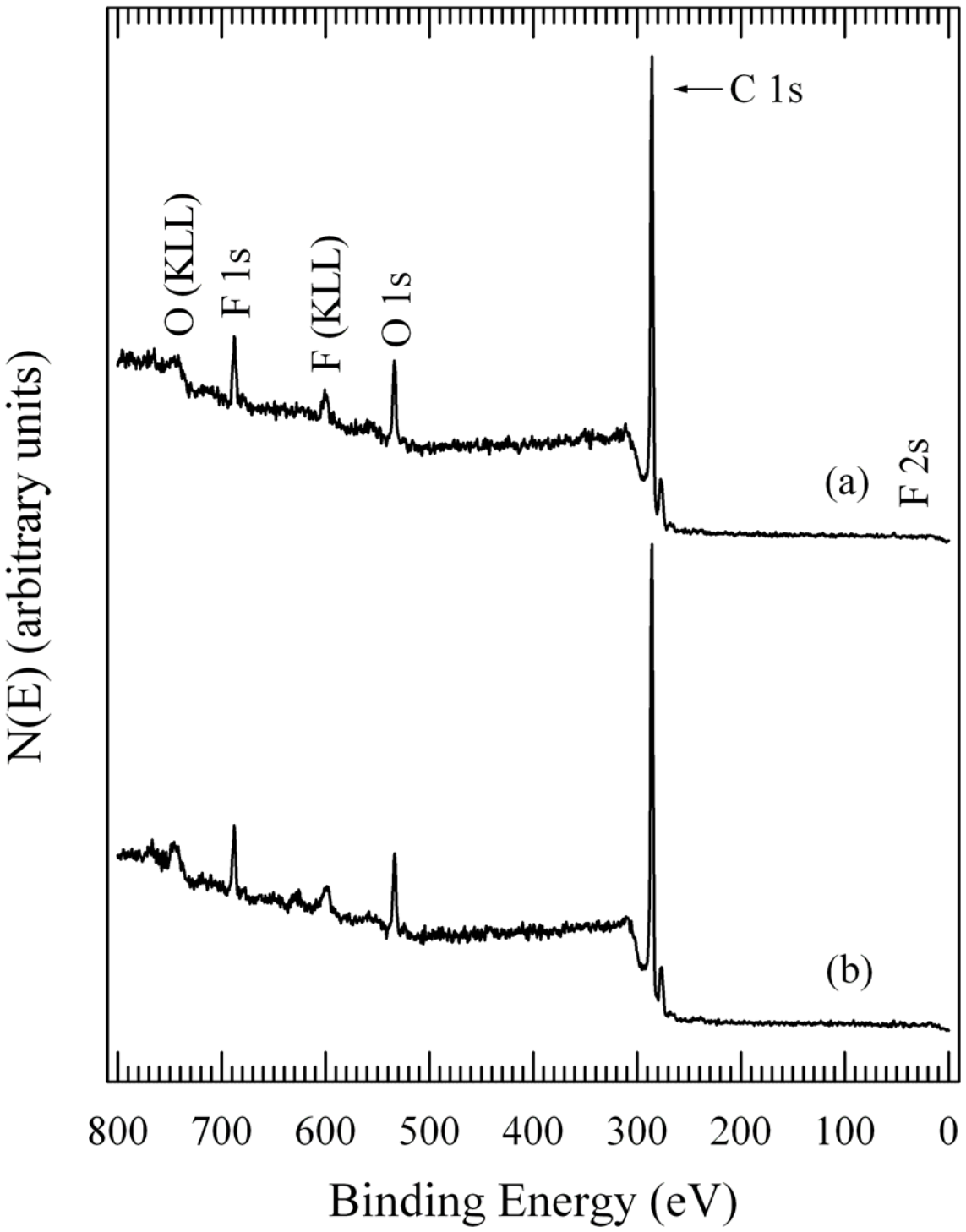

Figure 4-4. XPS survey spectra obtained from VUV-exposed Tedlar (a) after a 27-h exposure to VUV (3 h of UV after the O_2 exposure) and (b) after a total of 29 h exposure to VUV.

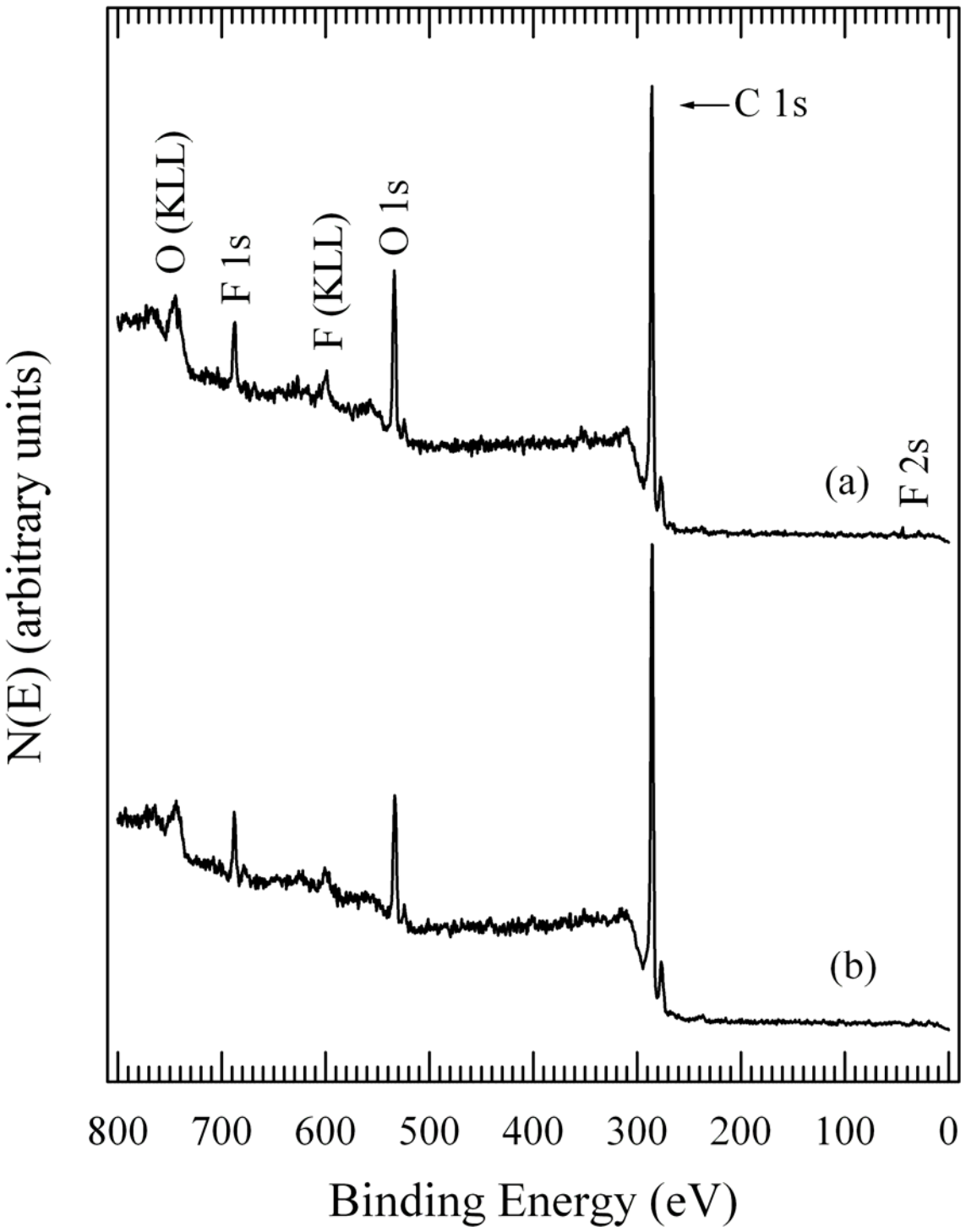

Figure 4-5. XPS survey spectra obtained from VUV-exposed Tedlar (a) after an 11-h exposure to air at room temperature and (b) after a total of 31 h exposure to VUV (2 h of VUV exposure after the air exposure).

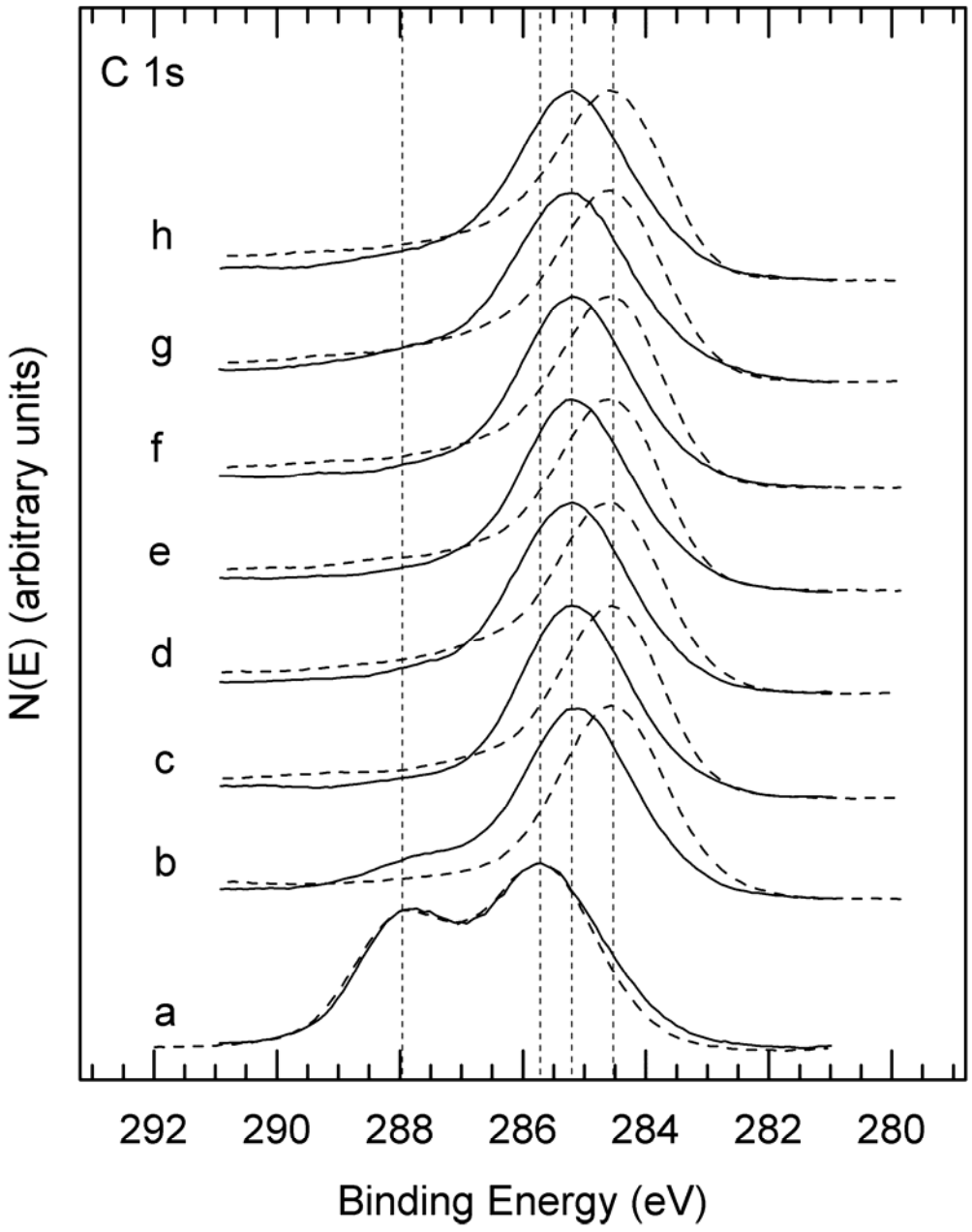

Figure 4-6. Overlays of XPS C 1s spectra obtained from Tedlar after various VUV (solid lines) and AO (dashed lines) exposures (a) as entered, (b) after 2 h VUV and 2 h AO, (c) after 24 h VUV and 24 h AO (d) after 20 min O_2, (e) after 27 total h VUV and 25 total h AO, (f) after 29 total h VUV and 27 total h AO, (g) after exposure to air, and (h) after 31 total h VUV and 70 total h AO.

CHAPTER 5
CHEMICAL ALTERATION OF POLY (ETHYLENE TETRAFLUOROETHYLENE) TEFZEL INDUCED BY HYPERTHERMAL ATOMIC OXYGEN

One of the main constituents in LEO is hyperthermal AO, which is known to degrade polymers. In this study XPS was used to characterize the surface of a Tefzel film before and after exposures of varying lengths to AO, as well as O_2 and air. The goal of the study was to determine how hyperthermal AO affects the TFE Teflon surface so that a better understanding of its space survivability can be obtained.

Experimental

An as-received E.I. du Pont Nemours & Co., Inc. Tefzel film was wiped with methanol and inserted into the UHV chamber (base pressure $<1.3 \times 10^{-10}$ Torr). XPS measurements were performed using a double-pass cylindrical mirror analyzer (DPCMA) (PHI Model 25-270AR). XPS survey spectra were taken in the retarding mode with a pass energy of 50 eV, and high-resolution XPS spectra were taken with a pass energy of 25 eV using Mg $K\alpha$ X-rays (PHI Model 04-151 X-ray source). Data collection was accomplished using a computer interfaced, digital pulse-counting circuit [28] followed by smoothing with digital-filtering techniques [29]. The sample was tilted 30 degrees off the axis of the DPCMA, and the DPCMA accepted electrons emitted into a cone 42.6 ± 6 degrees off the DPCMA axis.

XPS spectra were first obtained from the as-entered, solvent-cleaned sample. The sample was then transferred into an adjoining UHV chamber that houses the ESD AO source via a magnetically coupled rotary/linear manipulator. The characteristics of the atom source are described in Chapter 1. There the surface was exposed to the hyperthermal AO flux and re-examined after various exposure times. The samples were not exposed to air after the AO

exposures and before collecting XPS data. However, after the AO exposures the surface was exposed to O_2 to determine how this would affect the AO-exposed surfaces. The approximate normal distance between the sample face and source in this study was 15 cm, at which distance the flux was about 2.0 x 10^{15} atoms/cm^2-s for the instrument settings used. The sample was maintained at room temperature during the AO exposures with a temperature increase to about 50°C due to exposure to the X-ray source during XPS data collection. The substrate temperature was determined using a chromel-alumel thermocouple. Polymer structural repeat units, F-to-C ratios and reference XPS binding energies (BEs) used in this study are given in Table 5-1.

Results and Discussion

XPS survey spectra obtained from the as-entered Tefzel before and after 2 h of AO exposure are shown in Figure 5-1a and b respectively. The predominant peaks apparent in these spectra include the C 1s, O 1s, F 1s, F Auger (KLL) and F 2s. A small C1 2p peak is also present near 200 eV. Significant changes in relative peak heights are observed for the C and F features following the AO exposure. Estimates of the near-surface compositions have been made from the peak areas in the high-resolution spectra using published atomic sensitivity factors [31] with the assumption of a homogeneous surface region. XPS probes the near-surface region of the sample and yields a weighted average composition with the atomic layers near the surface being weighted more heavily since the photoemitted electrons from these layers have a lower probability of scattering inelastically. The sampling depth is ~4-6 nm, and ~10% of the signal originates from the outermost atomic layer [32]. This near-surface region is nonhomogeneous because the AO reacts most strongly with the outermost few atomic layers. Therefore, the region that reacts to the greatest extent with AO also makes the largest contribution to the XPS signal. This fact implies that XPS is an excellent technique for studying AO erosion of spacecraft materials. Even though the distribution functions involving the depth of chemical reactions in

the near-surface region and the XPS determination of the weighted average composition of the near-surface region are complex, the compositional values provide a trend which is indicative of the chemical alterations occurring during AO exposure.

The compositions determined using the homogeneous assumption are shown in Table 5-2 before and after various exposures to AO and O_2. The F/C atom ratio obtained from the as-entered sample is 0.74, which is lower than the stoichiometric value of 1.0. The near-surface region also contains about 2.3 at% of O giving an O/C atom ratio of 0.04. The source of this surface O is not known. It may have accumulated during preparation of the Tefzel, and it may be present in the bulk of the polymer. It possibly is due to an oxygen-containing termonomer such as terfluoropropyl vinyl ether, which may have been added to Tefzel to improve cracking resistance.

After a 2-h AO exposure (survey spectrum shown in Figure 5-1b), the F/C atom ratio is decreased from 0.74 to 0.17 and the O/C atom ratio is significantly reduced from 0.04 to 0.01. Furthermore, the chemical composition of the outermost 30-50 Å consists of 84.8 at% C. Stoichiometric Tefzel consists of equal atomic percents of C, F and H. Unfortunately, XPS is relatively insensitive to H because it has no core level electrons. Therefore, H is not measured although it is certainly present at least initially. Both AO and H are highly reactive. AO most likely reacts with H in the near-surface region to form H_2O, which desorbs leaving a carbonaceous layer. The structure of this carbonaceous layer has not been determined and most likely is quite complex. It may be partially graphitic, and it may contain amorphous regions as well as double and triple unsaturated bonds. It may be considered to be a charcoal-like layer produced after just 2 h of AO exposure. All further experiments are carried out on this layer and not on a Tefzel layer. The XPS spectrum obtained after a 24-h AO exposure (Figure 5-2a)

differs significantly from the spectrum obtained after the 2-h AO exposure in that the F 1s peak is much smaller relative to the C 1s peak and the O 1s peak size is increased. The latter is probably due to adsorption of O at unsaturated bonds formed by further erosion of the C-rich layer. According to the compositional data in Table 5-2, the C content is increased to 94.7 at%, the O content is increased to 3.5 at% and the F content is decreased from 14.5 to 1.9 at%. This layer is considerably more carbonaceous than that obtained after the 2-h AO exposure.

After exposure of this surface to O_2 at 150 Torr and room temperature for 20 min, the XPS O 1s peak is clearly increased (Figure 5-2b). The compositional data in Table 5-2 indicate that the O/C atom ratio is increased from 0.04 to 0.08. This increase is due to dissociative chemisorption of O_2 at reactive sites formed during the erosion process. The amount of O_2 adsorbed provides a measure of the concentration of reactive sites formed during AO exposure. A charcoal or graphite surface would not adsorb any O_2 under these exposure conditions. The O_2-exposed surface was then exposed to AO for 1 h (25 h total) and another 3 h (28 h total). The resulting XPS survey spectra are shown in Figure 5-3a and b respectively. The O 1s peak is slightly decreased in size relative to the C 1s peak. This is supported by the compositional information in Table 5-2 in which the O/C atom ratio decreases from 0.08 to 0.07. Furthermore, the F/C atom ratio decreases from 0.04 to 0.02. After another 3 h of AO exposure, the survey spectrum shown in Figure 5-3b was obtained. From Table 5-2 the F/C and O/C atom ratios are 0.01 and 0.05 respectively. These are quite similar to the values obtained after the 24-h AO exposure. The composition of this surface is probably similar to the steady-state composition during the AO process. Since the C concentration is very large, the formation of CO and/or CO_2 is the slow step in the erosion process. Surface F is most likely removed by a physical sputtering

process by the hyperthermal AO while surface O may be removed by either physical sputtering or chemical reaction to form O_2 or both at different rates.

The high-resolution XPS C 1s, O 1s and F 1s features are shown in Figure 5-4A, B and C respectively. The C 1s feature obtained from the as-entered Tefzel (Figure 5-4Aa) consists of two peaks with maxima at 286.4 and 291.0 eV. This is consistent with reference spectra obtained from Tefzel [30]. The feature at 286.4 eV is assigned as due to C bonded as $-\overset{H}{\underset{H}{\overset{|}{\underset{|}{C}}}}-$, and the feature at 291.0 eV is assigned to C bonded as $-\overset{F}{\underset{F}{\overset{|}{\underset{|}{C}}}}-$. The peaks should be the same size since these two types of C are present in stoichiometric Tefzel in equal amounts, and this is the case in the reference spectra [30]. Stoichiometric Tefzel also contains no O whereas the as-entered sample in this study contained about 2.3 at%. This O is most likely bonded in the near-surface region as $-\overset{OH}{\underset{H}{\overset{|}{\underset{|}{C}}}}-$ groups, which have a C 1s binding energy (BE) of about 286.5 eV [30]. The presence of these groups adds structure to the lower BE feature thereby increasing its intensity and broadening it to the low BE side. It seems reasonable that $-\overset{OH}{\underset{H}{\overset{|}{\underset{|}{C}}}}-$ groups

would have a C 1s BE between the two peaks observed in Figure 5-4Aa. Since features are not apparent at these BEs, $-\overset{\overset{OH}{|}}{\underset{\underset{F}{|}}{C}}-$ species are not present. The O 1s feature obtained from the as-entered Tefzel (Figure 5-4Ba) is consistent with the assertions above in that it is small and symmetrical. This latter point indicates the presence of only one chemical state of O. Furthermore, the BE of this peak is 532.9 eV which is the median of the narrow range ($\Delta E = 0.35$ eV) reported by Beamson and Briggs [30] for the proposed species. The F 1s peak is also symmetrical with a BE of 688.3 eV. This is characteristic of F in $-\overset{\overset{F}{|}}{\underset{\underset{H}{|}}{C}}-$ groups [30].

The C 1s, O 1s and F 1s spectra obtained after the 2-h AO exposure are shown in Figure 5-4Ab, 5-4Bb and 5-4Cb respectively. The C 1s feature consists of a predominant symmetrical peak with a BE of 284.6 eV, which is characteristic of a graphitic or an amorphous charcoal-like C film. This is reasonable since the near-surface region contains 84.8 at% C, 14.5 at% F and 0.7 at% O (Table 5-2). The C 1s feature also contains a shoulder on the high-BE side of the predominant feature. This shoulder is due to carbon which is bonded to the remaining F. Since the BE is lower than that of C bonded to two fluorines, this shoulder is probably due to C bonded to just one F species. The other F is most likely removed by physical sputtering. Another very slight shoulder is apparent at 289.6 eV. This is probably due to C which is still bonded to two fluorines. By comparing Figures 5-4Ba and 5-4Bb, it is apparent that the chemical nature of O in the near-surface region is changed by the 2-h AO exposure. This exposure decreases the O

concentration from 2.3 to 0.7 at%. The chemical state at 532.9 eV is reduced in intensity while chemical states with BEs in the range from 530.6 to 532.3 eV are formed. The chemical nature of these O species is not known, but they may be C-O-C, C-OH or C=O groups [30]. The fact that these AO-exposed surfaces are quite damaged makes species assignment very difficult. The F 1s peak is significantly decreased in size (the F/C atom ratio is reduced from 0.74 to 0.17), and the BE of the predominant feature is shifted to 686.5 eV and broadened toward lower BEs. These values are lower than any reported F 1s values for organic materials containing F. One possibility is that the F may be interacting with radical species capable of donating electrons to the F thereby lowering the F 1s BE.

After the 24-h AO exposure, the predominant peak in the C 1s feature remains unchanged but the higher-BE shoulders are significantly reduced in intensity. This is consistent with the compositional information since these shoulders are due to bonding with O or F. The F content is reduced from 14.5 to 1.9 at% while the O content is increased from 0.7 to 3.5 at%. This increase in O content is most likely due to bonding of AO with carbon-centered radicals remaining after F removal. At least four chemical states of oxygen are apparent after the 24-h AO exposure (Figure 5-4Bc). The corresponding F 1s feature (Figure 5-4Cc) is small and broad indicating that F is bonded in many chemical environments in this heavily damaged near-surface region.

After the O_2 exposure the C 1s feature (Figure 5-4Ad) is broadened slightly on the high-BE side. The corresponding O 1s feature (Figure 5-4Bd) is fairly symmetrical around the predominant peak with a BE of 532.7 eV. This is quite likely due to a C=O species formed by dissociative chemisorption of O_2 at reactive C sites. The F 1s peak (Figure 5-4Cd) is narrower

after the O_2 exposure possibly due to saturation of the reactive species formed during AO exposure.

After another 1 h and then 3 h of AO exposure, only a few small changes are observed in the high-resolution spectra. The small shoulder on the high-BE side of the C 1s peak (Figure 5-4Ae and 5-4Af) are more similar to that obtained after the 24-h AO exposure (Figure 5-4Ac). The O 1s feature (Figure 5-4Be and 5-4Bf) is broadened and is quite similar to that obtained after the 24-h AO exposure (Figure 5-4Bc). The F 1s peak (Figure 5-4Ce and 5-4Cf) becomes quite small with further AO exposure but retains its narrow, symmetrical nature.

These spectra along with the compositional data shown in Table 5-2 indicate that the surface produced by the 24-AO exposure is the steady-state surface formed during AO erosion of Tefzel. The fact that the C content of the near-surface region is about 95 at% indicates that removal of C from the surface either by reaction with AO to form CO and/or CO_2 or by physical sputtering by the hyperthermal AO is the slow step in the erosion process. The F is removed rapidly, and the H most likely is removed rapidly as well since it is very reactive toward AO. Oxygen in the near-surface region apparently is not removed as fast as F.

Comparison to Tedlar and Teflon

Similar AO-exposure studies have been carried out on poly (vinyl fluoride) (PVF) $(CHF-CH_2)_n$ (Tedlar) [35] and poly (tetrafluoroethylene) $(CF_2-CF_2)_n$ (PTFE Teflon) [33] and the XPS compositional results corresponding to Table 5-2 for Tefzel are shown in Tables 5-3 and 5-4 respectively. The F content of the near-surface region decreases very rapidly for Tedlar, less rapidly for Tefzel and relatively slowly for Teflon with increasing AO fluence. This behavior correlates with the hydrogen content of these polymers. Tedlar is 50 at% H, Tefzel is 33.3 at% H and Teflon is 0 at% H. This information suggests that H atoms i.e.: H-C bonds provide an attack point for AO possibly through formation of HF, which desorbs. After the surface

structure is damaged, the F is susceptible to removal by AO. Since Teflon does not contain H, the F is more difficult to remove. Furthermore, the C removal rate by AO is not much slower than the F removal rate so the F/C atom ratio only decreases from 1.66 to about 0.58 [33] for the steady-state surface composition. This is quite different than Tedlar where the F/C atom ratio drops from 0.45 to ~0.01 (Table 3-2) and Tefzel where the F/C atom ratio drops from 0.74 to 0.01 (Table 5-2). The steady-state compositions of Tedlar and Tefzel are nearly identical containing 92.1 and 93.9 at% C respectively while that for Teflon is very different containing only 63.4 at% C [33]. The reactions of the steady-state AO eroded surfaces with O_2 are also quite different. The O contents of both Tedlar and Tefzel are significantly increased after the O_2 exposure (O/C atom ratios increase from 0.07 to 0.12 for Tedlar and from 0.04 to 0.08 for Tefzel) while that for Teflon only increases from 0.0 to 0.015. Again, this behavior correlates with the initial H content of the polymer. Polymers containing more H initially form more damage-laden films during AO exposure, which adsorb more O_2.

Summary

In this study a Tefzel film has been exposed to a flux of $2x10^{15}$ atoms/cm^2-s of 5-eV AO for various times, and the chemical alterations at the surface have been monitored using XPS. After a 2-h exposure, the F/C and O/C atom ratios decrease from 0.74 and 0.04 to 0.17 and 0.01 respectively. Most of the F is removed, the O content is decreased from 2.3 to 0.7 at% and the C content is increased from 56.2 to 84.8 at%. A longer exposure of 24 h results in a further decrease of the F/C atom ratio to 0.02. This AO exposure transforms the near-surface region of Tedlar into a carbonaceous layer (94.7 at% C), which may be graphitic or amorphous according to the high-resolution XPS data. This surface is the steady-state surface formed during the AO erosion of Tefzel since longer AO exposures do not significantly alter the chemical composition or nature of the carbonaceous film. This film is attacked chemically by AO to form CO and/or

CO_2 resulting in erosion, but the erosion rate has not been determined in this study. Based on the XPS data, the thickness of the carbonaceous film is at least 4 nm. The fact that this surface consists mostly of C indicates that reaction of C with AO is the slow step in the erosion process. Comparison of the AO-erosion data of Tefzel with similar data taken from Tedlar and Teflon indicate that C-H bonds are sites that are highly susceptible to attack by AO.

Exposure of the AO-exposed carbonaceous film to O_2 increases the oxygen content of the near-surface region by a factor of about two. The oxygen adsorbs at reactive sites formed during AO exposure. These reactive sites most likely do not cross bond due to geometrical bond constraints. The amount of O_2 that chemisorbs provides a measure of the concentration of these reactive sites in the near-surface region. Further exposure to AO removes this chemisorbed oxygen to the level prior to the O_2 or air exposure.

Table 5-1. Polymer Name, XPS Binding Energies, F/C Ratio and Structure

Polymer	Binding Energy (eV)			
	C 1s 1	2	F 1s	F:C
Tefzel, Poly (ethylene tetrafluoroethylene) $[-CH_2-CH_2-CF_2-CF_2-]_n$	286.44	290.90	688.15	1:1

Table 5-2. Near-surface compositions of Tefzel after Various Treatments (at%)

	F	O	C	F/C	O/C
as entered	41.5	2.3	56.2	0.74	0.04
AO 2 h	14.5	0.7	84.8	0.17	0.01
AO 24 h	1.9	3.5	94.7	0.02	0.04
O_2 20 min	3.7	7.2	89.1	0.04	0.08
AO 25 h	1.7	6.8	91.5	0.02	0.07
AO 28 h	1.2	4.9	93.9	0.01	0.05

Table 5-3. Near-surface compositions of Tedlar after Various Treatments (at%)

	F	O	C	F/C	O/C
as entered	29.0	7.2	63.7	0.45	0.11
AO 2 h	1.7	4.0	94.2	0.018	0.04
AO 24 h	2.0	6.3	91.7	0.022	0.07
O_2 20 min	1.1	10.4	88.5	0.012	0.12
AO 25 h	1.3	7.0	91.7	0.014	0.08
AO 27 h	1.7	6.7	91.6	0.018	0.07

Table 5-4. Near-surface compositions of Teflon after Various Treatments (at%)

	F	O	C	F/C	O/C
as entered	62.4	0.0	37.6	1.66	0.0
AO 2 h	53.6	0.0	46.4	1.15	0.0
AO 24 h	47.4	0.0	52.6	0.90	0.0
O_2 20 min	46.8	0.8	52.4	0.90	0.015
AO 25 h	44.9	0.1	55.0	0.81	0.002
AO 28 h	45.2	0.0	54.8	0.82	0.0

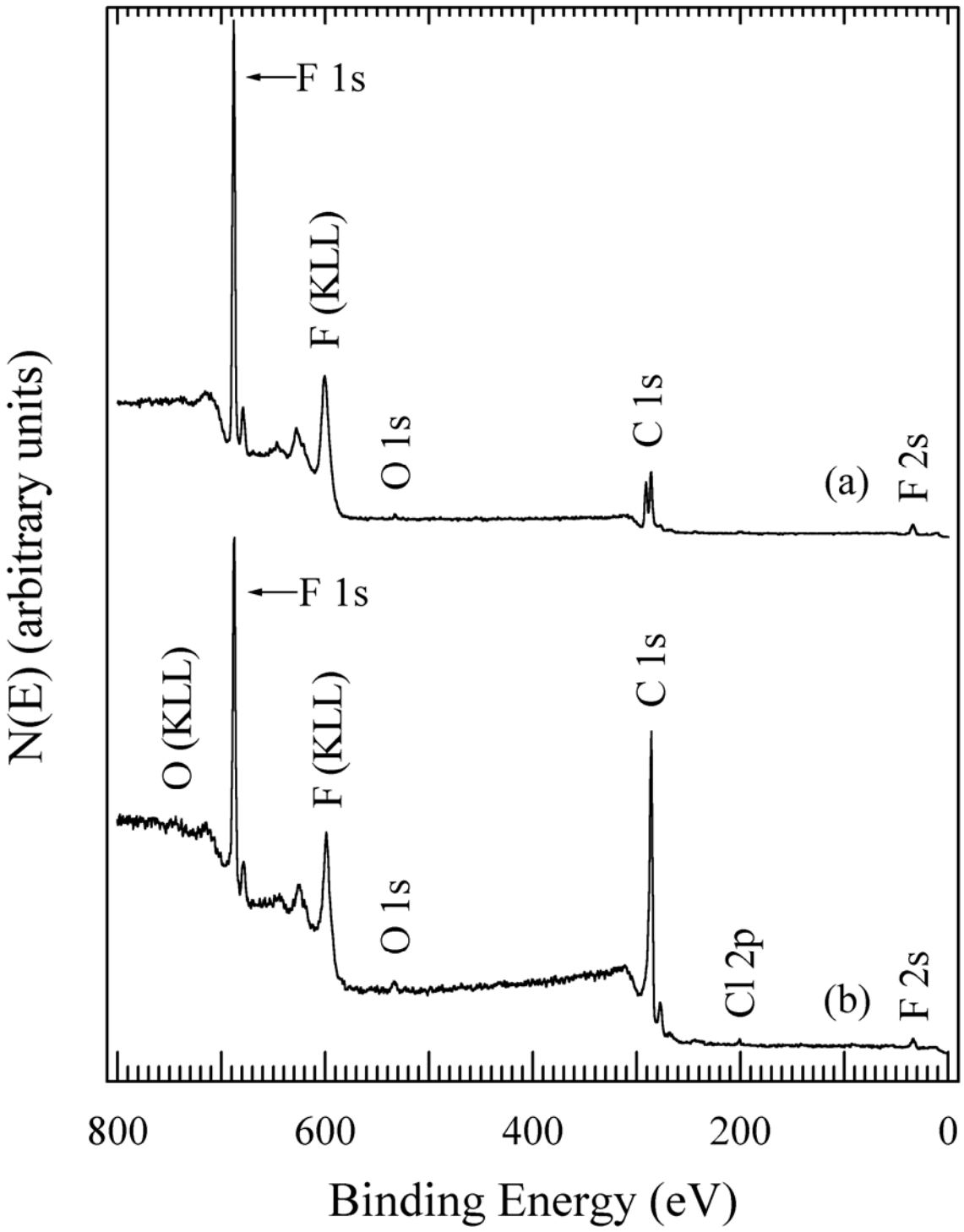

Figure 5-1. XPS survey spectra obtained from AO-exposed Tefzel (a) as entered and (b) after 2 h exposure to AO.

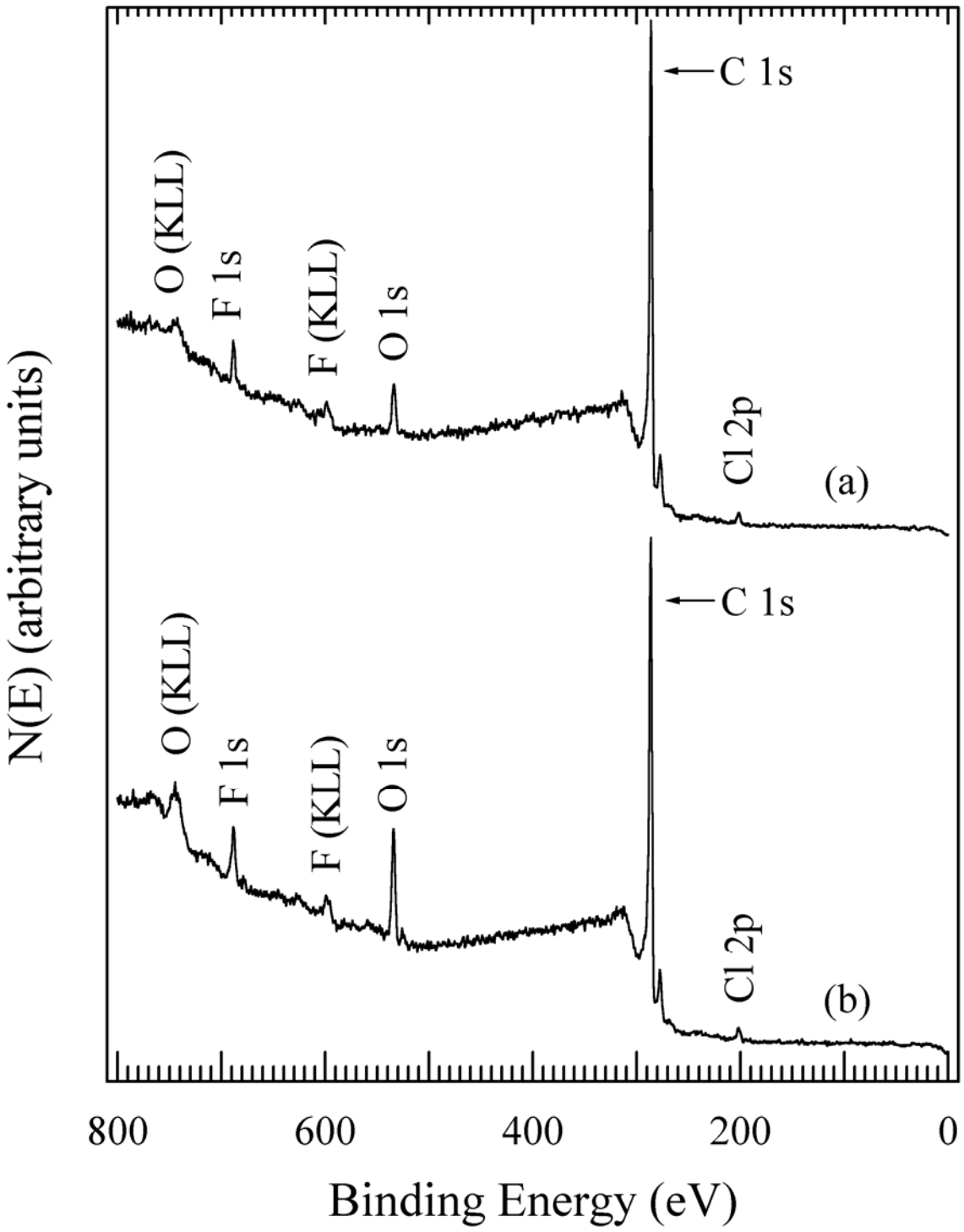

Figure 5-2. XPS survey spectra obtained from AO-exposed Tefzel (a) after 24 h exposure to AO and (b) after 20 min exposure to O_2 at 150 Torr and room temperature.

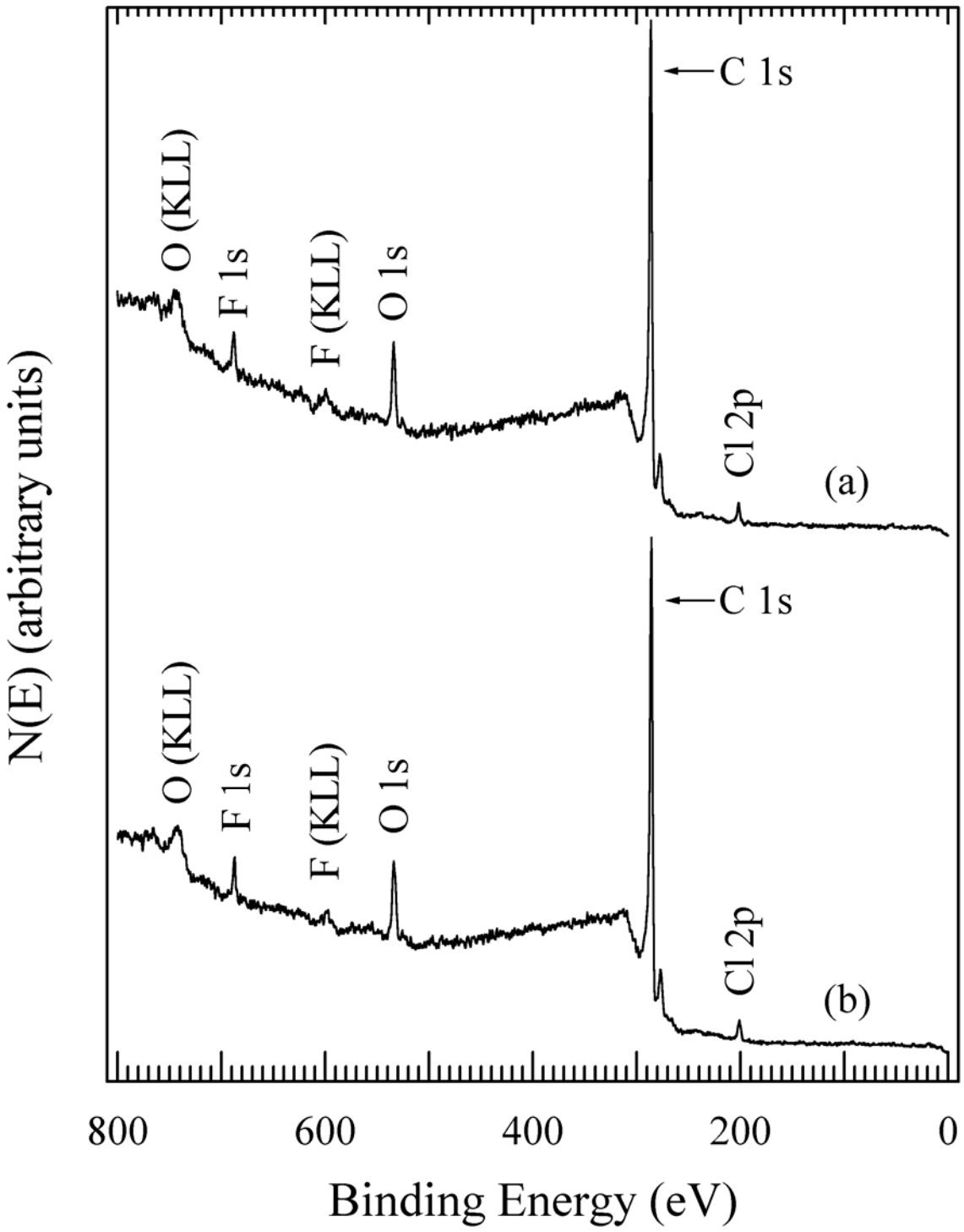

Figure 5-3. XPS survey spectra obtained from AO-exposed Tefzel (a) after 25 h exposure to AO and (b) after 28 h exposure to AO.

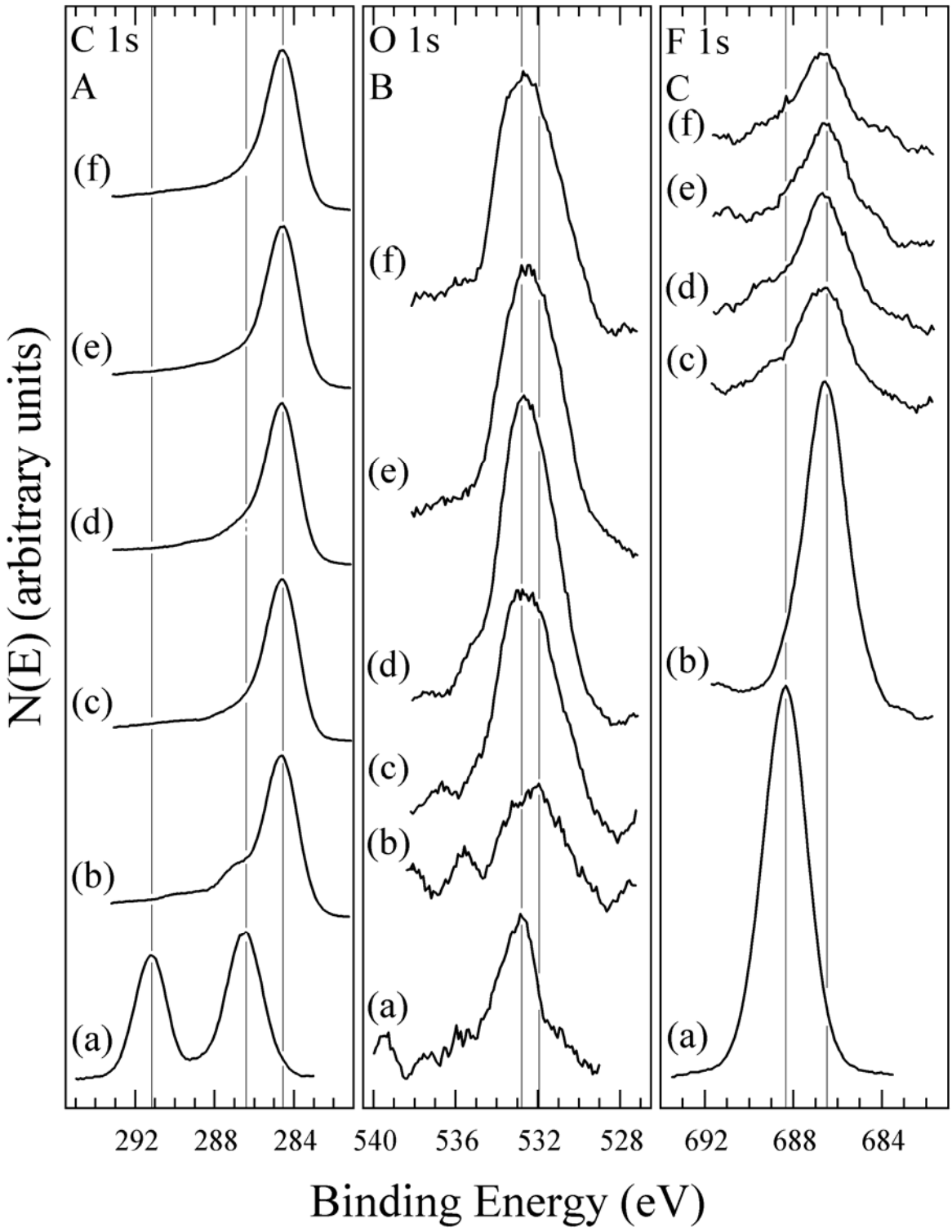

Figure 5-4. High-resolution spectra obtained from AO-exposed Tefzel (A) C 1s, (B) O 1s and (C) F 1s (a) as-entered, (b) after a 2-h AO exposure, (c) after a 24-h AO exposure, (d) after a 20-min exposure to O_2 at 150 Torr and room temperature, (e) after a 25-h exposure to AO and (f) after a 28-h exposure to AO.

CHAPTER 6
CHEMICAL ALTERATION OF POLY (ETHYLENE TETRAFLUOROETHYLENE) TEFZEL INDUCED BY EXPOSURE TO VACUUM ULTRAVIOLET RADIATION

In LEO objects are subjected to the full spectrum of solar radiation. One such range of light is VUV (115-200 nm), which is known to degrade polymers. In this study XPS was used to characterize the surface of a Tefzel film before and after exposures of varying lengths to UV radiation (115-400 nm), as well as O_2 and air. The goal of the study was to determine how VUV radiation affects the Tefzel surface so that a better understanding of its space survivability can be obtained.

Experimental

An as-received E.I. du Pont Nemours & Co., Inc. Tefzel film was wiped with ethanol and inserted into the UHV chamber (base pressure $<1.0 \times 10^{-10}$ Torr). XPS measurements were performed using a double-pass, cylindrical-mirror analyzer (DPCMA) (PHI Model 25-270AR). XPS survey spectra were taken in the retarding mode with a pass energy of 50 eV, and high-resolution XPS spectra were taken with a pass energy of 25 eV using Mg $K\alpha$ X-rays (PHI Model 04-151 X-ray source). The X-ray source was a flood source, and the DPCMA accepted photoelectrons from a spot 4 mm in diameter. The precision manipulator used allowed for analysis of the same spot after each treatment. The sample was tilted 30 degrees off the axis of the DPCMA, and the DPCMA accepted electrons emitted into a cone 42.6 ± 6 degrees off the DPCMA axis. The sample temperature was maintained at room temperature during the VUV exposures but rose to 50°C during exposure to the X-ray source according to a chromel-alumel thermocouple. The analysis chamber was pumped by a 400 l/s ion pump, a 180 l/s turbomolecular pump and a 4000 l/s cryopump containing a Ti sublimation system. The pressure was maintained at $\sim 2 \times 10^{-10}$ Torr during collection of XPS data. Under these conditions carbon

contamination did not accumulate on the surfaces studied. Data collection was accomplished using a computer-interfaced, digital-pulse-counting circuit [28] followed by smoothing with digital-filtering techniques [29]. Charging did not present a difficulty in this study. The spectrum taken from Tedlar was shifted so that the C 1s and F 1s peaks were at the same binding energies (BEs) of reference spectra [30]. All other spectra were shifted by this same value.

XPS spectra were first obtained from the as-entered, solvent-cleaned sample. The sample was then transferred into an adjoining UHV chamber that houses the VUV source via a magnetically coupled rotary/linear manipulator. This chamber contains a 120 l/s ion pump, which produces a base pressure in the low 10^{-9} Torr range during operation of the VUV source. An atomic oxygen (AO) source is also housed in this chamber. This chamber is kept very clean because AO reacts with any contamination to form products, which are pumped away. Many experiments have been performed including the oxidation of a cleaned Si(111) surface by AO which demonstrates that hydrocarbon contamination does not accumulate at surfaces in this chamber. This also keeps the VUV source window clean so periodic cleaning with diamond paste was not necessary. There the surface was exposed to a VUV radiation and re-examined after various exposure times. The samples were not exposed to air after the VUV exposures and before collecting XPS data. However, after the VUV exposures the surfaces were exposed to O_2 or air to determine how this would affect the VUV-exposed surfaces. The specific treatments used were (1) exposure to VUV for 2 h, (2) exposure to VUV for a total of 24 h, (3) exposure to research-grade O_2 at room temperature and 150 Torr for 20 min, (4) exposure to VUV for a total of 27 h, (5) exposure to VUV for a total of 29 h, (6) exposure to VUV for a total of 53 h, (7) exposure to VUV for a total of 99 h, (8) exposure to VUV for a total of 163 h, (9) exposure to air

for 43 h at room temperature and (10) exposure to VUV for a total of 200 h. XPS spectra were collected after each treatment.

Results and Discussion

XPS survey spectra obtained from the Tefzel film before and after a 2-h VUV exposure are shown in Figure 6-1a and b respectively. Spectrum a shows C 1s, F 1s, F 2s and F (KLL) features as expected. There are two distinct C 1s peaks corresponding to the two C atoms in the Tefzel structure. There is also the presence of Cl 2p and O 1s peaks, likely contaminants from processing the polymer. Estimates of the near-surface compositions have been made from the peak areas in the high-resolution spectra using published atomic sensitivity factors [31] with the assumption of a homogeneous surface region. XPS probes the near-surface region of the sample and yields a weighted average composition with the atomic layers near the surface being weighted more heavily since the photoemitted electrons from these layers have a lower probability of scattering inelastically. The sampling depth is ~4-6 nm, and ~10% of the signal originates from the outermost atomic layer [32]. This near-surface region is nonhomogeneous because the VUV radiation reacts most strongly with the outermost few atomic layers. Therefore, the region that reacts to the greatest extent with VUV radiation also makes the largest contribution to the XPS signal. This fact implies that XPS is an excellent technique for studying erosion of spacecraft materials by VUV radiation. Even though the distribution functions involving the depth of chemical reactions in the near-surface region and the XPS determination of the weighted average composition of the near-surface region are complex, the compositional values provide a trend which is indicative of the chemical alterations occurring during VUV exposure. The compositions determined using the homogeneous assumption are shown in Table 6-1 before and after various exposures to VUV radiation, O_2 and air. The F/C atom ratio obtained from the as-entered sample is 0.70, which is less than the stoichiometric value of 1.0.

This difference could be attributed to C contamination from hydrocarbons and the presence of surface O and Cl.

After a 2-h VUV exposure there is a substantial decrease in F content in the near-surface region as well as notable changes to the C 1s features. This spectrum is shown in Figure 6-1b. The F/C atom ratio is cut nearly in half by the 2-h VUV exposure, from 0.70 to 0.39. There is also a small decrease in the O 1s feature. Changes to the C 1s features are more evident in the high resolution spectra shown in Figure 6-2. The C 1s, O 1s and F 1s features obtained from the as-entered Tefzel are shown in Figure 6-2Aa, 6-2Ba and 6-2Ca respectively and in Figure 6-2Ab, 6-2Bb and 6-2Cb for the surface exposed to VUV for 2 h. The C 1s spectrum obtained from the as-entered Tefzel (spectrum 6-2Aa) features two peaks at 290.9 and 286.0 eV, the latter of which is broadened on the low-BE side most likely due to hydrocarbon contamination. These peaks correspond to C bonded to only F and C bonded to only H, respectively. The F 1s feature is a single well-defined peak centered at 688.1 eV. The O 1s feature is a small, broad peak centered at 532.8 eV.

The C 1s feature obtained after the 2-h VUV exposure (spectrum 6-2Ab) consists of one predominant peak at 286.0 eV with only a small hump remaining where the 290.9 eV peak was. The shoulder on the low-BE side of the 286.0 eV peak has disappeared leaving an even, well-defined peak. This is because the hydrocarbon contamination was easily removed by the VUV treatment. The F 1s feature maintains its shape but decreases in size (spectrum 6-2Cb) indicating F is being removed from the Tefzel surface. High resolution O 1s spectrum from the 2-h VUV exposure was not available however it is estimated from the XPS survey spectrum that the O composition dropped nearly in half.

An XPS survey spectrum obtained from the Tefzel surface after a 24-h VUV exposure is shown in Figure 6-3a. The increased VUV exposure results in a decrease in the F/C atom ratio from 0.39 to 0.22 (Table 6-1). Accordingly, the F 1s peak continued to decrease in size while the C 1s peak increased. The O 1s peak also increased, doubling the amount of surface O present. Cl in the surface also increased significantly from 0.1 to 0.6, though still a very small amount is present. These are also shown in high resolution spectra 6-2Ac, 6-2Bc and 6-2Cc. In spectrum 6-2Ac the hump at 290.9 eV is further reduced as is the F 1s peak in 6-2Cc. The O 1s feature in 6-2Bc broadens significantly to the high BE side. Assigning the peaks to specific species is quite difficult for several reasons. As explained in Chapter 2, defining localized species, which yield features at specific BEs, is difficult and may not be possible. Since there are distinct peaks in these spectra, there are distinct chemical environments, but defining the nature of this chemical environment may not be possible. Furthermore, the VUV-exposed surface is a damaged surface in that the composition is altered to a great extent.

Next the 24-h VUV exposed surface was exposed to 150 Torr of O_2 *in vacuo* for 20 min at room temperature. The XPS survey spectrum obtained from this surface is shown in Figure 6-3b. As expected, the O 1s peak increased significantly. This is seen more so in the high resolution spectrum 6-2Bd. The O 1s features become larger and broader on the high-BE side. There could be three different O 1s peaks in the feature due to various species formed during the chemisorption of O_2 at reactive sites which were formed during the VUV exposures. The O/C atom ratio increases from 0.02 to 0.05 while the F/C atom ratio remains unchanged. No changes to the F 1s peak in spectrum 6-2Cd are evident but there is some broadening on the high-BE side of the C 1s peak in spectrum 6-2Ad. This is also due to the chemisorption of O_2 at reactive sites. The amount of O_2 that chemisorbs provides a measure of the concentration of reactive sites in the

near-surface region. These reactive sites are probably present because cross bonding cannot occur due to geometrical constraints. The amount of molecular oxygen chemisorbed on VUV-exposed Tefzel is similar to that of AO-exposed Tefzel [36] and VUV-exposed Tedlar [37], indicating that the concentration of reactive species is quite appreciable.

Following the O_2 exposure the Tefzel surface was exposed to an additional 3 h of VUV radiation. The surface was then exposed for another 2 h for a total of 29 h of VUV exposure. The XPS survey spectrum for the 27-h exposure is not shown but the 29-h exposure is shown in Figure 6-4a. There are negligible changes to the C 1s and F 1s features but a slight decrease in the O 1s peak is observed as well as an increase in Cl. The compositions obtained from this surface show that the F/C atom ratio decreased from 0.21 to 0.19 and the O/C atom ratio from 0.05 to 0.04. In high-resolution spectra 6-2Ae and f, 6-2Be and f and 6-2Ce and f no changes are apparent in the F 1s spectra. The C 1s hump at 290.9 eV decreases further and the O 1s feature becomes more symmetrical centered about 533.8 eV. The mechanism of both F and O removal is photon stimulated desorption (PSD) which breaks the chemisorption bonds and creates an antibonding potential [36].

After another 24 (53 h total) of VUV exposure more systematic decrease in F 1s features are observed in XPS survey spectrum 6-4b and high resolution spectrum 6-2Cg. In spectrum 6-2Ag further reduction of the C 1s hump at 290.9 eV is observed. The F/C atom ratio is decreased from 0.19 to 0.15. The O/C atom ratio remains the same, a slight increase in Cl composition is observed (0.6 to 0.7 at%) and the appearance of N 1s features are observed (1.6 at%, Table 6-1). The presence of N could be due to contamination from the processing of the polymer and did not appear in earlier spectra until a certain degree of VUV-induced erosion brought it to the surface. Fluctuations in Cl content could also be attributed to this cause.

The Tefzel surface was then exposed to VUV radiation two more times. XPS survey spectra obtained from the 99-h and 163-h VUV exposures are shown in Figure 6-5a and b respectively while high resolution spectra for are shown in Figures 6-2Ah, 6-2Ai, 6-2Bh, 6-2Bi, 6-2Ch and 6-2Ci. Continued decrease in the C 1s hump at 290.9 eV is observed as well as in the F 1s peak. The F/C atom ratio drops from 0.15 to 0.09 after the 99-h VUV exposure and then to 0.07 following the 163-h exposure. The O/C atom ratio increases from 0.04 to 0.06 and then to 0.08 following the 99-h and 163-h exposures respectively. In spectra 6-2Bh and 6-2Bi the O 1s features broaden as the surface O concentration increases. The Cl 2p composition decreases from 0.7 to 0.3 at% following the 99-h exposure. It then increases to 0.5 at% following the 163-h exposure. The N 1s composition decreases from 1.6 at% to 0.4 at% then to 0.3 at% with the same two treatments.

The Tefzel sample was then removed from the UVH chamber and exposed to atmospheric conditions for 43 h, at which point it was returned to the UHV chamber. This treatment is quite different than an exposure to research purity O_2 because air contains water, hydrocarbons, alcohols and CO_2 which can adsorb at a surface. The XPS survey spectrum is shown in Figure 6-6a and the C 1s, O 1s and F 1s high resolution spectra are shown in Figures 6-2Aj, 6-2Bj and 6-2Cj respectively. The C 1s spectra appears broader on the high-BE side, similar to 6-2Ad after the O_2 exposure. The F 1s peak is further reduced and is approaching noise level. The O 1s peak becomes larger and more-well defined. The F/C atom ratio is reduced to 0.04 while the O/C atom ratio doubles to 0.16. The N 1s composition increases from 0.3 to 1.1 at%. The large increase in O and N concentration further indicates that a large amount of reactive sites form during VUV radiation.

Following the air exposure the Tefzel surface was exposed to another 37 h of VUV radiation, giving a total exposure time of 200 h. In the XPS survey spectrum in Figure 6-6b, little change to the C and F features are observed. The O 1s, O (KLL), N 1s and Cl 2p peaks are all decreased in size. In the high resolution XPS spectra in Figure 6-2 there are no noticeable changes to the C 1s features (spectrum 6-2Ak). The O 1s feature (spectrum 6-2Bk) gets smaller and broader as does the F 1s peak (spectrum 6-2Ck). The removal of surface oxygen is also evident in the compositional data obtained from the XPS spectra, as the O/C atom ratio is decreased from 0.16 to 0.12. The F/C ratio decreases to 0.03, which is believed to be the steady-state value.

Comparison: Tefzel Erosion by VUV Versus AO

Both VUV and AO [35] induce chemical alterations at a Tefzel surface, which result in erosion. A comparison of the high-resolution C 1s spectra obtained from VUV-exposed Tefzel (solid lines) and AO-exposed Tefzel (dashed lines) is shown in Figure 6-7. The spectra obtained from the two as-entered samples (Figure 6-7a) are almost identical as expected, with the low-BE peak shifted to a slightly higher BE (0.5 eV) in the AO-exposed Tefzel spectrum. There is also no evidence of hydrocarbon contamination on the AO-exposed sample. Both the AO- and VUV-exposed Tefzel spectra from the 24-h exposures and beyond are all quite similar in that the two peaks have been reduced to one peak at a lower BE (Figure 6-7c to f). The main difference is that the AO-exposed spectra have a main peak centered at 284.6 eV whereas the VUV-exposed spectra have a main peak centered at 286.0 eV. This shift is consistent throughout all of the spectra and suggests that AO and VUV lead to the formation of different carbon species at the surface of Tefzel. Also the AO-exposed spectra do not have a hump on the high-BE side of the main peak and the peak at ~290 eV is decreased to nothing after 24-h of AO exposure.

Comparison to Tedlar and Teflon

Similar VUV-exposure studies were performed on Tedlar (Chapter 4) [37] and Teflon [34] and the C 1s XPS spectra are compared in Figure 6-8. The F content of the near-surface region decreases very rapidly for Tedlar, similarly but less rapidly for Tefzel and relatively slowly for Teflon with increasing VUV radiation time. This behavior correlates with the hydrogen content of these polymers. Tedlar is 50 at% H, Tefzel is 33.3 at% H and Teflon is 0 at% H. This information suggests that H atoms i.e.: H-C bonds provide an attack point for VUV radiation. After the Tefzel structure is damaged the F becomes susceptible to removal by further VUV radiation. Since Teflon does not contain H the F is more difficult to remove. The C removal rate is not much slower than the F removal rate in Teflon so the steady state F/C atom ratio is 1.60 (from 1.98) compared to Tedlar where it drops from 0.34 to 0.04 and Tefzel dropping from 0.70 to 0.03. Also, compared to Tedlar and Tefzel, Teflon does not chemisorb much oxygen after erosion from VUV radiation. Following air exposure the O/C atom ratio for Tedlar went from 0.06 to 0.18 and for Tefzel from 0.08 to 0.16. In Teflon no O was adsorbed to the surface. Therefore, polymers containing more H initially form more damage-laden films during VUV radiation, which adsorb more O_2.

Summary

In this study a Tefzel film has been exposed to VUV radiation (115-400nm) for various times and the chemical alterations at the surface have been monitored using XPS. A 2-h exposure to VUV radiation results in a decrease in the F/C atom ratio from 0.70 to 0.39 and a significant decrease of carbon that is bonded to F. Another 22 h of VUV exposure results in a further decrease of the F/C atom ratio to 0.22. Exposure of this VUV-exposed surface to O_2 results in chemisorption of O due to bonding at reactive sites thereby raising the O/C atom ratio from 0.02 to 0.05. Further exposure of this surface to VUV radiation for 5 h results in a decrease

of the chemisorbed oxygen and the F/C ratio decreases to 0.19. Further treatments yield increased F removal and increased surface O. After 163 h total VUV exposure the F/C atom ratio is 0.07 and the O/C atom ratio is 0.08. This VUV-exposed surface was then exposed to air for 43 h and a large amount of O_2 is chemisorbed raising the O/C atom ratio to 0.16. Another 37 h of VUV exposure results in removal of some of the chemisorbed O (O/C atom ratio of 0.12) and attainment of a steady-state F/C atom ratio of 0.03.

Similar experiments were also carried out on Tefzel using hyperthermal AO, and the resulting XPS data have been compared with the corresponding XPS data obtained using VUV radiation. The results are similar with both methods removing much of the F within 2 h and nearly all of the F within 24 h. The two different treatments do however form carbon species with different BEs indicating that different carbonaceous structures form by the two treatments.

Similar experiments were also carried out by exposing PTFE Teflon and Tedlar to VUV radiation. The resulting XPS data have been compared and indicate that the C- H bonds in the polymer structure provide an attack point for VUV radiation and results in the rapid removal of F from the polymer.

Table 6-1. Near-surface compositions of Tefzel after various exposures (at%)

	F	C	O	Cl	N 1s	F/C	O/C
as entered	40.8	58.0	1.2	0.0	0.0	0.70	0.02
VUV 2 h	27.9	71.4	0.7	0.1	0.0	0.39	0.01
VUV 24 h	17.8	80.3	1.2	0.6	0.0	0.22	0.02
O_2 20 min	16.8	78.4	4.2	0.6	0.0	0.21	0.05
VUV 27 h	15.5	80.8	3.4	0.3	0.0	0.19	0.04
VUV 29 h	15.6	80.4	3.4	0.6	0.0	0.19	0.04
VUV 53 h	12.3	81.9	3.5	0.7	1.6	0.15	0.04
VUV 99 h	7.8	86.0	5.5	0.3	0.4	0.09	0.06
VUV 163 h	6.0	86.5	6.7	0.5	0.3	0.07	0.08
Air 43 h	3.3	82.3	12.8	0.6	1.1	0.04	0.16
VUV 200 h	2.7	86.2	10.1	0.2	0.8	0.03	0.12

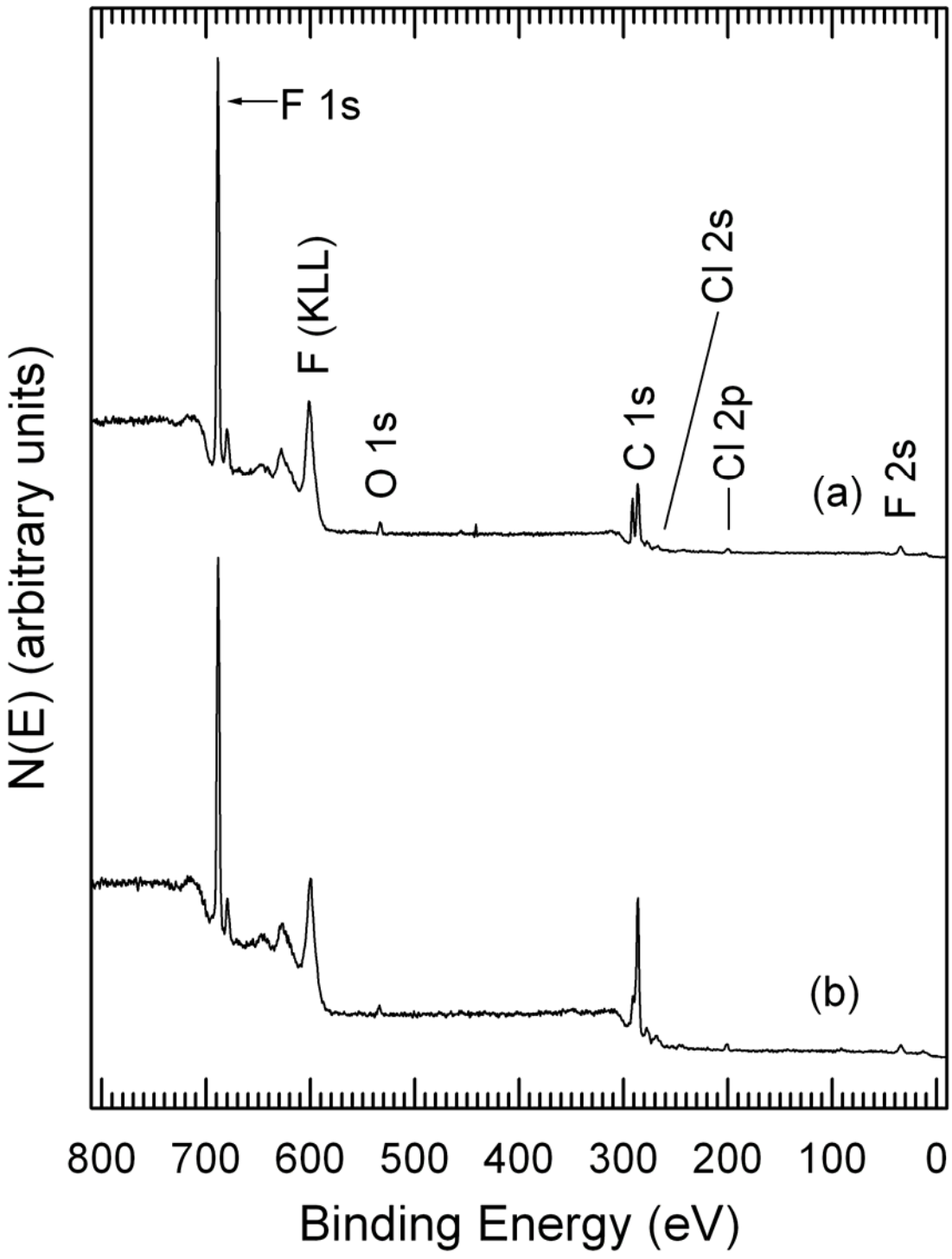

Figure 6-1. XPS survey spectra obtained from VUV-exposed Tefzel (a) as entered and (b) after a 2-h exposure to VUV radiation.

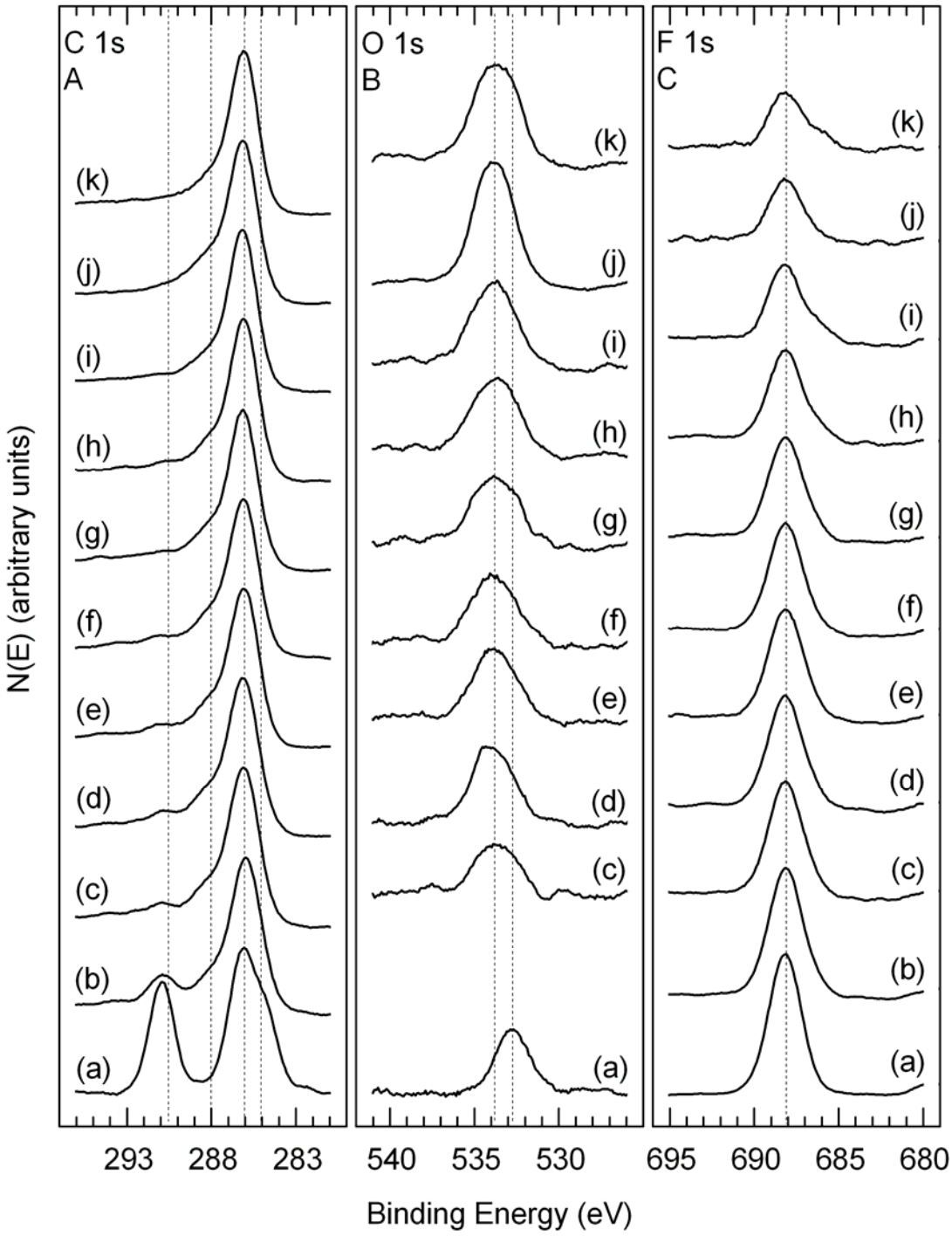

Figure 6-2. High-resolution XPS obtained from VUV-exposed Tefzel (A) C 1s, (B) O 1s and (C) F 1s (a) as entered, (b) after exposure to VUV for 2 h, (c) after exposure to VUV for a total of 24 h, (d) after exposure to O_2 at room temperature and 150 Torr for 20 min, (e) after exposure to VUV for a total of 27 h, (f) after exposure to VUV for a total of 29 h, (g) after exposure to VUV for a total of 53 h, (h) after exposure to VUV for a total of 99 h, (i) after exposure to VUV for a total of 163 h, (j) after exposure to air for 43 h at room temperature and (k) after exposure to VUV for a total of 200 h.

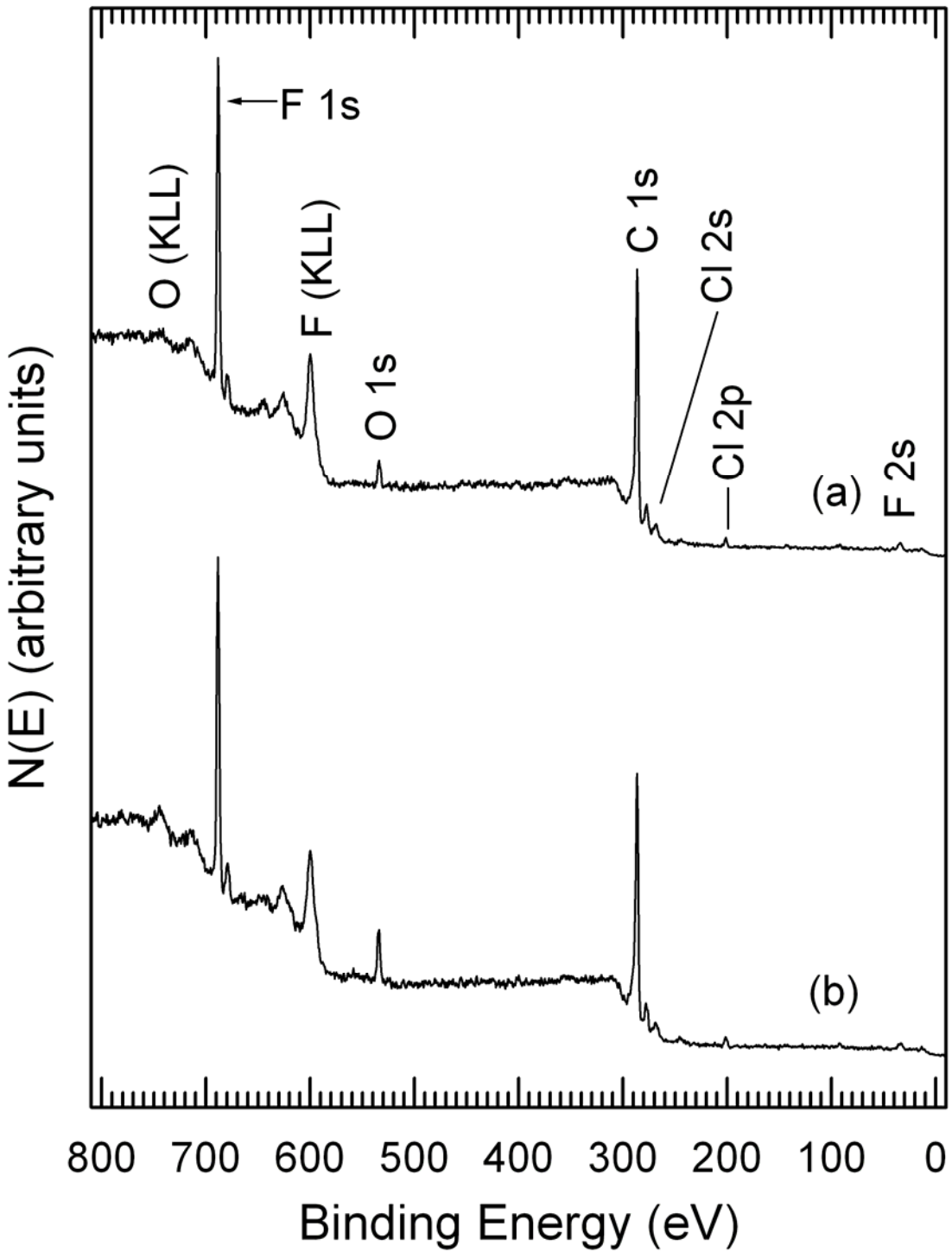

Figure 6-3. XPS survey spectra obtained from VUV-exposed Tefzel (a) after a 24-h exposure to VUV radiation and (b) after a 20-min exposure to O_2 at room temperature and 150 Torr.

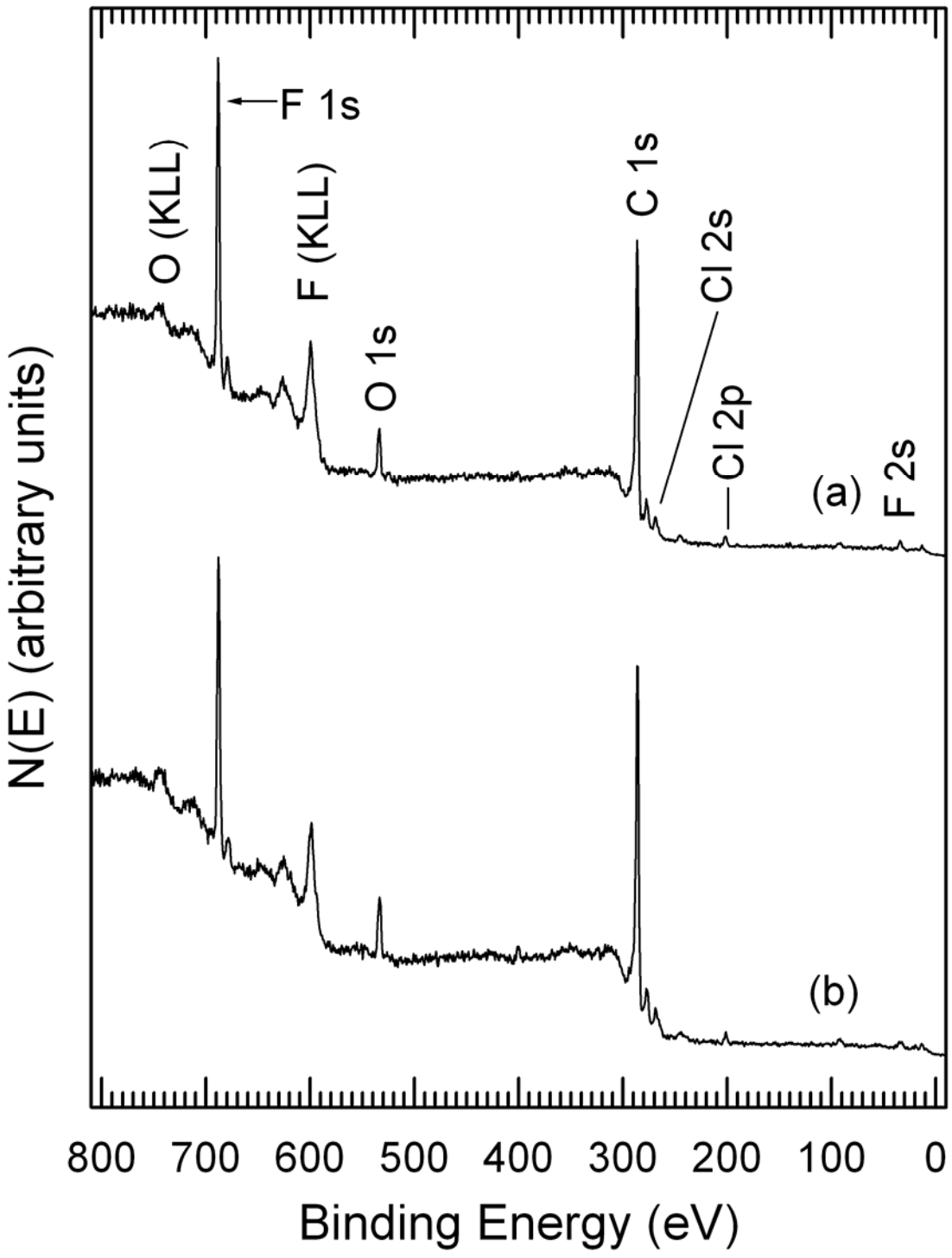

Figure 6-4. XPS survey spectra obtained from VUV-exposed Tefzel (a) after a 29-h exposure to VUV (5 h of VUV after O_2 exposure) and (b) after a total of 53 h exposure to VUV.

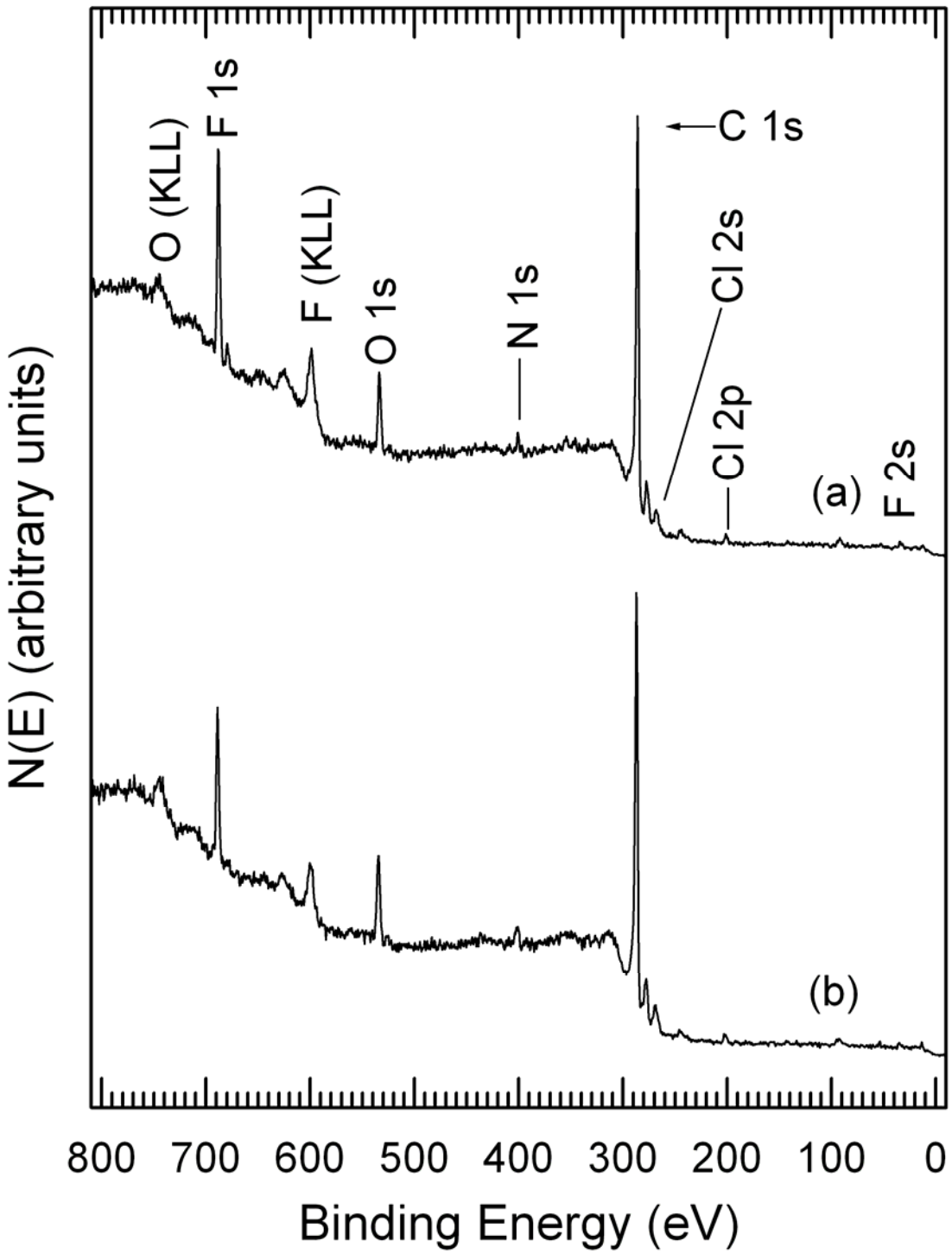

Figure 6-5. XPS survey spectra obtained from VUV-exposed Tefzel (a) after a 99-h exposure to VUV and (b) after a total of 163 h exposure to VUV.

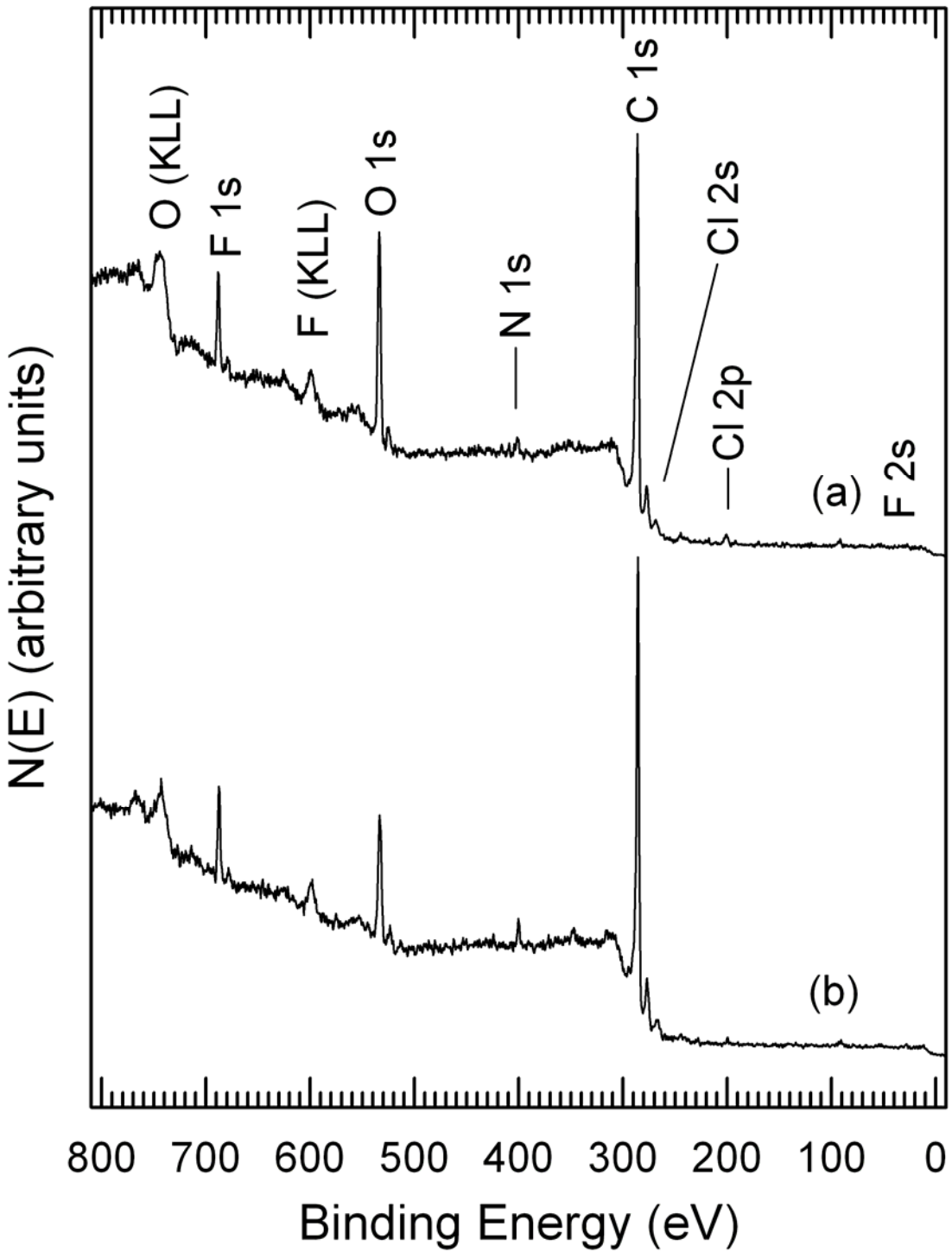

Figure 6-6. XPS survey spectra obtained from VUV-exposed Tefzel (a) after a 43-h exposure to air at room temperature and (b) after a total of 200 h exposure to VUV (37 h of VUV exposure after the air exposure).

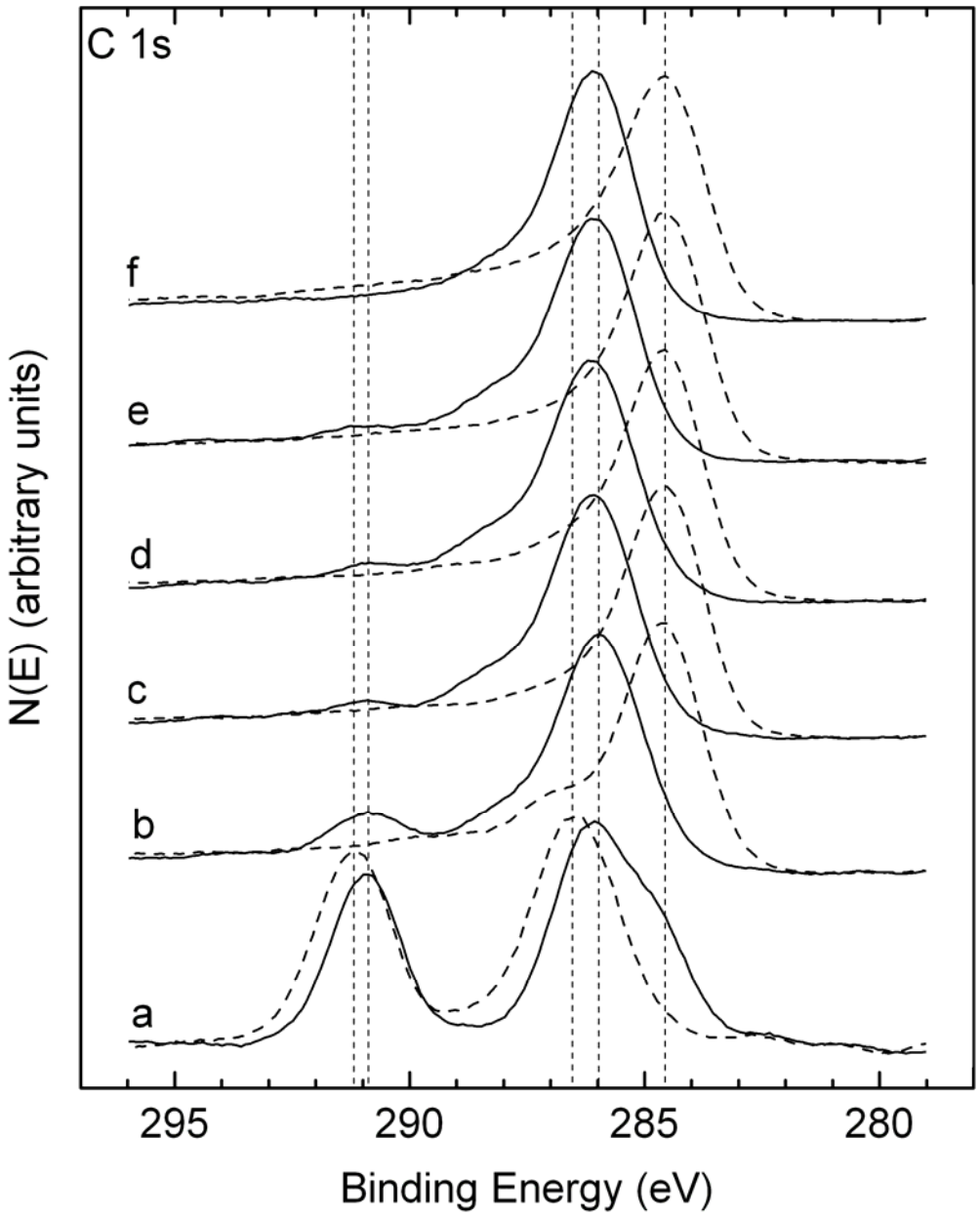

Figure 6-7. Overlays of XPS C 1s spectra obtained from Tefzel after various VUV (solid lines) and AO (dashed lines) exposures (a) as entered, (b) after 2 h VUV and 2 h AO, (c) after 24 h VUV and 24 h AO (d) after 20 min O_2, (e) after 27 total h VUV and 27 total h AO, (f) after 200 total h VUV and 98.5 total h AO (steady state).

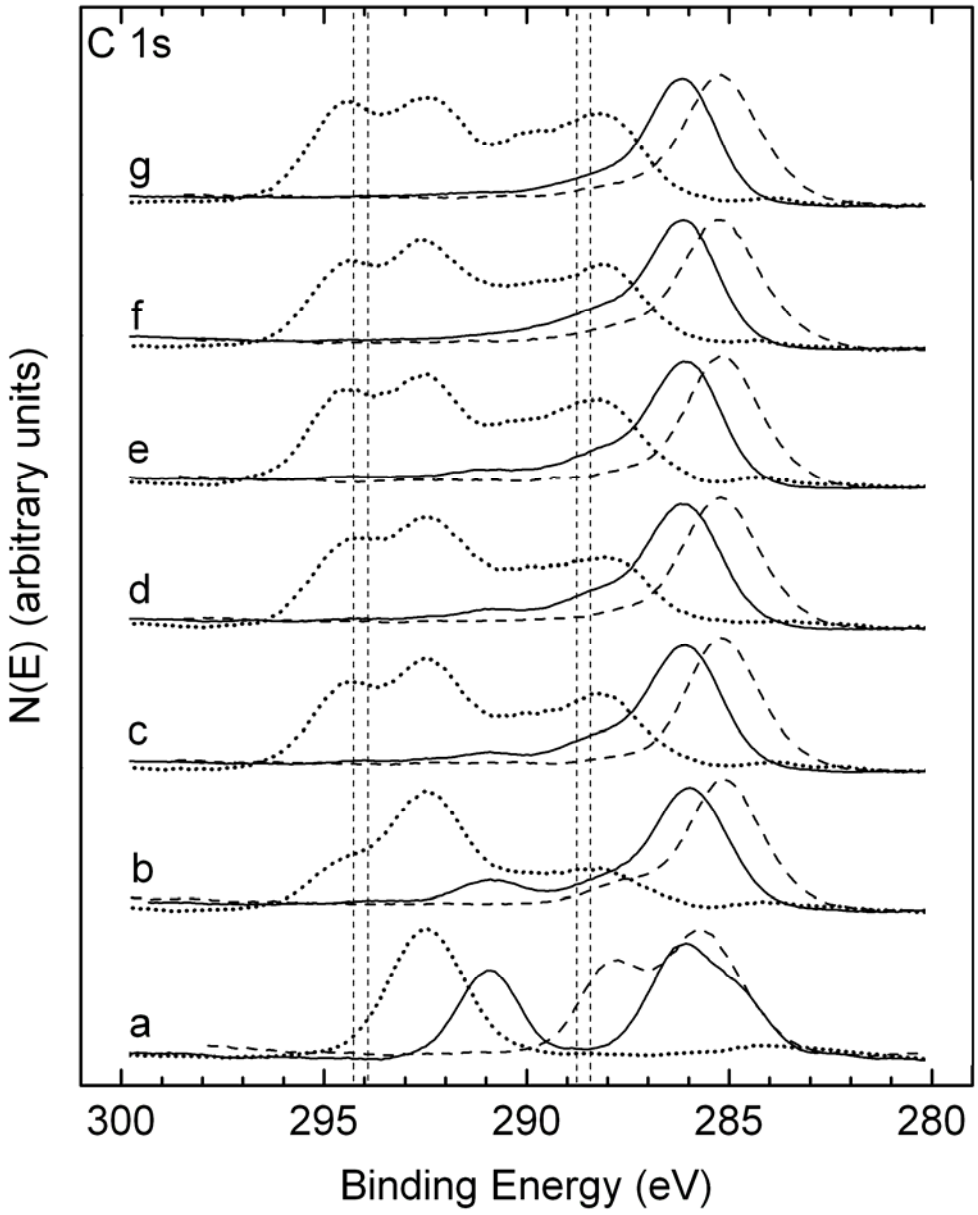

Figure 6-8. Overlays of XPS C 1s spectra obtained from various VUV exposures of Tedlar (dashed lines), Tefzel (solid lines) and Teflon (dotted lines) (a) as entered, (b) after 2 h VUV, (c) after 24 h VUV for Tedlar and Tefzel and 25 h for Teflon (d) after 20 min O_2, (e) after 3 additional h VUV or AO following O_2 exposure, (f) after exposure to air and (g) after steady state exposure.

LIST OF REFERENCES

1. B.A. Banks, The Use of Fluoropolymers in Space Applications. Modern Fluoropolymers, John Wiley & Sons, New York 1997.

2. L.J. Leger and J.T. Visentine, J. Spacecraft Rockets, 23, 505 (1986).

3. S.L. Koontz, L.J. Leger, J.T. Visentine, D.E. Hunton, J.B. Cross and C.L. Hakes, J. Spacecraft Rockets, 32, 483 (1995).

4. R.C. Tennyson, Can. J. Phys, 69, 1190 (1991).

5. S.L. Koontz, L.J. Leger, S.L. Rickman, C.L. Hakes, D.T. Bui, D.E. Hunton and J.B. Cross, J. Spacecraft Rockets, 32, 475 (1995).

6. M. R. Reddy, J. Mater. Sci., 30, 281 (1995).

7. S. Packirisamy, D. Schwam and M.H. Litt, J. Mater. Sci., 30, 308 (1995).

8. M.R. Reddy, N. Srinivasamurthy and B.L. Agrawal, Eur. Space Agency J., 16, 193 (1992).

9. K. K. de Groh and B.A. Banks, J. Spacecraft Rockets, 31, 656 (1994).

10. E. Grossman, Y. Lifshitz, J.T. Wolan, C.K. Mount and G.B. Hoflund, J. Spacecraft Rockets, 36, 75 (1999).

11. R.I. Gonzalez, S.H. Phillips and G.B. Hoflund, J. Spacecraft Rockets, 37, 463 (2000).

12. S.H. Phillips, G.B. Hoflund and R.I. Gonzalez, Proc. 45th International SAMPE Symposium, 45, 1921 (2000).

13. G. B. Hoflund, R. I. Gonzalez, S. H. Phillips, J. Adhesion Sci. Technol., 15, 1199 (2001).

14. K.K. DeGroh, J.R. Gaier, M.P. Espe, D.R. Cato, J.K. Sutter and D.A. Scheiman, High Perform. Polym., 12, 83 (2000).

15. J.A. Dever, K.K. DeGroh, B.A. Banks, J.A. Townsend, J. L. Barth, S. Thomson, T. Gregory and W. Savage, High Perform. Polym., 12, 125 (2000).

16. F.A. Rasoul, D.J.T. Hill, J.S. Forsythe, J.H. O'Donnell, G.A. George, P.J. Pomery, P.R. Young and J.W. Connell, J. Appl. Polym. Sci., 58, 1857 (1995).

17. A. Gindulyte, L. Massa, B.A. Banks and S.K.R. Miller, J. Phys. Chem. A, 106, 5463 (2002).

18. G. R. Corallo, G.B. Hoflund and R.A. Outlaw, Surf. Interface Anal., 12, 185 (1988).

19. M.R. Davidson, G.B. Hoflund and R.A. Outlaw, Surf. Sci., 281, 111 (1993).

20. R.A. Outlaw, G.B. Hoflund and G.R. Corallo, Appl. Surf. Sci., 28, 235 (1987).

21. E. Wisotzki, A.G. Balogh, H. Horst, J.T. Wolan and G.B. Hoflund, J. Vac. Sci. Technol. A, 17, 14 (1999).

22. E. Wisotzki, H. Hahn and G.B. Hoflund, in Trends and New Applications of Thin Films, Horst Hoffman, Ed., Trans Tech Publications LTD, Switzerland, 1998, 181, pp. 277-278.

23. M. R. Davidson, G. B. Hoflund and R. A. Outlaw, J Vac. Sci. Technol. A, 11, 264 (1993).

24. ASTM Designation: E 490-00a, Standard Solar Constant and Zero Air Mass Solar Spectral Irradiance Tables, ASTM, West Conshohocken, PA (2000).

25. G.B. Hoflund and J.F. Weaver, Measure. Sci. Technol. 5 (1994) 201.

26. C.D. Wagner, W.M., Riggs, L.E Davis, J.F. Moulder and G.E. Muilenberg, Eds., Handbook of X-ray Photoelectron Spectroscopy, Perkin-Elmer Corp.: Eden Prairie, MN, (1979).

27. A. Joshi, L.E. Davis and P.W. Palmberg, in Methods of Surface Analysis; A.W. Czanderna, Ed., Elsevier Scientific Publ. Co.: Amsterdam, (1975) p 160.

28. R.E. Gilbert, D.F. Cox and G.B Hoflund, Rev. Sci. Instrum. 53 (1982) 1281

29. A. Savitzky and M.J.E. Golay, Anal. Chem. 36 (1964) 1627.

30. High Resolution XPS of Organic Polymers: The Scienta ESCA300 Database; G. Beamson and D. Briggs, Eds.; Wiley: Chichester, 1992; pp 54, 226-236.

31. Handbook of X-ray Photoelectron Spectroscopy; C.D. Wagner, W.M. Riggs, L.E. Davis, J.F. Moulder and G.E. Muilenberg, Eds.; Perkin-Elmer Corp.: Eden Prairie, MN, 1979.

32. G.B. Hoflund in Handbook of Surface and Interface Analysis: Methods in Problem Solving; Rivière, J. C.; Myhra, S., Eds.; Marcel Dekker: New York, 1998; pp 57-158.

33. G.B. Hoflund and M.L. Everett, J Phys. Chem. B 108 (2004) 15721.

34. M.L. Everett and G.B. Hoflund, J. Poly. Sci. 43 (2004) 552.

35. G.B. Hoflund and M.L. Everett, Appl. Surf. Sci. 239 (2005) 367.

36. M.L. Everett and G.B. Hoflund, Macromolecules 37 (2004) 6013.

37. M.L. Everett and G.B. Hoflund, Appl. Surf. Sci. 252 (2006) 3789.

BIOGRAPHICAL SKETCH

Michael L. Everett was born on February 23, 1978, in Springfield, Massachusetts, to Wayne R. Everett and Kathleen S. Everett. He graduated from Springfield Central High School in 1996. That fall Michael began his college education at Worcester Polytechnic Institute in Worcester, Massachusetts. In May 2000 he received his Bachelor of Science in chemical engineering. Michael then entered the Graduate School at the University of Florida in Gainesville, Florida, to further his education in chemical engineering. As a graduate student he began working under Dr. Gar B. Hoflund, performing research in surface science and received a Master of Science in chemical engineering. He then continued working under Dr. Hoflund towards a PhD.